

# **Probiotic Mucoadhesive Polymer Films for Treatment of Periodontitis**

Dissertation

zur Erlangung des Grades  
des Doktors der Naturwissenschaften  
der Naturwissenschaftlich-Technischen Fakultät  
der Universität des Saarlandes

von

**Charlotte Eckermann**

Saarbrücken

2025

Tag des Kolloquiums: 06.06.2025

Dekan: Prof. Dr.-Ing. Dirk Bähre

Berichterstatter: Prof. Dr. Marc Schneider  
Prof. Dr. Andriy Luzhetskyy

Vorsitz: Prof. Dr. Markus Gallei

Akd. Mitarbeiter: Dr. Brigitta Loretz

Die Daten der vorliegenden Dissertation sind im Zeitraum zwischen September 2021 und August 2024 am Institut für Biopharmazie und Pharmazeutische Technologie der Universität des Saarlandes unter Betreuung von Prof. Dr. Schneider (Professor für Biopharmazie und Pharmazeutische Technologie) entstanden.

*„Man muss Geduld haben mit dem Ungelösten (im Herzen) und versuchen, die  
Fragen selbst lieb zu haben“ Rainer Maria Rilke*

## Table of Contents

Abbreviations.....	X
Summary .....	XII
Zusammenfassung .....	XIII
1. General Introduction .....	1
1.1. Probiotics and Oral Health .....	1
1.2. Microencapsulation of Probiotic Bacteria .....	3
1.3. Mucoadhesive Polymer Films.....	6
1.4. Cultivation of <i>Lactobacilli</i> .....	7
1.5. Aim of the Work.....	9
2. Materials and Methods .....	11
2.1. Materials.....	11
2.2. Frequently Used Methods .....	15
2.2.1. Analytical Methods.....	15
2.2.1.1. Scanning Electron Microscopy (SEM) .....	15
2.2.1.2 Atomic Force Microscopy (AFM) - Mucoadhesion .....	15
2.2.1.3 Tensile Tester .....	16
2.2.1.4 Plate Count Method .....	18
2.2.1.5 Confocal Laser Scanning Microscope (CLSM) .....	19
2.2.1.6 <i>In Vivo</i> Testing.....	20
2.2.2 Preparative Methods.....	21
2.2.1.1. Microencapsulation via Spray Drying .....	22
2.2.1.2 Film Casting.....	24
2.2.1.3 Lyophilization .....	25
2.2.1.4. 3D Bioprinting .....	26
3. Formulation Probiotic Mucoadhesive Polymer Films .....	27

3.1.	Introduction .....	28
3.2.	Methods .....	31
3.2.1.	Cultivation <sup>1</sup> .....	31
3.2.2.	Determination of Activity <sup>1</sup> .....	31
3.2.3.	Microencapsulation <sup>1</sup> .....	32
3.2.4.	Film Casting .....	33
3.2.5.	Film Properties .....	35
3.2.5.5.	<i>Dissolution Testing</i> <sup>1</sup> .....	38
3.3.	Results & Discussion.....	39
3.3.1.	Activity <sup>1</sup> .....	39
3.3.2.	Film Casting <sup>1</sup> .....	41
3.3.3.	Film Casting Thickness and Additional Formulations.....	43
3.3.4.	Film Properties .....	44
3.4.	Conclusion <sup>1</sup> .....	58
3.4.1.	Selection of Polymer Film.....	58
4.	Microencapsulation of <i>L. rhamnosus</i> and <i>L. reuteri</i> and incorporation inside mucoadhesive polymer films .....	60
4.1.	Introduction .....	61
4.2.	Methods .....	64
4.2.1.	Microencapsulation via Spray Drying <sup>2</sup> .....	64
4.2.2.	Morphology Analysis <sup>2</sup> .....	64
4.2.3.	Microbiological Analysis <sup>2</sup> .....	65
4.2.4.	Dissolution of Microencapsulated Bacteria and Polymer Film <sup>2</sup> .....	65
4.2.5.	Polymer Films Incorporating <i>L. reuteri</i> <sup>2</sup> and <i>L. rhamnosus</i> (Film Casting Device) .....	66
4.2.6.	Hand-cast Polymer Films .....	66
4.2.7.	Drying at Different Temperatures .....	66

4.2.8.	Freeze-Dried Polymer Films.....	66
4.2.9.	Foamed PVA Films with Incorporated Bacteria.....	67
4.2.10.	Foamed PVA Films with Bacteria filled Pores.....	68
4.2.11.	Covered Polymer Films with Bacteria.....	69
4.2.12.	Vacuum Dried Films .....	69
4.2.13.	Cultivation of <i>L. reuteri</i> and <i>L. rhamnosus</i> in Liquid Culture <sup>2</sup> .....	69
4.2.14.	Activation of Protection Mechanisms in Bacteria <sup>2</sup> .....	70
4.2.15.	Stability Testing .....	71
4.3.	Results .....	72
4.3.1.	Survival of <i>L. reuteri</i> after Spray Drying <sup>2</sup> .....	72
4.3.2.	Survival of <i>L. rhamnosus</i> after Spray Drying.....	73
4.3.3.	Morphology of Microencapsulated <i>L. reuteri</i> <sup>2</sup> .....	73
4.3.4.	Investigation of Core-Shell Structure <sup>2</sup> .....	75
4.3.5.	Dissolution of Microencapsulated <i>L. reuteri</i> <sup>2</sup> (Three-Way-Nozzle) .....	75
4.3.6.	Dissolution of Microencapsulated <i>L. reuteri</i> (Three-Way Nozzle).....	77
4.3.7.	Survival Embedding <i>L. reuteri</i> inside Polymer Films <sup>2</sup> .....	78
4.3.8.	Survival Embedding <i>L. rhamnosus</i> inside Polymer Films.....	79
4.3.9.	Survival Bacteria inside Hand-Cast Polymer Films .....	80
4.3.10.	Survival Probiotic Polymer Films at Different Drying Conditions.....	81
4.3.11.	Freeze-Dried Polymer Films .....	82
4.3.12.	Foamed PVA Films with Incorporated Bacteria .....	83
4.3.13.	Foamed PVA Films with Bacteria filled in Pores.....	84
4.3.14.	Polymer Films with Covered Bacteria.....	85
4.3.15.	Vacuum-Dried Polymer Films .....	86
4.3.16.	Liquid Cultivation and Determination of Growth Curve ( <i>L. reuteri</i> ) <sup>2</sup> .	87
4.3.17.	Liquid Cultivation and Determination of Growth Curve ( <i>L. rhamnosus</i> ) .....	89

4.3.18.	Microencapsulating after Cultivation under Osmotic Stress and Film Formation ( <i>L. reuteri</i> ) <sup>2</sup> .....	91
4.3.19.	Microencapsulation after Cultivation under Osmotic Stress and Film Formation ( <i>L. rhamnosus</i> ) .....	92
4.3.20.	Microencapsulation after Cultivation under Acidic Conditions and Film Formation ( <i>L. reuteri</i> ) <sup>2</sup> .....	93
4.3.21.	Microencapsulation after Cultivation under Acidic Conditions and Film Formation ( <i>L. rhamnosus</i> ).....	94
4.3.22.	Microencapsulation after Cultivation under Acidic Conditions and Osmotic Shock Followed by Film Formation <sup>2</sup> .....	96
4.3.23.	Microencapsulation after Cultivation under Acidic Conditions and Osmotic Shock Followed by Film Formation ( <i>L. rhamnosus</i> ) .....	97
4.3.24.	Dissolution of Polymer Film Containing Microencapsulated <i>L. reuteri</i> <sup>2</sup> .....	97
4.3.25.	Dissolution of Polymer Film Containing Microencapsulated <i>L. rhamnosus</i> .....	99
4.3.26.	Stability .....	99
4.4.	Discussion <sup>2</sup> .....	101
4.4.1.	Discussion <i>L. rhamnosus</i> and <i>L. reuteri</i> and Different Film Preparation Methods .....	103
4.5.	Conclusion <sup>2</sup> .....	106
5.	Biological Testing .....	109
5.1.	Introduction .....	110
5.2.	Methods <sup>1</sup> .....	111
5.3.	Results and Discussion <sup>1</sup> .....	112
5.3.1.	Influence of Bacterial Concentration <sup>1</sup> .....	112
5.3.2.	Incubation in Oral Cavity <sup>1</sup> .....	113
5.4.	Summary .....	120
6.	Bioprinting.....	122
6.1.	Introduction .....	122
6.2.	Methods .....	124



6.2.1.	Formulation .....	124
6.2.2.	Surface Morphology .....	126
6.2.3.	Dissolution.....	126
6.3.	Results and Discussion .....	127
6.3.1.	Formulation .....	127
6.3.2.	Surface Morphology .....	127
6.3.3.	Activity.....	128
6.3.4.	Release .....	129
6.3.5.	Bioprinted Grid .....	130
6.3.6.	Bioprintingformulation – Filmcasting Device.....	133
6.4.	Summary .....	134
7.	Summary & Outlook.....	136
7.1.	Film Formulation.....	136
7.2.	Microencapsulated Bacteria .....	137
7.3.	Embedding Bacteria inside Polymer Films .....	137
7.4.	Biological Testing .....	138
7.5.	Outlook.....	138
8.	References .....	141
	Publication Report .....	153
	Paper .....	153
	Posters.....	153
	Oral Talk .....	154
	Acknowledgements .....	155
	Curriculum Vitae .....	157

# Abbreviations

<b>2WN</b>	Two-Way Nozzle
<b>3WN</b>	Three-Way Nozzle
<b>AFM</b>	Atomic force microscopy
<b>CFU</b>	Colony forming units
<b>CLSM</b>	Confocal laser scanning microscope
<b>DMSO</b>	Dimethyl sulfoxide
<b>EDC</b>	Carbodiimide
<b>Encap</b>	Microencapsulated
<b>HPMC</b>	Hydroxypropyl methylcellulose
<b>LAB</b>	Lactic acid bacteria
<b>MO</b>	Microorganisms
<b>MRS</b>	Man Rogosa Sharpe
<b>MWCO</b>	Molecular weight cut-off
<b>NaCl</b>	Sodium chloride

<b>NHS</b>	N-Hydroxysuccinimide
<b>OD</b>	Optical density
<b>PVA</b>	Polyvinyl alcohol
<b>SEM</b>	Scanning electron microscope

# Summary

The oral microbiome plays a pivotal role in maintaining oral health, with dysbiosis leading to conditions such as periodontitis. Probiotics, including *Lactobacillus rhamnosus* and *Lactobacillus reuteri*, have demonstrated efficacy in restoring microbial equilibrium within the oral cavity. To address the challenges inherent to the survival and delivery of probiotics, this work explores innovative approaches involving microencapsulation and mucoadhesive polymer films for effective therapeutic applications.

The probiotics were microencapsulated using spray drying with Eudragit® EPO and RL30D, ensuring gradual release. Stress preconditioning enhanced bacterial resilience. The bacteria were embedded in two polymer films: a thin, flexible film, out of HPMC and PVA, and a foamed one, out of PVA. The objective was to design films that show mucoadhesion, flexibility, tensile strength, bacterial viability and controlled bacterial release.

The treatment was evaluated through *in vivo* experiments on two volunteers. It demonstrated strong mucoadhesion and effective bacterial release. Both film types facilitated the adhesion of probiotic bacteria to enamel surfaces, reducing the colonization of cocci.

This demonstrates the efficacy of combining microencapsulation with mucoadhesive films to improve delivery. The approach offers a non-invasive, targeted therapy for periodontitis, with the potential to improve oral health by restoring microbial balance and reducing pathogenic colonization.

# Zusammenfassung

Das orale Mikrobiom ist entscheidend für die Mundgesundheit, wobei eine Dysbiose zu Erkrankungen wie Parodontitis führen kann. Probiotika wie *Lactobacillus rhamnosus* und *Lactobacillus reuteri* helfen, das mikrobielle Gleichgewicht wiederherzustellen. Diese Arbeit untersucht innovative Ansätze zur verbesserten Verabreichung von Probiotika mittels Mikroverkapselung und mukoadhäsiven Polymerfilmen.

Die Mikroverkapselung mit Eudragit® EPO und RL30D per Sprühtrocknung gewährleistete eine hohe Überlebensrate, Mukoadhäsion und kontrollierte Freisetzung. Eine Stressvorbehandlung erhöhte die Widerstandsfähigkeit der Bakterien. Zwei Polymerfilmtypen wurden getestet: ein flexibler Film aus HPMC-PVA und ein geschäumter PVA-Film. Beide Filme bewahrten die bakterielle Aktivität und boten gute mechanische Eigenschaften.

In vivo zeigten die Filme starke Mukoadhäsion, kontrollierte Bakterienfreisetzung und eine Reduktion pathogener Kokken auf der Zahnschmelzoberfläche. Die Kombination aus Mikroverkapselung und Polymerfilmen bietet einen vielversprechenden, nicht-invasiven Ansatz zur gezielten Behandlung von Parodontitis und zur Förderung der Mundgesundheit.

# 1. General Introduction

## 1.1. Probiotics and Oral Health

Probiotics are defined as live microorganisms that confer health benefits to the host when administered in appropriate amounts.<sup>[1,2]</sup> They exert a direct inhibitory effect on the adhesion, growth and metabolic processes of competing pathogenic bacteria.<sup>[3]</sup> The study of probiotics has expanded considerably in recent years, particularly in light of the growing understanding of the human microbiome. Microbiota play a multifaceted role in health and disease. There is compelling evidence that disruptions in microbial balance, or dysbiosis, is associated with a wide range of health issues<sup>[4]</sup>. However, it remains challenging to determine the direction of causality, i.e. whether dysbiosis triggers disease, the disease disrupts microbial balance, or both are mutually reinforcing. Nevertheless, targeting specific probiotic strains has shown promise in restoring microbiome equilibrium, with potential applications in targeted local treatments.<sup>[5–8]</sup>

The oral microbiome is now recognized as the second largest in the human body, after the gut microbiome.<sup>[9]</sup> It is a highly intricate microbiome, comprising bacteria, archaea, fungi and viruses. The coexistence is a very fine balanced system<sup>[8]</sup>. The microbiome forms a biofilm to adapt to environmental conditions. In the absence of regular biofilm removal, gram-negative bacteria proliferate and undergo mineralization, resulting in the accumulation of calcium and phosphorus. This process also induces inflammation.<sup>[10–12]</sup> A disbalance in the microbiome is frequently associated with a range of pathological conditions, including caries and periodontitis. Periodontitis is a highly prevalent condition, affecting an estimated 20–50% of the global population. Periodontitis is a chronic infection associated with the accumulation of dental plaque and characterized by inflammation and the progressive destruction of tooth-supporting structures. It is an irreversible pathological disease of the periodontium. The onset of this condition is marked by reversible gingivitis, which is characterized exclusively by involvement of the gingival tissues.<sup>[13,14]</sup> The process commences with an overgrowth of gram-negative bacteria in the periodontal area, which initially manifests as gingivitis and subsequently progresses to periodontitis, characterized by the loss of soft and

hard tissue. The aforementioned bacteria are responsible for the production of metabolites, for example lipopolysaccharides, which elicit an inflammatory response and the subsequent production of matrix metalloproteinases.<sup>[15–17]</sup> These enzymes contribute to the degradation of collagen fibers within periodontal tissue. The bacteria then penetrate the periodontal tissue, forming periodontal pockets.<sup>[18]</sup> Advanced periodontitis has the potential to result in tooth loss as soon as it reaches the tooth attachment system. Furthermore, periodontitis is linked to an increased risk of developing other metabolic diseases, such as cardiovascular disease and diabetes.<sup>[5,9,19]</sup> The delicate equilibrium between commensal and pathogenic microbes in the oral cavity is of great importance for oral health. <sup>[4,6,8]</sup> Furthermore, the colonization patterns of bacteria in the oral cavity, in terms of duration is a crucial factor influencing oral health outcomes.<sup>[7]</sup> Antibiotics and surgical interventions are primarily used to treat periodontitis.<sup>[19]</sup> However, antibiotic therapies have been linked to negative consequences for the entire microbiome, and surgical approaches have frequently neglected the microbiome.<sup>[19]</sup> Another method for rebalancing the microbiome is through the introduction of probiotic bacteria. Probiotics are non-pathogenic microorganisms that are considered to have a beneficial effect on the health of the host.<sup>[2,7]</sup>

Probiotic delivery methods for periodontitis prioritize therapeutic approaches over simplified consumer products, reflecting the severity of the disease and its prevalence beyond childhood. Probiotic formulations for periodontitis include lozenges, tablets, and mouthwashes, which facilitate localized application within the oral cavity. It is important to ensure a long resistance time in the mouth, allowing the probiotics to adhere effectively with the oral cavity and prevent the bacteria from being swallowed too quickly, thereby maximizing their therapeutic potential.<sup>[5,19,20]</sup>

Clinical studies have demonstrated the efficacy of *L. reuteri* in the management of gingivitis and periodontitis. It was demonstrated that the bacteria inhibited the growth of periodontopathogens through the release of bacteriocins, hydrogen peroxide, and organic acids.<sup>[21–24]</sup> The administration of *L. reuteri* lozenges resulted in enhanced outcomes for patients presenting with moderate and deep periodontal pocket depths. Furthermore, it was observed that the intervention resulted in a reduction in both

periodontal bleeding and plaque formation. No adverse effects associated with the use of *L. reuteri* lozenges were reported. Further research indicated that *L. reuteri* lozenges may impede the recolonization of pathogenic bacteria, thereby enhancing clinical outcomes.<sup>[20,24–27]</sup>

*L. rhamnosus* is a probiotic strain that has been extensively researched and has shown various health benefits, especially in relation to gastrointestinal, immune, and oral health. Studies have focused on its potential in treating periodontitis and gingivitis by positively influencing the oral microbiome and reducing inflammation. *L. rhamnosus* can promote periodontal health through competitive inhibition of pathogenic bacteria, production of antimicrobial compounds, and modulation of local immune responses. It can prevent the colonization of harmful bacteria by competing for adhesion sites and producing bacteriocins that inhibit their growth. Clinical studies have demonstrated that supplementation with *L. rhamnosus*, alongside traditional cleaning methods, can improve periodontal parameters such as plaque, bleeding, and gingival indices without disturbing the overall composition of the salivary microbiome. This suggests that *L. rhamnosus* can reduce oral pathogenicity while maintaining microbial balance, potentially due to its immunomodulatory properties that reduce proinflammatory cytokines and contribute to a healthier gum environment.<sup>[28–31]</sup>

As the bacteria cannot be administered directly in pure powder form, they must be incorporated into a suitable dosage form. The initial step in this process is the microencapsulation of the bacteria, which serves to safeguard them and facilitate the controlled release of the active ingredient. Subsequently, the microencapsulated bacteria are embedded within polymer films for the purpose of ensuring effective delivery.

## 1.2. Microencapsulation of Probiotic Bacteria

Microencapsulation of probiotic bacteria represents a crucial technique for enhancing stability, viability, and targeted delivery in both pharmaceutical and biomedical applications.<sup>[32–34]</sup> This process involves the entrapment of bacteria within a protective matrix, thereby shielding them from harsh environmental conditions such as pH



fluctuations, temperature changes, and enzymatic degradation. Microencapsulation not only ensures bacterial survival during processing and storage but also allows for controlled release and localized activity at the site of action.<sup>[34–38]</sup> This capability holds promise for advancing applications in probiotic therapies, oral drug delivery, and other bacterial-based treatments, offering improved therapeutic outcomes and user compliance.

In particular, spray drying has emerged as a prominent technique for microencapsulation. Spray drying is renowned for its rapid and gentle drying process.<sup>[35,39]</sup> When combined with appropriate encapsulating agents, such as trehalose, maltodextrin, and whey protein, it can achieve high bacterial survival rates.<sup>[40–42]</sup> This technique can be employed to produce highly uniform, small-diameter applications that require a consistent dosage and controlled release properties. The selection of nozzle also permits flexibility in structural outcomes.<sup>[35,36,41,43,44]</sup> To illustrate, a two-way nozzle facilitates encapsulation through the combination of drying gas and bacterial dispersion into a matrix.<sup>[38,45–47]</sup> In contrast, a three-way nozzle configuration, in which the drying gas and spray dispersion converge at the tip, enables the formation of multi-layer encapsulation.<sup>[47–49]</sup>

Spray drying with a three-way nozzle represents a sophisticated technique for the microencapsulation of probiotics. This technique enables more precise control over the structure and functionality of the particles, resulting in the formation of multi-layered particles. In the process, an inner stream transports the probiotic bacteria, while an outer stream provides encapsulating materials that coat the core. The layered microcapsule acts as a protective barrier, safeguarding the probiotics from external factors such as heat, moisture, and stomach acid. The application of low temperatures during spray drying helps to maintain high survival rates of the bacteria in question, as this minimizes the impact of thermal stress. Furthermore, the outer encapsulation layer can be tailored to regulate the release rate, thereby ensuring targeted delivery to specific regions of the gastrointestinal tract. The incorporation of materials such as Eudragit® in the outer layer can enhance mucoadhesion and prolong retention time within the gastrointestinal tract. Overall, the three-way nozzle spray drying technique

is a valuable method for producing stable, viable, and controlled-release probiotic formulations suitable for oral consumption.<sup>[38,50–54]</sup>

This advanced technique, frequently incorporating polymers such as Eudragit® E (Figure 1.1 A) and RL, ensures bacterial protection and allows for controlled delivery.<sup>[55]</sup> Eudragit® RL (Figure 1.1 B), for instance, has the capacity to enhance mucoadhesion, thereby prolonging the residence time of the formulation within the oral cavity and reducing the likelihood of immediate swallowing. The positive charge is capable of interacting with negatively charged mucins.<sup>[56–59]</sup> This attribute is highly beneficial for local therapies.

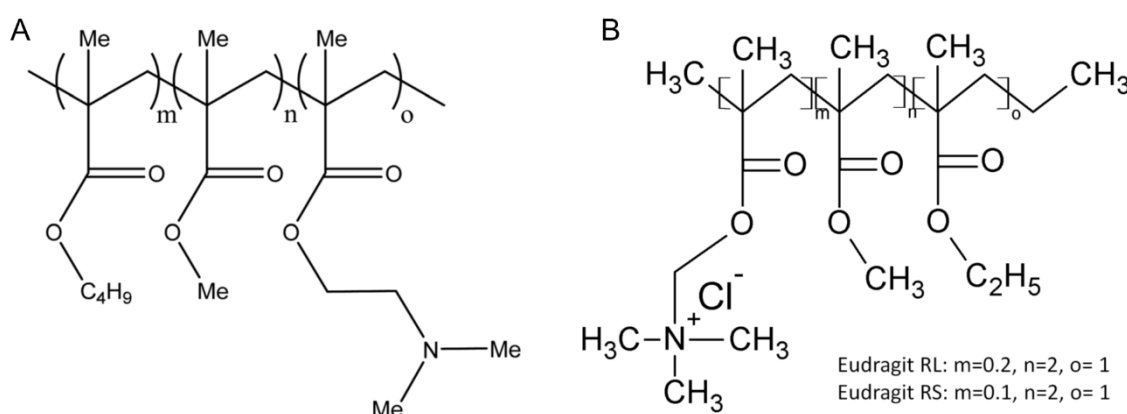


**Figure 1.1.** A. Chemical structure of Eudragit® E B. Chemical structure of Eudragit RL/RS®

The encapsulating matrix plays a pivotal role in safeguarding bacterial cells. Alginate-chitosan coatings, for instance, provide dual protection, withstanding gastric acidity while releasing bacteria in the more neutral pH of the intestines. Similarly, spray drying with formulations such as trehalose and maltodextrin provides a glassy structure around the bacteria, offering protection from thermal and oxidative stress.<sup>[33]</sup> Maltodextrin with a low dextrose equivalent (DE) has been demonstrated to enhance cell survival due to its robust encapsulating properties.<sup>[60–62]</sup>

Spray drying for microencapsulation represents a practical, scalable, and effective method for the preservation of viable probiotics.<sup>[44]</sup> By modifying parameters such as nozzle type and encapsulating matrix composition, manufacturers can enhance

bacterial survival, stability, and targeted release, which are essential for the efficacy of probiotics in health applications.

The microencapsulated bacterial powder is embedded in mucoadhesive polymer films, thus creating an applicable dosage form.

### **1.3. Mucoadhesive Polymer Films**

The microencapsulated bacteria were embedded in mucoadhesive polymer films, thereby enhancing their applicability and increasing mucoadhesion.<sup>[63–66]</sup> In recent years, the development of oral films has emerged as a novel therapeutic strategy for combating oral diseases. These films, designed for local or systemic drug delivery, offer several advantages, including improved drug stability, targeted release, and patient compliance.<sup>[67–70]</sup>

Mucoadhesive films are composed of polymers that interact with the mucosal membrane, forming adhesive bonds through a variety of mechanisms, including van der Waals forces, hydrogen bonds, ionic interactions, and chain entanglements.<sup>[65,66,69,71–75]</sup> The selection of polymers is of great consequence, as it determines a number of properties, including adhesion strength, film flexibility, dissolution rate, and drug release kinetics. The utilized polymers include hydroxypropyl methylcellulose (HPMC) and polyvinyl alcohol (PVA), which are combined with glycerol, acting as a plasticizer, to enhance flexibility. These films offer several advantages over traditional dosage forms, including ease of administration and minimal invasiveness.<sup>[71,76–78]</sup> Additionally, they provide prolonged adhesion and the potential for local drug delivery. Consequently, they are particularly efficacious in the treatment of local oral diseases, such as periodontitis.

In the development of effective mucoadhesive films, it is essential to optimize essential properties such as flexibility, tensile strength and mucoadhesion in order to ensure durability and functional performance within the oral cavity.<sup>[75,79]</sup> The capacity of a film to bend without breaking, as determined by folding endurance tests, is indicative of its resilience during storage, transport, and use. Tensile strength is evaluated through

tensile testing, which assesses the film's mechanical robustness and capacity to withstand physical stress without disintegrating. Mucoadhesion, a critical factor influencing the duration of drug release, is influenced by the interactions between the polymer and mucosal tissues. It is therefore a key factor in maintaining the film's position in the mouth for effective drug delivery.<sup>[78,80]</sup>

The combination of these characteristics with the controlled drug release capabilities of mucoadhesive films makes them a promising option for the management of localized oral conditions. They offer a non-invasive, efficient and user-friendly therapeutic alternative. In this study, polymeric films comprising hydroxypropyl methylcellulose (HPMC) and polyvinyl alcohol (PVA) were fabricated for the encapsulation of probiotics, leveraging the distinctive interaction capabilities of the polymers. The processes of spray-drying and film formation entail the drying of the system, which exerts stress on the microorganisms and results in a significant reduction in viability.

### **1.4. Cultivation of *Lactobacilli***

The cultivation of *Lactobacillus* species, particularly *L. reuteri* and *L. rhamnosus*, has attracted considerable attention due to their probiotic benefits in supporting oral health and immune functions. It is of paramount importance to enhance the activity, stability, and robustness of these strains during formulation processes, storage, and delivery, as this is a prerequisite for their efficacy. To enhance survivability and functional activity, a number of cultivation and environmental strategies have been explored, with a particular focus on nutrient composition, growth-phase conditioning, and stress response mechanisms.<sup>[81–83]</sup>

The composition of the optimal growth media, the implementation of stress preconditioning, and the process of environmental adaptation are of great importance in order to achieve the greatest possible resilience of the cells. It has been demonstrated that the use of controlled fermentation environments with specific pH and temperature settings can enhance bacterial survival during the processes of freeze-drying and gastrointestinal transit.<sup>[84–88]</sup> For instance, *L. rhamnosus* has been observed to exhibit heightened resilience to heat and oxidative stress when cultivated

with particular nitrogen sources, indicating that nutritional modifications can confer cross-protection against diverse environmental stressors.<sup>[89]</sup>

It has been demonstrated that distinct metabolic pathways are activated during different growth phases. Lactic acid bacteria, in particular, have been observed to demonstrate enhanced resilience to external influences during the stationary phase.<sup>[83,90]</sup> The application of growth-induced stressors, such as osmotic or pH stress, to bacteria prior to a process of conditioning enables the adaptation of specific metabolic pathways, thereby enhancing tolerance to drying processes. For example, exposure of *Lactobacillus* species to elevated salt concentrations induces alterations in cell wall composition, thereby conferring increased resistance to osmotic stress encountered during desiccation.<sup>[91–93]</sup> In particular, *Lactobacillus delbrueckii subsp. lactis* has been observed to demonstrate enhanced survival rates during freeze-drying and elevated autolytic activity following exposure to hyperosmolar conditions.<sup>[91]</sup> Furthermore, the manipulation of pH during cultivation has been observed to influence cell wall composition, thereby enhancing osmotic tolerance and resilience to environmental fluctuations.<sup>[84]</sup>

The use of encapsulation and other protective carrier matrices represents a valuable strategy for enhancing the stability and efficacy of *Lactobacillus* strains. The use of encapsulation techniques serves to protect probiotic cells from environmental stressors, such as fluctuations in pH and temperature during the processing and storage phases.<sup>[92]</sup>

In conclusion, the combination of optimised growth conditions, targeted stress adaptations and encapsulation strategies has been demonstrated to enhance the viability of *L. reuteri* and *L. rhamnosus*. It is of great importance to ensure that these probiotics retain their beneficial properties when incorporated into mucoadhesive polymer films.

## **1.5. Aim of the Work**

The objective of this thesis was to develop an innovative approach to the treatment of periodontitis by utilizing microencapsulated probiotics embedded within mucoadhesive oral films. Specifically, *L. reuteri* and *L. rhamnosus*, which have been demonstrated to exert beneficial effects on oral health, were microencapsulated using Eudragit® EPO and RL30D through a spray-drying process. The objective of this encapsulation was to safeguard the bacteria during storage and to facilitate a controlled release with enhanced mucoadhesion within the oral cavity.

Subsequently, the probiotic particles were incorporated into mucoadhesive polymer films, fabricated from hydroxypropyl methylcellulose (HPMC) and polyvinyl alcohol (PVA), following microencapsulation. The objective of the film development was to achieve optimal adhesion to the oral mucosal surfaces, thus enabling prolonged retention and targeted release of the probiotics at the site of action. The film design incorporated glycerol as a plasticizer, thus enhancing flexibility and ensuring ease of application under oral conditions. Additionally, the tensile strength and dissolution properties of the film were evaluated.

The main focus, in addition to the development of the film formulation, was the maintenance of bacterial activity throughout the microencapsulation and film formation processes. To optimize bacterial activity, particular cultivation techniques were employed, including stress preconditioning during growth and harvesting at an optimal growth phase. The objective of this study was to develop a localized, non-invasive and efficacious treatment for periodontitis, utilizing the benefits of probiotics within an innovative oral film delivery system. In vivo testing was conducted on two volunteers to evaluate the probiotic effect of the films within the oral cavity. This approach has the potential to become an advanced, targeted therapy for periodontal disease, supporting oral microbiome balance and health.

Figure 1.2 presents a flowchart outlining the methodology employed in the structuring of the work.

## General Introduction

---

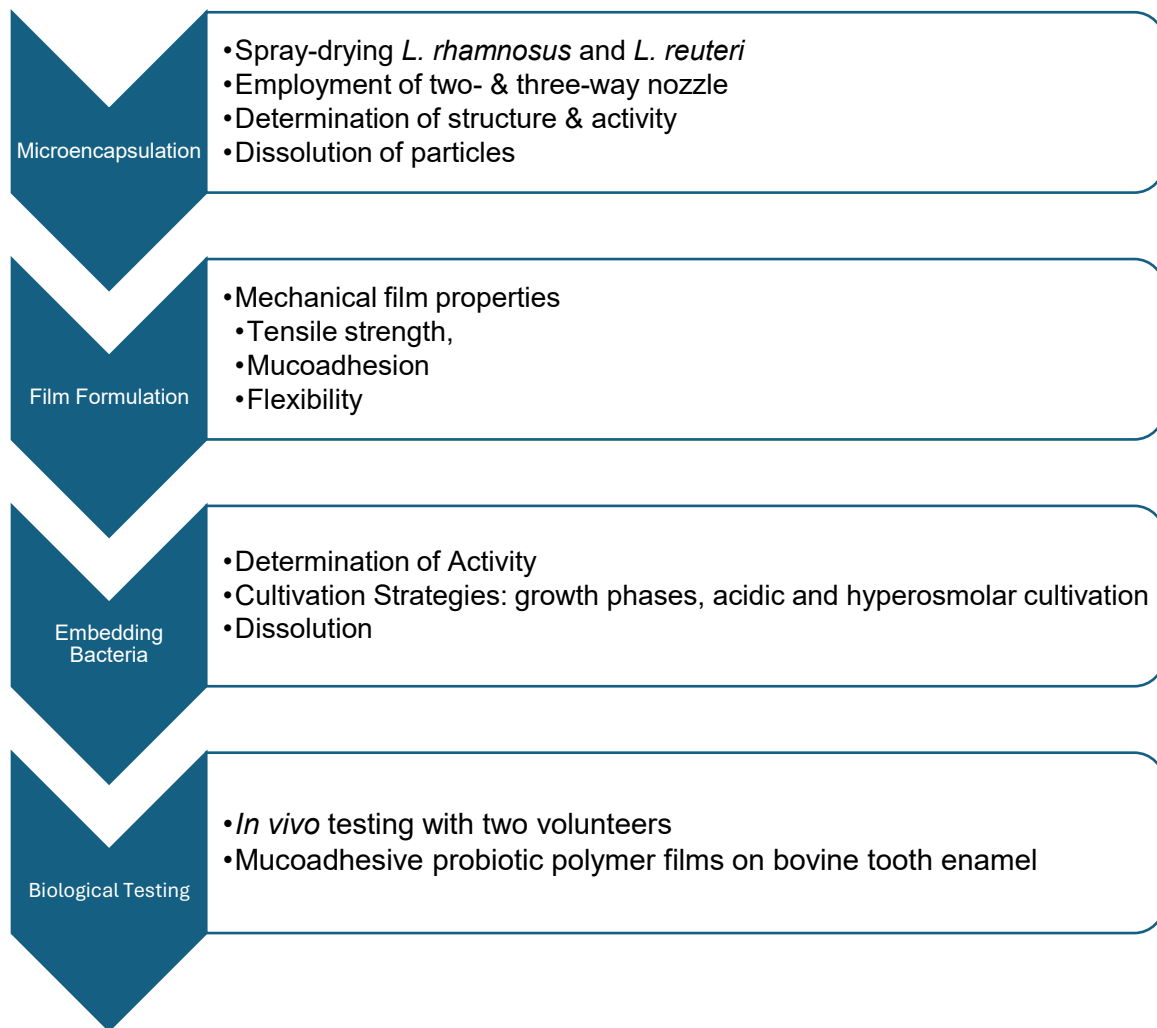


**Figure 1.2.** Flow chart of sequence of experiments. First microencapsulation of bacteria, second film formulation, third embedding of bacteria and fourth biological testing.

## 2. Materials and Methods

### 2.1. Materials

**Table 1: Bacteria and cultivation**

Substance	Comment	Supplier
<i>Lactobacillus reuteri</i>	1:5 (in Maltodextrin)	Lactopia, Saarbrücken, Germany
<i>Lactobacillus rhamnosus</i>	1:5 (in Maltodextrin)	Lactopia, Saarbrücken, Germany
MRS-Agar		Carl Roth GmbH, Karlsruhe, Germany
MRS-Boullion		Carl Roth GmbH, Karlsruhe, Germany

**Table 2: Polymers**

Substance	Comment	Supplier
Eudragit EPO	Butyl methacrylate	Evonik, Essen, Germany
Eudragit RL30D	Ammonio methacrylate copolymer type A	Evonik, Essen, Germany
Eudragit S	Poly(methyl methacrylate-co-methacrylic acid)	Evonik, Essen, Germany
HPMC	Hydroxypropyl methylcellulose Viscosity 15 mPa*s	Shin-Etsu Chemical, Chiyoda, Japan
PVA	Polyvinyl alcohol 18-88	Sigma Aldrich, Darmstadt, Germany

**Table 3: Acids, bases and solvents**

Substance	Comment	Supplier
Aceton	technical	Zentrale Chemikalienausgabe UdS, Saarbrücken, Germany
H <sub>2</sub> O	MilliQ water Grad-2	Merck Millipore, Billerica, USA
H <sub>2</sub> SO <sub>4</sub>	Sulfuric acid	Bernd Kraft, Duisburg, Germany
HCl	Hydrochloric acid	Analytichem, Oberhausen, Germany
Isopropyl alcohol	technical	Zentrale Chemikalienausgabe UdS, Saarbrücken, Germany
NaOH		Zentrale Chemikalienausgabe UdS, Saarbrücken, Germany



## Materials & Methods

**Table 4:** Other chemicals

Substance	Comment	Supplier
BODIPY		Sigma Aldrich, Darmstadt, Germany
Bovine tooth enamel		Slaughterhouse, Germany
CaCl <sub>2</sub>	Calcium chloride	Arcos organics, New Jersey, USA
EDTA	Ethylenediaminetetraacetic acid	Sigma Aldrich, Darmstadt, Germany
Gelatin Type A	Gel strength 300	Sigma Aldrich, Darmstadt, Germany
Glycerol	Propan-1,2,3-triol	Caelo, Hilden, Germany
Mucin	Mucin from porcine stomach Type II	Sigma Aldrich, Darmstadt, Germany
NaCl	Sodium chloride	Grüssing, Filsum, Germany
PEI	Polyethylenimine, branched	Sigma Aldrich, Darmstadt, Germany
Polyvinylsiloxane	Addition-type, Type 3, low consistency	Coltene Holding, Altstätten, Swiss
Sodium alginate		Sigma Aldrich, Darmstadt, Germany
SYTO 9		Thermo Fisher, Waltham, USA
Trypsin		Thermo Fisher, Waltham, USA

**Table 5:** Consumables

Consumables	Comment	Supplier
Cannulas	Sterican®	B. Braun, Melsungen, Germany
AFM Cantilevers for force measurement	High density carbon tip biosphere B1000-FM	Nanotools, Munich, Germany
Carbon discs		Plano, Wetzlar, Germany
Cuvette	UV-Transparent Cuvettes	Sarstedt AG & Co KG, Nümbrecht, Germany
Disposable syringes	Injekt® 1,2 & 5 mL	B. Braun, Melsungen, Germany

## Materials & Methods

<b>Consumables</b>	<b>Comment</b>	<b>Supplier</b>
Eppendorf reaction tubes	1.5 & 2 mL, Polypropylene microreaction vessel	Greiner Bio-One, Kremsmünster, Austria
Falcon tubes	15, 50 mL, Polypropylene	Greiner Bio-One, Kremsmünster, Austria
Glass vessels	Beakers, measuring cylinders, bottles, etc.	Brand/Schott, Wertheim/Mainz, Germany
Parafilm	Parafilm M®	Pechiney Plastic Packaging, Chicago, USA
Petri dishes	92 x 16mm sterile	Sarstedt AG & Co KG, Nümbrecht, Germany
Pin stubs		Plano, Wetzlar, Germany
Pipet tips	10, 200 & 1000 µL, autoclaved	Greiner Bio-One, Kremsmünster, Austria
Silica wafer		Plano, Wetzlar, Germany
Teflon foil		Amazon, Seattle, USA
Drigalski spatula		VWR International, Radnor, USA

**Table 6: Devices**

<b>Devices</b>	<b>Comment</b>	<b>Supplier</b>
3D Bioprinter		RegenHU Sa, Villaz- Saint-Pierre, Swiss
AFM	JPK NanoWizard III	Bruker, Berlin, Germany
Analytical balance	Quintix & CP225D	Sartorius, Göttingen, Germany
Autoclave	FGV G3	Fedegari, Albuzzano, Italy
Biophotometer	6131	Eppendorf, Hamburg Germany
Centrifuge	Heraeus Multifuge X1R	Thermo Fisher Scientific, Waltham, USA
	Rotina 420R	Andreas Hettich GmbH, Tuttlingen, Germany
CLSM	LSM710	Carl Zeiss AG, Oberkochen, Germany
Electromotive film casting device	Coatmaster 510	Erichsen, Hemmer, Germany
Freeze dryer	Alpha 3-4 LSCbasic	Martin Christ, Osterode am Harz, Germany
Freezer – 80 °C	Ultra Guard ULT	Binder GmbH, Tuttlingen, Germany
Heating cabinet (forced ventilation)	027101	Memmert, Schwabach, Germany

## Materials & Methods

<b>Devices</b>	<b>Comment</b>	<b>Supplier</b>
Incubator	BF 260	Binder GmbH, Tuttlingen, Germany
Laboratory balance	MC1	Sartorius, Göttingen, Germany
Laboratory shaker	MHR 13	Andreas Hettich GmbH, Tuttlingen, Germany
LAF bench	3F180-II GS	Integra Biosciences AG, Biebertal, Germany
Magnetic stirrer	Arec Connect	VELP Scientifica Srl, Usmate Velate, Italien
Mini Spray Dryer	B290	Büchi Labortechnik, Flawil, Swiss
Osmometer	Osmomat 010	Gonotec GmbH, Berlin, Germany
pH-Meter pH-Electrode	SevenCompact & Education Line	Mettler-Toledo, Gießen, Germany
Pipettes	Eppendorf Research, 10, 20, 200 & 1000 µL	Eppendorf, Hamburg, Germany
Rotary-pumped sputter coater	Q150R	Quorum Technologies Ltd., Lewes UK
SEM	EVO HD15 SEM	Carl Zeiss Microscopy GmbH, Jena, Germany
Squeegee	Multicator 411	Erichsen, Hemmer, Germany
Ultra fine balance	MC 5	Sartorius, Göttingen, Germany
Ultra Turrax	IKA Homogenisator	IKA-Werke, Staufen im Breisgau, Germany
Ultrapure water system	Millipore Q-Grad 2	Merck Millipore, Billerica, USA
Ultrasound bath	Elmasonic P	Elma Schmidbauer GmbH, Singen, Germany
Vortex	Genie 2	Scientific Industries Inc., Bohemia, USA
Water bath		Memmert, Schwabach, Germany

## **2.2. Frequently Used Methods**

### **2.2.1. Analytical Methods**

#### **2.2.1.1. Scanning Electron Microscopy (SEM)**

Scanning electron microscopy (SEM) is a technique allowing to visualize the surfaces of samples. In this case, it is important to visualize the microencapsulation, dissolution, and surface of polymer films. In order for this method to be effective, the surface in question must be conductive. If the surface is not naturally conductive, it can be rendered so by coating it with a conductive material, such as gold. The sample is then scanned with a focussed electron beam in a high vacuum, and a detector records the backscattered electrons.<sup>[94–97]</sup> This process provides the images with a distinct depth of focus.

A SEM, EVO HD15, Zeiss, Germany was used. The samples were attached to SEM holders via adhesive carbon plates and followed by 100 s gold sputtering using a Quorum Q150R ES sputter coater (Quorum Technologies Ltd., East Grinstead, UK), for better conductivity. The images were captured at an acceleration voltage of 5 kV and different magnifications.

#### **2.2.1.2 Atomic Force Microscopy (AFM) - Mucoadhesion**

Atomic force microscopy (AFM) is a high-resolution scanning probe microscopy technique that permits the imaging and characterization of surfaces at the nanometer scale. AFM operates based on the interactions between a tip mounted on a flexible cantilever and the surface of a sample. As the cantilever scans the surface, the interaction forces between the tip and the sample cause the cantilever to deflect, which is recorded in order to generate detailed topographical maps.<sup>[98,99]</sup>

The fundamental principle of AFM is the detection of forces, including van der Waals, electrostatic, or repulsive forces, which are dependent on the distance between the tip and the surface. There are also methods where the cantilever does not touch the surface. This requires the measurement to be made in a vacuum. The cantilever

deflection is typically quantified through the reflection of a laser beam off the reverse surface of the cantilever and onto a position-sensitive photodetector, thereby enabling the precise detection of nanometer-scale vertical displacements.<sup>[100,101]</sup>

In addition to its imaging capabilities, AFM can also be used to measure the interaction energy (adhesion forces) between the tip and the sample surface.<sup>[65,72,102]</sup>

AFM force measurements were conducted using a JPK NanoWizard III (Bruker, Berlin, Germany), equipped with a spherical-shaped cantilever with a diameter of 1  $\mu\text{m}$  (Biosphere B1000-FM). The cantilever was coated with mucins. The preparation process involved an initial immersion of the cantilever in concentrated sulfuric acid (95-97%) for cleaning purposes, followed by coating with a polyethyleneimine (PEI) solution in water (2%). Subsequently, a mucin suspension (8% w/w) was applied, enabling the mucins to adhere to the cantilever via electrostatic interactions with the PEI. The AFM experiment was conducted in three phases. In the initial phase, the cantilever approached under ambient conditions the sample at a speed of 2  $\mu\text{m/s}$  with a force of 5 nN. In the second phase, the cantilever remained in contact with the sample for 20 seconds under the same force, allowing interaction formation. In the final phase, the force-displacement curve was recorded as the cantilever retracted from the sample at 2  $\mu\text{m/s}$ . Measurement in air may cause inaccuracies in force-displacement measurements. These would be more accurate in an aqueous environment. However, the mucoadhesion measurement was performed in air to mimic the system as closely as possible involving an air interface.

The polymer films used for AFM measurement were carefully mounted on a glass slide using double-adhesive tape to ensure stability during the scanning process.

### **2.2.1.3 Tensile Tester**

A tensile tester is a mechanical device used to measure the tensile strength and other mechanical properties of materials by applying a controlled pulling force until the material ruptures. It consists of a fixed clamp and a movable clamp that holds the material sample in place. The machine applies a uniaxial force to the sample at a specified rate while recording the force and displacement. The data collected is used

to generate a force-displacement curve, which can be analyzed to determine parameters such as tensile strength, elongation, and Young's modulus. In this study, the tensile tester was used to assess both the mechanical strength of polymer films and their mucoadhesive properties.<sup>[103]</sup>

### **2.2.1.3.1 Tensile Strength Testing of Polymer Films**

The tensile strength of polymer films, both with and without bacterial incorporation, was evaluated using a Kappa20 tensile tester (ZwickRoell GmbH & Co. KG, Ulm, Germany) in accordance with the DIN EN ISO 527 standard.<sup>[104]</sup> Polymer films were cut into samples with dimensions of 10 × 15 mm. These samples were clamped into the tensile tester, ensuring that no preload was applied to the films prior to the test. The ends of the polymer film were each clamped and then pulled apart vertically. This is schematically shown in chapter 3.2.5.

The tensile tester applied a pulling force at a constant rate of 50 mm/min until the polymer films ruptured. The tensile strength of each film was calculated based on the measured film thickness, which was determined beforehand using an optical microscope. Each polymer formulation was tested five times to ensure reproducibility, and the results were recorded as force-displacement curves, enabling the calculation of the tensile strength of the films.

### **2.2.1.3.2 Mucoadhesion Testing**

Mucoadhesion was evaluated using a tensile tester to measure the interaction between the polymer films and mucins derived from porcine stomach tissue. This method provided a macroscale analysis of the adhesive properties of the films.<sup>[102,105]</sup>

For the mucoadhesion testing, polymer film samples were cut into 1 cm<sup>2</sup> sections and attached to microscope slides. The counterpart slide was prepared by cleaning a glass microscope slide with concentrated sulfuric acid (95 – 97%) followed by thorough washing with MilliQ water. The cleaned slide was then coated with a PEI solution (2% in water) to promote adhesion. After an additional wash with MilliQ water, a mucin

suspension (8% w/w in water) was applied to the slide. The mucins adhered to the glass via electrostatic interactions with the PEI layer.

Once the polymer film and mucin-coated slides were prepared, the two slides were pressed together using a tensile tester (Instron 8513, Instron GmbH, Darmstadt, Germany). A force of 5 N was applied for 5 minutes to ensure adequate contact between the polymer and the mucins. Following this, the slides were separated at a controlled rate of 0.020 mm/s over a distance of 2 mm. A force-displacement curve was recorded throughout the separation process, allowing for the evaluation of the tensile strength of the mucoadhesive interaction between the polymer film and the mucins.

By analyzing the force-displacement curve, the adhesion force and work of adhesion were calculated, providing insights into the strength of interaction between the polymer films and the mucins. This method enabled the quantification of mucoadhesive properties in a controlled, repeatable manner. Furthermore, this was compared to control measurements without mucins.

### **2.2.1.4 Plate Count Method**

#### **2.2.1.4.1 Sample Preparation and Dilution**

The bacterial activity was evaluated through the plate count method, conducted in a manner that ensured sterility. This entailed working in a sterile environment, beneath a sterile bench, and utilizing sterile substances and devices, with the objective of preventing contamination at all times. The bacterial sample was initially dissolved in isotonic saline solution (0.9% NaCl) at 37 °C and then thoroughly dispersed using a vortexer to create a uniform suspension. The suspension was subjected to serial dilutions using isotonic saline, with the dilution steps being either 1:100 or 1:10, depending on the anticipated concentration of bacteria. The serial dilution process was repeated until the expected bacterial activity fell within the quantifiable range of 20 to 200 colonies per plate.<sup>[106,107]</sup>

### **2.2.1.4.2 Plating and Incubation**

Once the appropriate dilutions had been prepared, 100  $\mu$ L of each diluted sample was evenly distributed across MRS agar plates using a sterile Drigalski spatula, in order to ensure uniform distribution of bacteria across the agar surface. The inoculated plates were incubated at 36 °C for 48 hours in an incubator set at 100% relative humidity and 5% CO<sub>2</sub> to allow for optimal growth conditions.<sup>[106]</sup> This specific incubation environment was selected to provide optimal conditions for the growth of *L. reuteri* and *L. rhamnosus*.

### **2.2.1.4.3 Colony Counting and Quantification**

Following the 48-hour incubation period, the number of bacterial colonies was manually counted. The colony-forming units per gram (CFU/g) of the original sample were calculated based on the number of colonies observed on plates. The CFU/g was determined by multiplying the number of colonies by the dilution factor and accounting for the volume of the sample plated. This quantification provided an estimate of the viable bacterial count in the original sample.

### **2.2.1.5 Confocal Laser Scanning Microscope (CLSM)**

Confocal Laser Scanning Microscopy (CLSM) is a powerful imaging technique that is widely employed in the biological, material, and medical sciences to obtain high-resolution, three-dimensional images of samples.<sup>[108,109]</sup> In this project, the technique was employed primarily for the visualization of stained bacteria, with an additional objective of detecting a core-shell structure. The fundamental principle underlying CLSM is the utilization of lasers for the precise excitation of fluorescent dyes (Syto 9 and BODIPY) within the sample. The optical sectioning allows for the visualization of fine details at various depths without the necessity for physical sectioning of the sample.<sup>[110]</sup>

CLSM was conducted using a LSM710 (Carl Zeiss AG, Oberkochen, Germany) with a 100x oil immersion objective. The microscope was operated using ZEN Blue software.



A laser source was employed to excite the sample at wavelengths that were specific to the fluorophores or dyes that were present in the sample. Further details can be found in the specific methods section. The laser beam was collected through a pinhole to ensure that only light from the focal plane was detected, thus providing high-resolution, optically sectioned images with reduced out-of-focus light. The emission signals were collected by the detector type. Different emissions were passed through appropriate emission filters to ensure the separation of different fluorescence channels.<sup>[108–110]</sup>

The preparation of the samples is described in brief in the specific methods sections. Subsequently, the images were processed and analyzed using ImageJ and Zen Blue software.

### **2.2.1.6 *In Vivo* Testing**

#### ***Preparation of Bovine Tooth Enamel***

The adhesion of bacteria was evaluated using bovine tooth enamel as a substrate. Prior to testing, the enamel was prepared by rehydration. This involved submerging the bovine teeth in demineralized water for a period of 24 hours. This process ensured that the enamel closely resembled its natural hydrated state, as would be found in the oral cavity.

Once rehydrated, the sample (comprising mucoadhesive polymer films with and without *L. rhamnosus* or *L. reuteri*) was applied to the enamel surface. The polymer film was attached to the tooth enamel by partially dissolving it in MilliQ water and then applying it to the enamel surface. The samples were then allowed to dry until the polymer film reached its initial stage.

#### ***Attachment to Dental Splints and In Vivo Testing***

The treated enamel samples were mounted onto dental splints using a two-component silicone adhesive (Polyvinylsiloxane), with the objective of ensuring attachment during the experiment. The dental splints, with the enamel attached, were then placed in the

oral cavities of two volunteers, where they were incubated for a period of eight hours, depending on the specific test being conducted. This *in vivo* exposure permitted the replication of bacterial adhesion under conditions approximating those of the natural oral environment. Pure, uncoated, rehydrated bovine tooth enamel was also incubated in the oral cavity as a reference but at the opposite side of the mouth (opposite cheek). This was assumed to be far enough away to have no crosstalk between the samples.

### ***Visualization and Quantification of Adhered Bacteria***

Following the incubation period, the enamel samples were removed from the oral cavity, washed in MilliQ water and prepared for visualization. The bacteria that had adhered to the enamel surface were stained with Syto 9, a nucleic acid stain that facilitated the detection of the bacteria. Subsequently, the stained samples were examined under CLSM in order to visualize the bacterial adhesion.

The differentiation of bacterial cells was based on their morphological characteristics, allowing for the identification of specific types of adhered bacteria. Given that the lactobacilli native to the oral cavity require a longer period than eight hours to adhere to tooth enamel,<sup>[111]</sup> it is possible to identify these bacteria with a high degree of reliability from the sample. This was verified via the incubated tooth enamel references. For the purposes of quantification, twelve randomly selected images were taken from each sample, and the number of bacteria present in each image was counted. This process permitted a robust estimation of the total bacterial adhesion to the enamel surfaces.

Following the conclusion of the experiment, the enamel samples were subjected to reactivation through treatment in an ultrasonic bath, initially in MilliQ water and subsequently in 30% ethanol. The samples were subsequently stored in 30% ethanol.

## **2.2.2 Preparative Methods**

In accordance with the principles of aseptic technique, all preparative methods were conducted within a sterile bench environment whenever feasible. All substances and equipment that were in contact with the bacteria were obtained in a sterile state or

underwent sterilization by autoclaving. If this was not possible, everything was disinfected with 70% isopropanol and worked as germ-free as possible.

### **2.2.1.1. Microencapsulation via Spray Drying**

Spray drying is a gentle and widely used technique for transforming liquid dispersions or solutions into dry powders. This makes it particularly useful for temperature-sensitive materials, such as probiotics, which would otherwise be adversely affected by the high temperatures typically required for other drying techniques. Furthermore, probiotics can be subjected to both drying and microencapsulation with polymers as part of the same process.<sup>[112–115]</sup> In this process, the liquid feed is atomized into fine droplets using either a two-way or three-way nozzle, thereby enabling the generation of different patterns of microencapsulation.

We used two types of nozzles for microencapsulation.

A two-way nozzle utilizes compressed air or nitrogen in conjunction with the liquid feed to generate the spray. This technique is frequently utilized when a uniform droplet size is of paramount importance, rendering it an optimal choice for straightforward formulations and controlled particle sizes. In the context of microencapsulation, it is assumed that the components will form a matrix structure, given that they are mixed together in a single dispersion.<sup>[42,115]</sup>

A three-way nozzle incorporates an additional liquid feed, which enables the formation of core-shell structures. This type of nozzle is particularly useful for more complex formulations or when a highly controlled drying process is required, such as in the case of microencapsulation. It is used to obtain a core shell structure.<sup>[38,45,116]</sup>

#### **Spraying Parameters**

A number of critical parameters exert a substantial influence on the spray drying process and the ultimate characteristics of the resulting product.<sup>[112–115]</sup>

Inlet temperature is defined as the temperature of the substance being introduced into the drying chamber. The temperature of the hot air introduced into the drying chamber is a crucial factor. This has an impact on the drying rate and the overall efficiency of the process.

The outlet temperature is defined as the temperature of the air as it exits the drying chamber. The temperature of the air as it exits the chamber is indicative of the maximum temperature to which the product is exposed. It is of paramount importance to maintain control over this temperature, particularly when working with heat-sensitive substances such as probiotics.

The feed rate is defined as the quantity of material introduced into the system per unit time. The rate at which the liquid solution is introduced into the atomizer has an impact on the droplet size and drying process. An increase in feed rate results in the formation of larger droplets due to an increase in the available material over a shorter period of time.<sup>[112]</sup>

Atomization pressure is defined as the pressure applied to atomize the liquid feed, which directly influences droplet size and distribution. By dispersing the feed into fine droplets, the total surface area of the liquid is greatly increased, allowing greater heat and mass transfer.<sup>[112]</sup>

The airflow rate is defined as the volume of air that passes through a given space in a given time. The velocity at which the air is conveyed through the drying chamber affects the residence time of the droplets and the efficiency of the drying process.<sup>[112]</sup>

The microencapsulation of probiotics via spray drying represents a crucial technique for enhancing the stability and viability of the microorganisms during storage and formulation. Furthermore, it can impact the release kinetics and adhesion of microencapsulated bacteria.<sup>[41,117]</sup>

The viability of the probiotics following the drying process represents a critical quality parameter, which is influenced by a number of factors including the inlet and outlet temperatures, the composition of the feed, shear forces and the drying rate.

Spray drying enables the production of probiotic powders that are stable, straightforward to handle, and suitable for incorporation into a diverse range of products or supplements while maintaining their efficacy.

### **2.2.1.2 Film Casting**

#### ***Electromotive Film Casting Device***

An electromotive film casting device represents a tool employed in the production of thin, uniform films characterized by high precision and reproducibility. In the context of polymer film production, this device plays a pivotal role in ensuring the regulated deposition of polymer solutions or dispersions onto a substrate, such as glass or metal, to create films with the desired thickness and properties.

The operational principle of the electromotive film casting device is as follows: a motor-driven mechanism is employed to move a casting squeegee across the surface of a substrate. The electromotive drive is defined as follows: The motorized system governs the movement of the squeegee, thereby providing highly controlled and repeatable casting conditions. This guarantees that the polymer film is applied in a uniform manner across the substrate (in this case Teflon foil), without the potential for manual inconsistencies. The regulation of casting parameters is essential for the attainment of optimal results. The device permits the modification of pivotal parameters, including casting velocity, solution volume, and film thickness, which exert a direct influence on the characteristics of the resulting polymer film. The control of these variables is crucial for the attainment of the desired mechanical properties, homogeneity, and surface smoothness in the final product.

In the field of pharmaceuticals, polymer films are frequently utilized for the purpose of drug-loaded films, where the precise control over the thickness of the film and the distribution of the drug is of paramount importance in order to guarantee the

consistency of the drug release profiles.<sup>[118,119]</sup> Furthermore, these devices are utilized in the production of mucoadhesive films for localized drug delivery, where the film's adhesion properties and uniformity are of paramount importance for optimal performance.<sup>[120,121]</sup>

### **2.2.1.3 Lyophilization**

Lyophilization, also referred to as freeze-drying, is a prevalent method for the dehydration of biological materials, pharmaceuticals, and food products. It is a very gentle drying method. The technique entails freezing the material and then reducing the surrounding pressure, thereby enabling the frozen water within the material to sublime directly from the solid phase to the gas phase.<sup>[122,123]</sup> This process is highly effective at preserving the structural integrity, bioactivity, and viability of sensitive compounds, rendering it an optimal method for the preservation of temperature-sensitive materials such as proteins, probiotics, and vaccines.

Lyophilization offers a number of advantages over conventional drying methods. The process occurs at low temperatures, which minimizes the risk of thermal degradation and thus preserves the functional properties of delicate compounds.<sup>[124,125]</sup>

For bacteria, particularly probiotics, lyophilization represents a crucial preservation method, offering long-term stability and maintaining cell viability during storage. Probiotic bacteria are highly susceptible to environmental stressors, which can impair their efficacy. Lyophilization provides a means of markedly reducing the water content of probiotic cultures, thereby safeguarding them from metabolic activity and degradation over time. The low-temperature nature of the lyophilization process minimizes damage to the cell membrane and other vital cellular components, thereby preserving the functionality and viability of the probiotic bacteria.<sup>[124,126]</sup>

Lyophilization ensures that probiotic bacteria maintain their stability, viability and potency during storage and shelf life, thereby making it a preferred method for the delivery of live, functional probiotics to consumers.

### **2.2.1.4. 3D Bioprinting**

3D bioprinting is an advanced technology that enables the precise fabrication of biological structures by layering bioinks composed of living cells, biomaterials, and growth factors.<sup>[127]</sup> This method has significant applications in tissue engineering, regenerative medicine, and drug delivery. In recent years, 3D bioprinting has gained attention for the encapsulation and delivery of probiotic bacteria within biocompatible matrices, offering a novel approach for ensuring the viability and targeted release of probiotics.<sup>[128,129]</sup>

We used a mixture of alginate and gelatin as bioink for 3D bioprinting. The formulation of the Bioink was described in Aliyazdi et al.<sup>[127]</sup> Alginate, a natural polysaccharide, forms hydrogels upon crosslinking with calcium ions, providing a supportive matrix that protects the bacteria while allowing for nutrient exchange and cell viability. Gelatin, a denatured form of collagen, enhances the mechanical properties of the bioink and improves the printability and structural integrity of the bioprinted constructs. Together, these materials create a stable, biocompatible environment for the encapsulated probiotic bacteria.

In this process, a pressure-based nozzle is used to extrude the bioink containing probiotics. The pressure nozzle system allows for precise control over the deposition of the bioink, ensuring uniform encapsulation of the bacteria within the alginate-gelatin matrix.<sup>[127]</sup> This method also permits the creation of intricate structures, enabling the design of customizable probiotic delivery systems that could improve the survivability of probiotics during gastrointestinal transit or controlled release in various environments.

By usage of 3D bioprinting, probiotic bacteria can be incorporated into advanced delivery vehicles that maintain bacterial viability, enhance stability, and enable site-specific release, thereby expanding the potential applications of probiotics in health and disease management.<sup>[128,130]</sup>

### **3. Formulation Probiotic Mucoadhesive Polymer Films**

Parts of this chapter have been previously prepared for publication. The corresponding sections are indicated with footnote 1.

## **Probiotic-Embedded Polymer Films for Oral Health: Development, Characterization, and Therapeutic Potential**

Charlotte Eckermann<sup>1</sup>, Florian Schäfer<sup>2</sup>, Marc Thiel<sup>3</sup>, Agnes-Valencia Weiss<sup>1</sup>, Christian Motz<sup>2</sup>, Karen Lienkamp<sup>3</sup>, Matthias Hannig<sup>4</sup>, Marc Schneider<sup>1\*</sup>

<sup>1</sup>Department of Pharmacy, Biopharmaceutics and Pharmaceutical Technology, PharmaScienceHub, Saarland University, 66123 Saarbrücken, Germany

<sup>2</sup>Chair of Materials Science and Methods, Department of Materials and Engineering, Science, Saarland University, 66123 Saarbrücken, Germany

<sup>3</sup>Chair of Polymer Materials, Department of Materials Science and Engineering, Saarland University, 66123 Saarbrücken, Germany

<sup>4</sup>Clinic of Operative Dentistry, Periodontology and Preventive Dentistry, Saarland University, 66421 Homburg, Germany



### 3.1. Introduction

At the outset of the project, a series of film formulations were developed and subjected to a series of evaluations to determine their characteristics. The formulations were assessed in terms of their visual appearance, thickness, mucoadhesion, flexibility, tensile strength and dissolution properties. The optimal film formulation was then selected. Additionally, several films were tested with varying loads of *L. reuteri* and *L. rhamnosus*, which demonstrated alterations in their properties with the load. There is also a brief overview of the methodology employed for the determination of activity and the loading of the bacteria, but this is comprehensively described in Chapter 4.

Mucoadhesive polymer films represent an approach to drug delivery, characterized by their ability to adhere to mucosal surfaces, such as the oral cavity. This property enables the localized or systemic release of drugs, offering a promising avenue for the development of targeted and effective therapeutic solutions. The development of these films requires the selection of suitable polymers, including natural (e.g., chitosan, alginate) and synthetic (e.g., PVA, HPMC) options, which offer both film-forming and mucoadhesive properties.<sup>[119,131]</sup>

It is of great importance to characterize mucoadhesive films in order to guarantee their efficacy and stability. The evaluation of mucoadhesive films entails the measurement of several key parameters, including mucoadhesive strength, which gauges the extent to which the film adheres to mucosal tissue, and mechanical properties, such as tensile strength and flexibility, which ensure the durability and patient comfort of the film. Furthermore, dissolution profiles are evaluated to ascertain the drug release profile, in this case, of the *L. rhamnosus* or *L. reuteri*.<sup>[71,120,121,132]</sup>

Mucoadhesion is a phenomenon whereby a material adheres to a mucous membrane, conferring a strategic advantage for probiotic delivery. This prolongs the retention time, thereby allowing the bacteria to colonize the oral mucosa.<sup>[133,134]</sup> Theories attempting to explain the phenomenon of mucoadhesion posit a number of different mechanisms, including:

**Wetting Theory:** This theory focuses on the adhesive polymer's ability to spread across and penetrate surface irregularities on the mucosal membrane.<sup>[135,136]</sup>

**Electronic Theory:** It posits that differences in electronic structures between mucin and polymer result in electron transfer, leading to attraction and adhesion.<sup>[134]</sup>

**Diffusion Theory:** This describes the interpenetration of polymer chains with mucin molecules to form a stable bond.<sup>[73,134]</sup>

**Fracture Theory:** It involves the force required to separate two surfaces after adhesion, suggesting that greater forces signify stronger mucoadhesion.<sup>[136]</sup>

Mucoadhesive polymers, which are central to this technology, are typically hydrophilic, thereby enabling them to interact effectively with mucus layers.<sup>[72,73]</sup> The advantages of mucoadhesive drug delivery systems include the prolonged retention of drugs at target sites, an enhanced bioavailability, the avoidance of first-pass metabolism, and a reduction in the required dosing frequency. These properties render mucoadhesive drug systems a valuable tool in the context of localized treatments, including oral, nasal, ocular and gastrointestinal drug delivery.<sup>[133]</sup>

In this instance, probiotic mucoadhesive polymer films were produced using HPMC and PVA, with glycerol serving as a plasticizer.

Hydroxypropyl methylcellulose (HPMC) is a highly versatile polymer that is widely employed in the development of pharmaceutical formulations, particularly in the creation of mucoadhesive oral films. HPMC is known for its non-toxic, hydrophilic, and biodegradable nature, which affords it desirable properties for mucoadhesion, defined as the adherence of materials to mucous membranes (Figure 3.1 A).<sup>[137–139]</sup> In mucoadhesive films, HPMC facilitates enhanced drug delivery by adhering to the mucosal surfaces of the oral cavity, which increases the retention time of the drug at the site of adsorption and allows for controlled drug release. The mucoadhesive strength of HPMC is attributed to its hydrophilic structure and the capacity to form hydrogen bonds with mucin, a glycoprotein present in mucus covering the respective

tissue surfaces. Furthermore, a range of HPMC grades with varying viscosities and molecular weights is available, allowing for the customization of film properties, such as swelling and adhesiveness, to optimize drug delivery.<sup>[137,139]</sup>

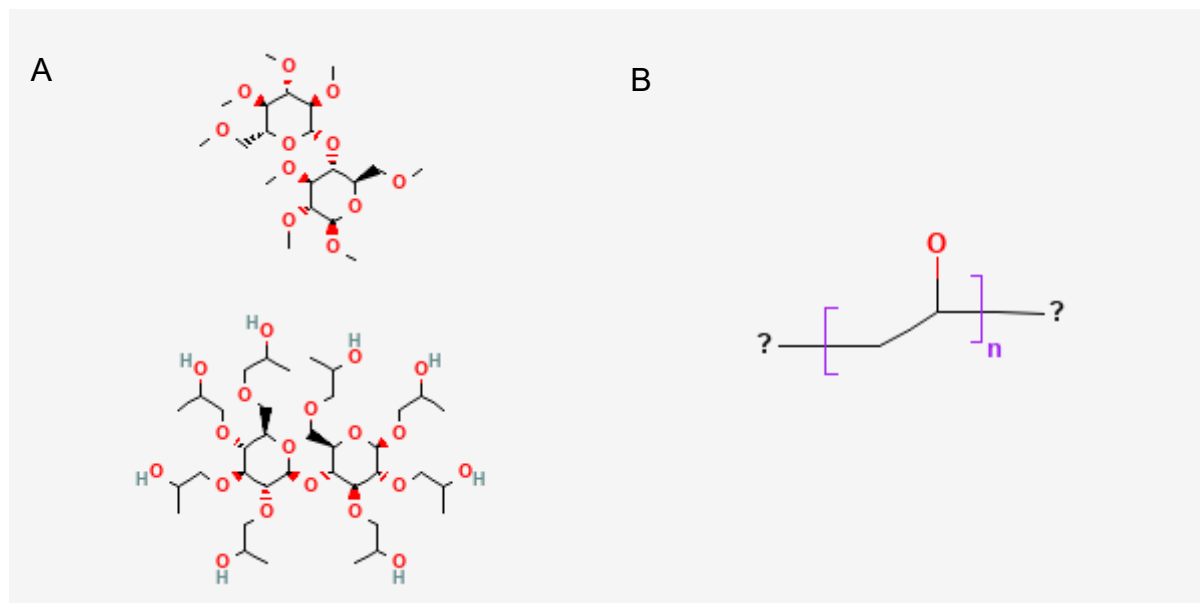


**Figure 3.1.** Chemical structure of HPMC (A) and PVA (B)

Polyvinyl alcohol (PVA) is a hydrophilic, biocompatible polymer that is widely employed in the development of mucoadhesive drug delivery systems, including oral films.<sup>[63,119,121]</sup> (Figure 3.1 B) PVA is renowned for its favorable mechanical strength, flexibility and transparency, and is frequently incorporated into mucoadhesive films with the objective of enhancing drug retention on mucosal surfaces. PVA exhibits mucoadhesive properties due to its capacity to form hydrogen bonds with mucin present in the mucus layer, thereby promoting prolonged contact with mucosal tissues.<sup>[140,141]</sup> In oral film applications, PVA is frequently combined with other polymers to enhance adhesion, film-forming capabilities, and drug release profiles. These films offer benefits such as increased patient compliance, ease of administration, and controlled drug release at the site of absorption.<sup>[142,143]</sup> Additionally, PVA displays self-emulsifying properties.<sup>[144]</sup>

## 3.2. Methods

### 3.2.1. Cultivation<sup>1</sup>

*L. rhamnosus* and *L. reuteri* were cultured in MRS broth. A single colony from a pregrown MRS-agar plate was selected and inoculated into 30 mL of MRS broth for preculture, followed by overnight incubation at 36 °C under 5% CO<sub>2</sub>. For the main culture, 1 mL of the preculture was transferred into 250 mL of MRS broth and incubated for 14 h (*L. rhamnosus*) and 16 h (*L. reuteri*) till the stationary phase. The bacterial cells were then harvested by centrifugation at 5000 × g for 5 min. (Figure 3.2)

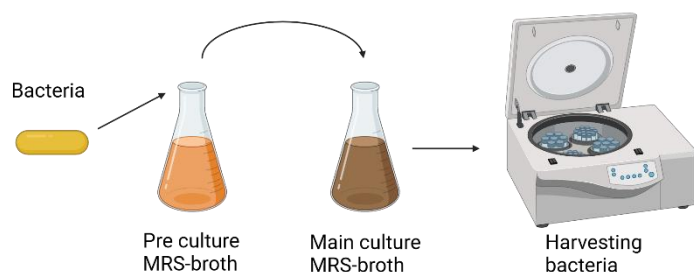


**Figure 3.2.** Schematic drawing of the cultivation of *L. rhamnosus* and *L. reuteri* in MRS broth.

### 3.2.2. Determination of Activity<sup>1</sup>

The viability of *L. rhamnosus* and *L. reuteri* was determined using the plate count method. Samples containing the bacterial cultures were incubated in a 0.9% NaCl solution at 37 °C for 45 min to dissolve the polymeric matrix or encapsulating shell. The resulting suspensions were serially diluted in 0.9% NaCl and subsequently spread on MRS agar plates. After incubation at 36 °C under 5% CO<sub>2</sub> for 48 h, colony counts were performed in triplicate (Figure 3.3). The data were expressed in logarithmic form, and the mean values with corresponding standard deviations were calculated.

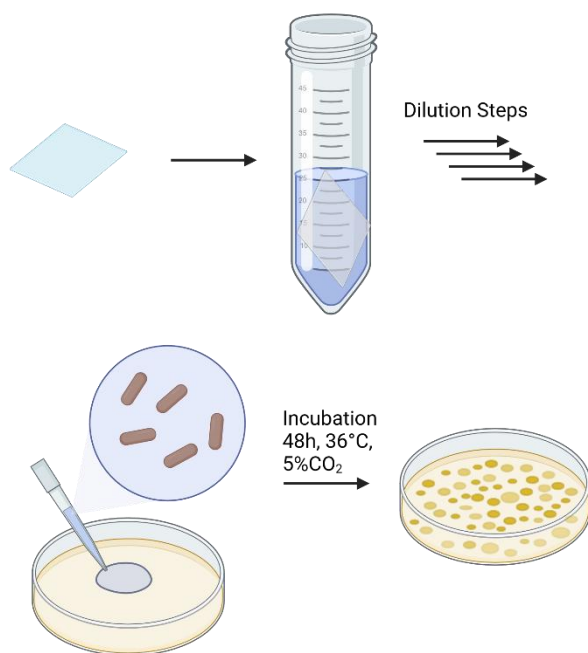


**Figure 3.3.** Assessment of *L. rhamnosus* and *L. reuteri* survival by plate count method on MRS Agar.

### 3.2.3. Microencapsulation<sup>1</sup>

Bacterial microencapsulation was achieved through spray drying, employing polymethacrylate derivatives. Specifically, a 1:1 mixture of Eudragit EPO and Eudragit RL30D, at a total polymer concentration of 10%, was used. The spray drying process was conducted using a laboratory-scale Mini spray dryer (Buchi B290, Flawil, Switzerland) under two different configurations. To reduce thermal stress on the bacteria, a three-way nozzle configuration was also used.<sup>[59]</sup> Consequently, the bacteria are shielded by the polymer dispersion that envelops them. The polymer solutions, consisting of Eudragit EPO and RL30D dispersed in water, were fed through the outer nozzle, while the purified bacterial suspension was introduced via the inner nozzle. To further mitigate thermal impact, the spray drying process was optimized with an inlet temperature of 55 °C and an outlet temperature of 42 °C, operating at a system pressure of 1.5 bar. The flow rate was maintained at 1 mL/min, with the rotameter set to 60 mm, and the aspirator running at full capacity.

### 3.2.4. Film Casting

#### 3.2.4.1. Handcast Polymer Films

Initially, polymer films were prepared using hydroxypropyl methylcellulose (HPMC) and polyvinyl alcohol (PVA). A polymer solution containing 3% total polymer (in a 1:1 ratio) was mixed with 20% (w/w) glycerol, based on the total polymer mass, to act as a plasticizer. Five milliliters of this polymer dispersion were poured into a polystyrene Petri dish with a diameter of 10 cm and a surface area of 78.54 cm<sup>2</sup> and left to dry for 12 h. (Figure 3.4) After drying, the film was carefully removed from the Petri dish using tweezers.

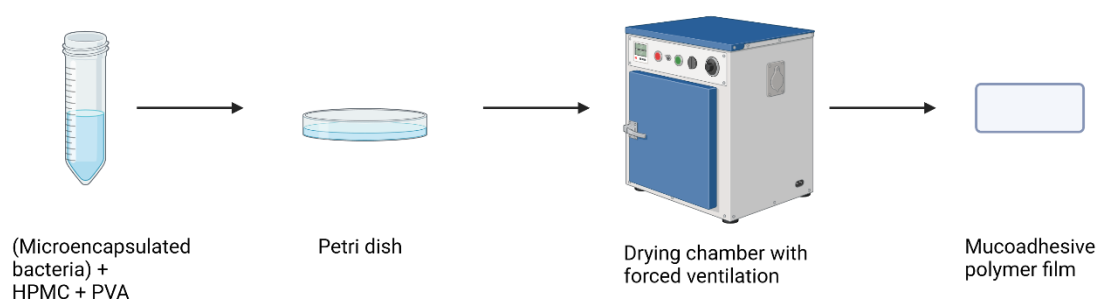


**Figure 3.4.** Workflow mucoadhesive polymer film production via hand casting.

#### 3.2.4.2. Electromotive Film Casting Device<sup>1</sup>

Polymer films were fabricated using an electromotive film casting system (Coatmaster 510, Erichsen, Hemer, Germany). Aqueous solutions of 1.5% HPMC and 1.5% PVA (18-88) were prepared, with glycerol added as a plasticizer at 20% of the total polymer weight. The solutions were sterilized by autoclaving. (Microencapsulated) bacteria, obtained from liquid cultures, were incorporated into the polymer mixture by gentle stirring. The resulting blend was uniformly spread onto Teflon foils using a squeegee (Erichsen, Hemer, Germany) with a slit width of 1000 µm and speed of 5 cm per min. The films were subsequently dried in a ventilated drying chamber at 37 °C for approximately 1.5 h (Figure 3.5).

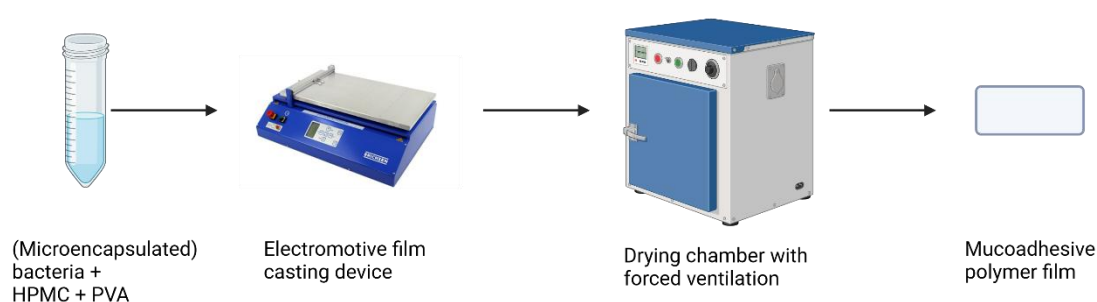


**Figure 3.5.** Mucoadhesive film casting workflow via electromotive film casting device.

### **3.2.4.3. Freeze-dried polymer films**

One method for drying the films in a manner that minimizes stress on the lactic acid bacteria is freeze-drying. For this process, films composed of 10% HPMC with glycerol and 10% PVA with glycerol were produced. The films were drawn using the film puller as previously described, frozen at -80 °C, and then placed in a Christ freeze dryer until fully dried. The (microencapsulated) bacteria were incorporated into the polymer dispersion and embedded within the films.

### **3.2.4.4. Foamed PVA-Films<sup>1</sup>**

To develop an additional film formulation with a higher loading capacity, foamed PVA films were produced. For this, PVA (18-88) with 20% (w/w) glycerol, relative to the polymer weight, was cooled to 4 °C and foamed using a homogenizer for 5 minutes, with continuous cooling of the sample. The foamed PVA solution was then spread with the help of the electromotive film casting device and dried as previously described.

## Film Formulation

This method resulted in films with a large surface area and increased loading capacity due to the porous structure.

For the loading process of the foamed films, the pores were filled with microencapsulated bacteria by mechanical mixing. The films were placed in a sample container together with the microencapsulated bacteria and subjected to vortex mixing for one minute at maximum speed (Figure 3.6). The loading capacity of the films was determined gravimetrically

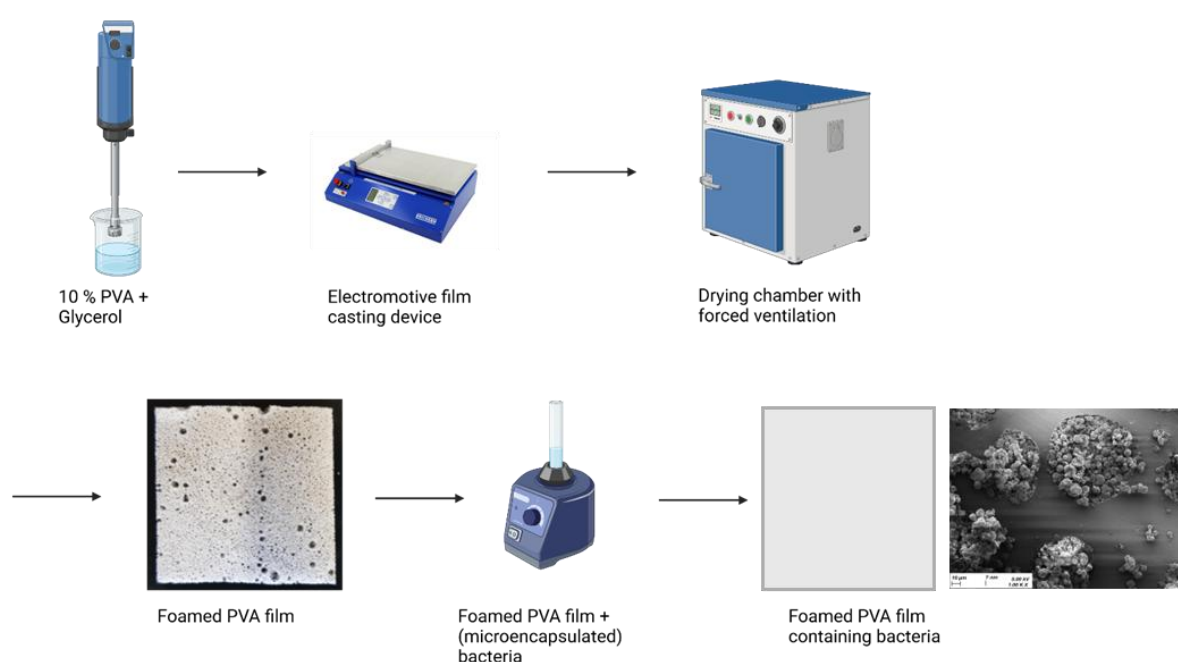


**Figure 3.6.** Schematic representation of the production of foamed PVA-films

### 3.2.5. Film Properties

#### 3.2.5.1. Determination of the film thickness

The thickness of the previously prepared polymer films was measured using SEM. The films were cut with a scalpel and mounted vertically on an SEM holder using a carbon disc. To improve conductivity, a 100-second gold sputtering process was carried out using a Quorum Q150R ES sputter coater (Quorum Technologies Ltd., East Grinstead, UK). Images were captured at an accelerating voltage of 5 kV and a magnification of



5,000x. The film thickness was determined from the cross-sectional images of the cut surfaces.

### 3.2.5.2. *Mucoadhesion (Mucoadhesive polymer films)<sup>1</sup>*

Mucoadhesion was evaluated using two complementary methods, both assessing the interaction between polymer films and mucins derived from porcine stomach tissue at ambient conditions. The first method analyzed interactions over a larger surface area using a tensile test set-up, while the second method focused on smaller surface interactions measured by AFM.

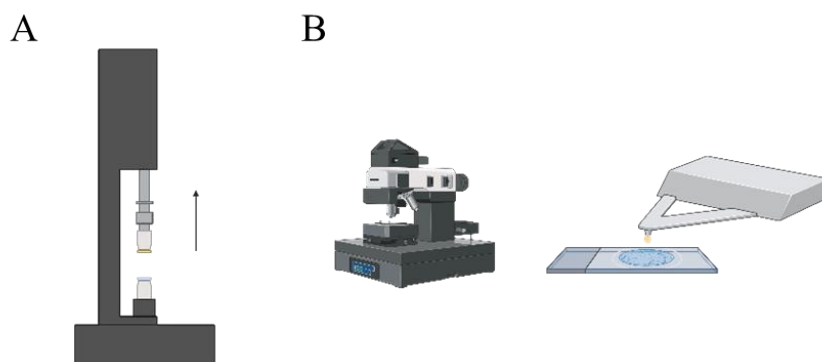


**Figure 3.7. A:** Schematic representation of the tensile tester for testing of mucoadhesive properties. **B:** Mucoadhesion testing via AFM measurements.

#### *Macroscale Analysis (Figure 3.7 A):*

For the tensile testing, film samples were cut into 1 cm<sup>2</sup> sections and attached to a microscope slide. A counterpart slide coated with mucins was prepared by initially immersing the glass in concentrated sulfuric acid (95–97%) for cleaning, followed by coating with a polyethyleneimine (PEI) solution in water (2%). After every step, the slide was washed in MilliQ water. A mucin suspension (8% w/w) was then applied, allowing the mucins to adhere to the slide via electrostatic interactions with the PEI. A force-displacement curve was recorded using a tensile test set-up (Instron 8513, Instron GmbH, Darmstadt, Germany). The slides were pressed together with a force

of 5 N for 5 minutes and subsequently separated at a speed of 0.020 mm/s over a distance of 2 mm.

### *Microscale Analysis (Figure 3.7 B):*

For interactions on a smaller surface area, an atomic force microscope (JPK NanoWizard III, Bruker, Berlin, Germany) was used. The AFM cantilever (Biosphere B1000-FM) was coated with mucins in a manner similar to the microscope slides, with the tip having a spherical shape and a diameter of 1  $\mu\text{m}$ . The AFM experiment consisted of three phases: in the first phase, the cantilever approached the sample at a speed of 2  $\mu\text{m/s}$  with a force of 5 nN. In the second phase, the cantilever remained in contact with the sample for 20 seconds under the same force, allowing interaction formation. In the final phase, the force-distance curve was recorded as the cantilever was retracted from the sample at 2  $\mu\text{m/s}$ . The adhesion was then evaluated using the area over the retraction curve to the zero level of the cantilever using JPKSPM Data Processing software.

#### **3.2.5.3. Folding endurance<sup>1</sup>**

The flexibility of the polymer films, both with and without bacterial incorporation, was assessed by measuring folding endurance. The films were repeatedly folded at a 360° angle for 300 cycles. Flexibility suitable for oral application was considered sufficient if the films did not rupture during the test.

#### **3.2.5.4. Tensile strength<sup>1</sup>**

The tensile strength of the films, both with and without bacterial incorporation, was evaluated using a tensile tester (Kappa20, ZwickRoell GmbH & Co. KG, Ulm, Germany) in accordance with DIN EN ISO 527<sup>[104]</sup> standards (Figure 3.8). Film samples were cut into dimensions of 10 × 15 mm and clamped into the tensile tester. The films were subjected to a pulling force at a rate of 50 mm/min until rupture, with no preload applied.

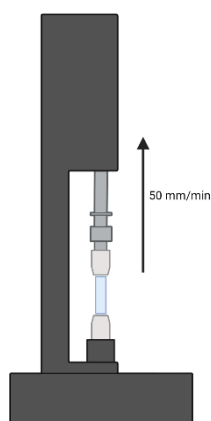


**Figure 3.8.** Schematic representation of a tensile tester used for measurement of tensile strength of the polymer films.

Tensile strength was calculated based on the film thickness, which was measured beforehand using an optical microscope. Each formulation was tested five times to ensure reproducibility.

$$\text{Tensile Strength} = \frac{\text{Force at failure}}{\text{Cross sectional area of film}} \times \frac{100}{\text{Film thickness}} \times \text{film width} \quad \text{Equation 1}$$

### 3.2.5.5. Dissolution Testing<sup>1</sup>

The dissolution behavior of the films, with bacterial loading, was assessed. A 1.5% agarose gel patch was prepared, and the film samples were placed on a polycarbonate membrane with a pore size of 50 nm, followed by incubation on the agarose patch at 36 °C under 100% relative humidity. Samples were collected at 0, 30, 60 and 120 min. The samples were analyzed using SEM (EVO HD15, Zeiss, Oberkochen, Germany). For SEM preparation, the samples were mounted on an SEM holder with a carbon adhesive disc, followed by a 100-second gold sputtering process using a Quorum Q150R ES sputter coater (Quorum Technologies Ltd., East Grinstead, UK) to improve conductivity. Images were captured at an acceleration voltage of 5 kV and a magnification of 5,000x. Three tests were conducted per formulation.

The dissolution of the final film formulations of the HPMC and PVA films, produced using the film applicator, was also tested in the oral cavity of a test subject. The films

were first attached to previously rehydrated bovine enamel, and these enamel samples were then fixed to a dental splint using two-component silicone. The samples were incubated in the mouth for 10, 20 and 30 minutes, after which they were analyzed using SEM under low vacuum conditions.

### **3.3. Results & Discussion**

#### **3.3.1. Activity<sup>1</sup>**

A more detailed description and discussion of microencapsulation and the embedding of bacteria in polymer films of varying formulations can be found in Chapter 2.

The activity of *L. rhamnosus* and *L. reuteri* was assessed by determining colony-forming units (CFU). Activity measurements were taken immediately after cultivation to the stationary phase, after microencapsulation by spray drying, and within the polymer film.

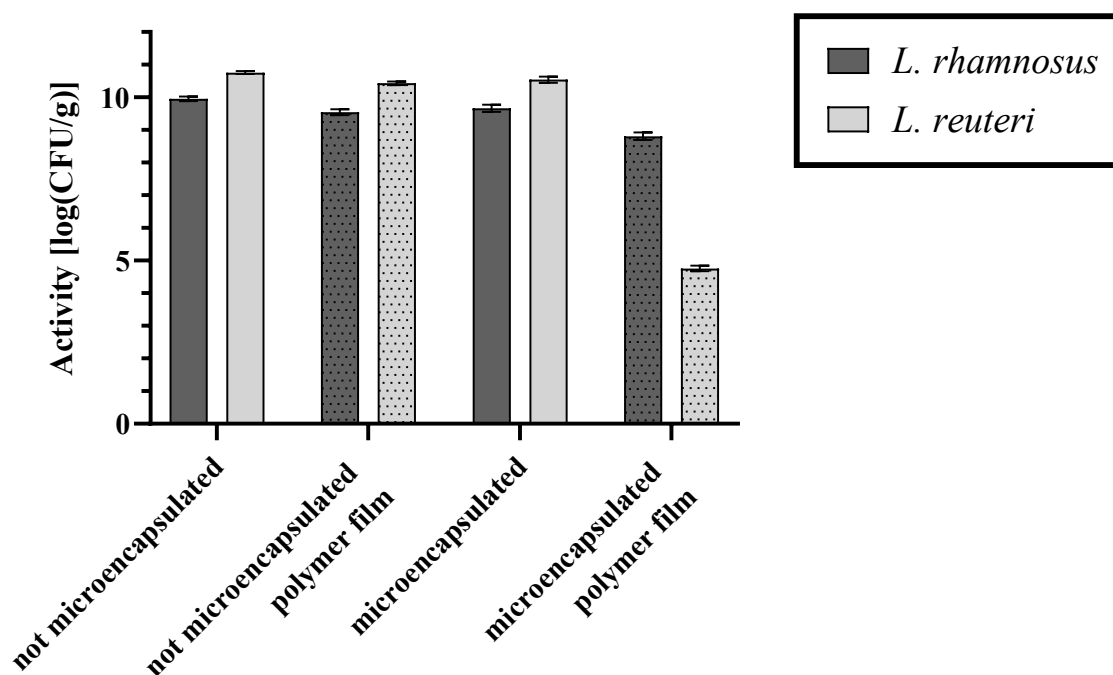


**Figure 3.9.** Survival of *L. rhamnosus* and *L. reuteri* before and after microencapsulation and embedding in polymer films, following prior cultivation in MRS broth till stationary phase for 14 h respective 16 h. n=3 with standard deviation.

As illustrated in Figure 3.9, high survival rates were observed for both *L. rhamnosus* and *L. reuteri* before and after microencapsulation, with minimal loss due to spray drying. For *L. rhamnosus*, CFU counts were 9.96 log(CFU/g) both before and after microencapsulation, while *L. reuteri* showed values of 10.76 log(CFU/g) prior to microencapsulation and 10.54 log(CFU/g) post-encapsulation. Spray drying proved to be a gentle drying method, as the thermal stress on the dried particles is expected to be highest on the surface and decreases towards the interior. Utilizing a three-way nozzle minimized the temperature load on the bacteria, with the polymers being exposed to the highest thermal stress while the bacterial cells experienced lower levels. This phenomenon can be attributed to the configuration of the particles, wherein the polymers are positioned externally, and the bacteria are located internally. The rapid drying characteristic of spray drying further reduced stress on the bacteria.

Two different polymer films were produced. In the first approach, the bacteria were incorporated into the polymer films immediately after cultivation, resulting in minimal activity loss. *L. rhamnosus* retained an activity of 9.54 log(CFU/g), while *L. reuteri*

maintained 10.43 log(CFU/g). However, when combining both steps—microencapsulation and incorporation into a polymer film consisting of HPMC and PVA—a significant reduction in bacterial activity was observed. *L. reuteri* showed a pronounced decrease in activity to 4.76 log(CFU/g), while *L. rhamnosus* showed a decrease to 8.81 log(CFU/g). In the calculations for the activity, the polymer mass was considered and mathematically excluded. This suggests that, while spray drying is a mild process, it may cause preliminary damage to the bacteria, which becomes more apparent in the form of reduced activity following incorporation into the polymer film.

The high survival rates of *L. rhamnosus* and *L. reuteri* after microencapsulation and within the polymer films highlight the effectiveness of the spray-drying process used in this study. Minimal CFU loss indicates that spray drying, especially with a three-way nozzle, is a mild drying method, exposing bacteria to low thermal stress. This supports the hypothesis that rapid drying reduces bacterial exposure to detrimental conditions, particularly those near the surface of the particles.<sup>[117]</sup>

However, while both bacteria retained their viability after microencapsulation, a notable reduction in colony-forming unit (CFU) counts was observed when the encapsulated bacteria were embedded into the polymer films. The decline in activity for *L. reuteri* (to 4.76 log(CFU/g)) and *L. rhamnosus* (to 8.81 log(CFU/g)) indicates that the microencapsulation process, though initially mild, may still inflict some damage that becomes more apparent when further incorporated into the films. Furthermore, the extended drying period may exert additional stress on the bacteria.<sup>[117,145–147]</sup>

### 3.3.2. Film Casting<sup>1</sup>

In order to facilitate the oral cavity applications, polymer films were fabricated and thereafter embedded with bacteria. A variety of methods for the production of polymer films were evaluated, commencing with two techniques: hand casting and the utilization of an electromotive film casting device. The thicker hand-cast films necessitated a drying period of 12 h, whereas the thinner films produced by the film casting device exhibited a shorter drying time of only 1 h. The prolonged drying time of the hand-cast films resulted in a notable loss of activity (3.2.2.), prompting the decision

to proceed with the thinner films produced by the film casting device. Two types of homogeneous films were produced using an electromotive film casting device. Figure 3.10 A depicts a transparent polymer film composed of HPMC and PVA, with glycerol (20% of the total polymer weight) incorporated to ensure adequate flexibility. The thickness of the film was determined to be 25  $\mu\text{m}$  using an optical microscope.

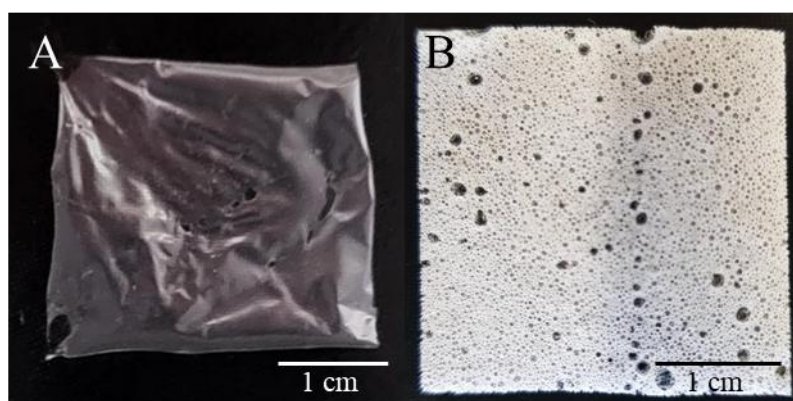


**Figure 3.10.** **A** Polymer film made of HPMC + PVA using the electromotive film casting device. **B** Polymer film made from foamed PVA using the electromotive film casting device.

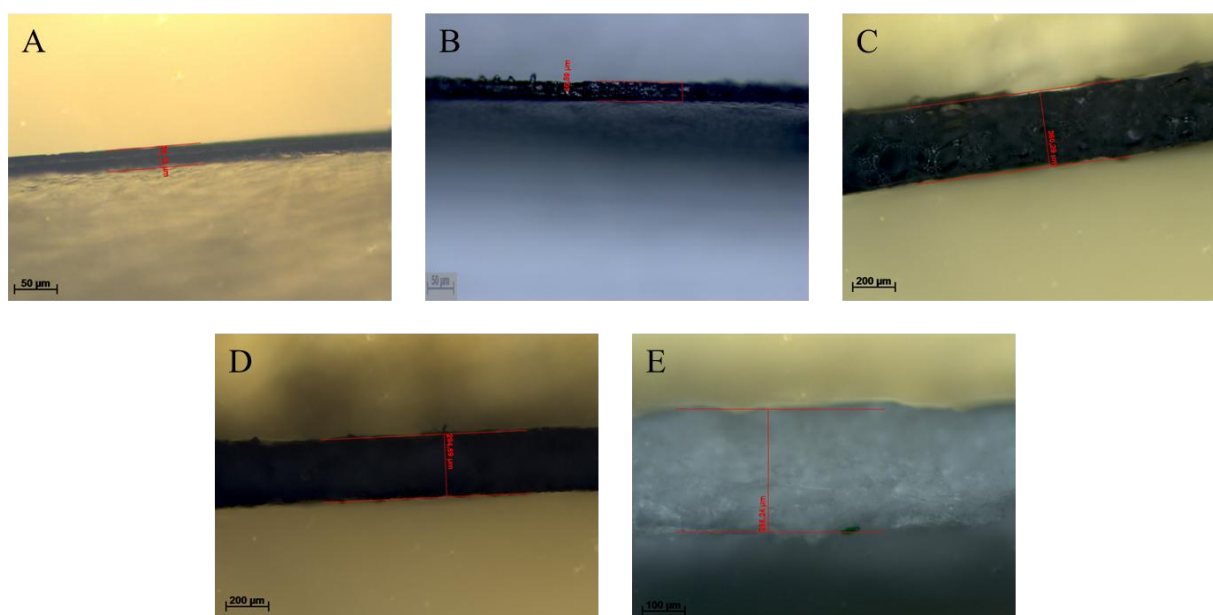
Figure 3.10 B depicts a foamed PVA film. This white polymer film displays a uniform distribution of pores, with a measured thickness of 360  $\mu\text{m}$  by optical microscopy.

The two distinct types of films produced—transparent HPMC-PVA and foamed PVA—differ significantly in structure and function. The HPMC-PVA film, with a thickness of 25  $\mu\text{m}$ , is thin and flexible, as demonstrated by the folding endurance test (3.3.4.3). Its homogeneity and transparency make it a suitable candidate for mucoadhesive applications in the oral cavity, where a thinner film might offer more comfort to the user.<sup>[71]</sup>

In contrast, the foamed PVA film, which is thicker (360  $\mu\text{m}$ ) and more porous, shows potential for applications requiring increased bacterial loading. The large pores enable the incorporation of higher quantities of bacteria, which may enhance therapeutic outcomes. However, this is accompanied by a reduction in tensile strength (3.3.4.5), as the pores act as weak points, leading to a lower tensile strength.

### 3.3.3. Film Casting Thickness and Additional Formulations

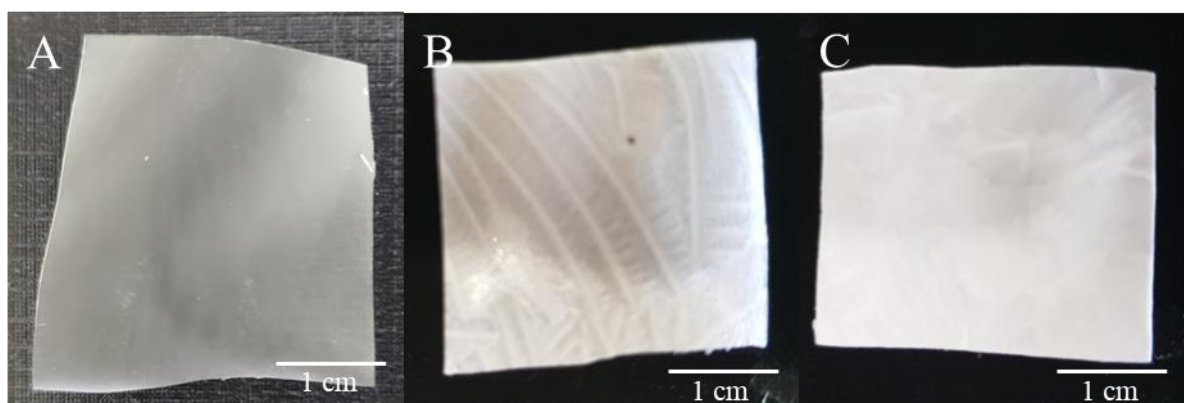
The thickness of the different polymer films was determined using an optical microscope. The thickness of the HPMC-PVA film produced with the electromotive film casting device is 25  $\mu\text{m}$ , and they exhibit a transparent appearance (Fig. 3.11 A). The thickness of the hand-cast PVA-HPMC film is 47  $\mu\text{m}$  (Figure 3.11 B). Figure 3.11 C shows the thickness of the foamed PVA Film (360  $\mu\text{m}$ ).



**Figure 3.11.** Determination of the thickness of the polymer films using cross-sections taken with an optical microscope (Examples). **A:** HPMC-PVA film electromotive film-casting device (25.16  $\mu\text{m}$ ) **B:** HPMC-PVA film hand-cast (46.59  $\mu\text{m}$ ) **C:** foamed PVA Film (360.29  $\mu\text{m}$ ) **D:** Freeze-dried HPMC Film (294.69  $\mu\text{m}$ ) **E:** freeze-dried PVA film (288.24  $\mu\text{m}$ ). n=5

Figure 3.11 D displays a freeze-dried film made from HPMC and glycerol, with a thickness of 295  $\mu\text{m}$ . In Figure 3.11 E, a film consisting of PVA and glycerol is shown, having a thickness of 288  $\mu\text{m}$ .





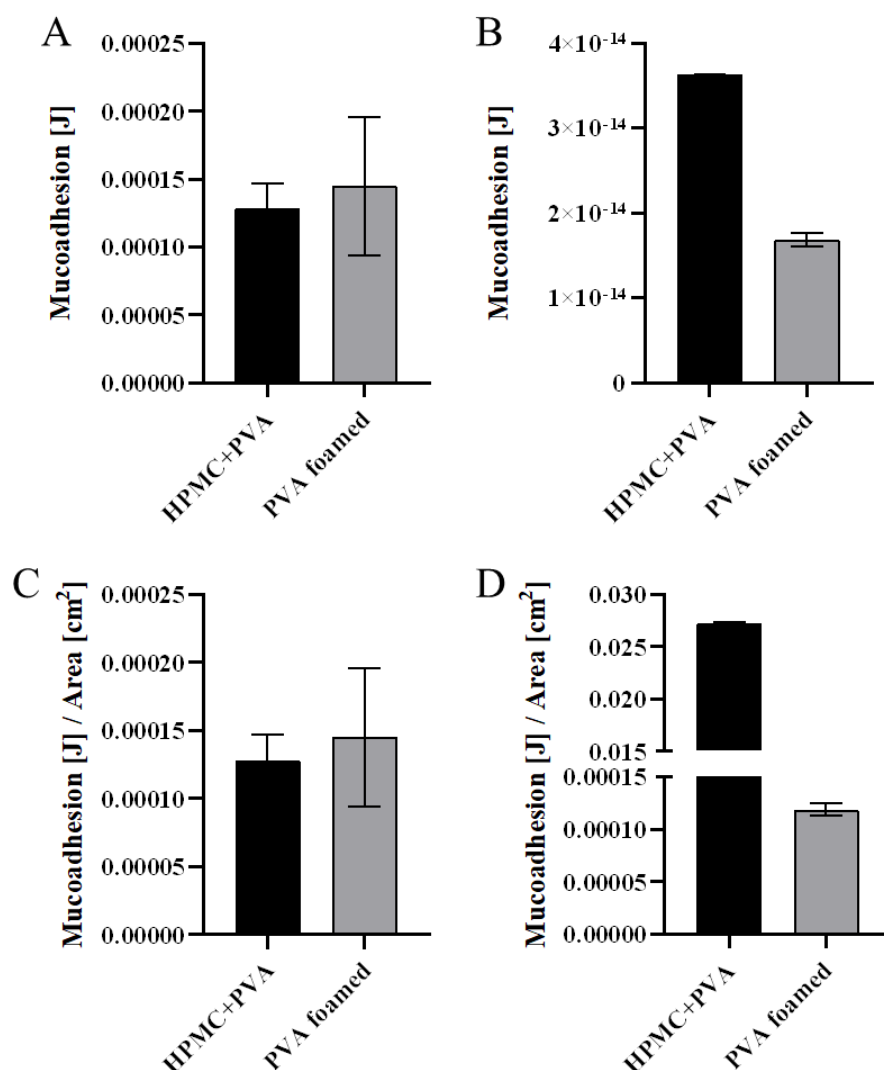
**Figure 3.12.** **A** Hand-cast polymer film made of HPMC + PVA. **B** Freeze-dried polymer film made from HPMC using the electromotive film casting device. **C** Freeze-dried polymer film made from PVA using the electromotive film casting device.

Figure 3.12 A illustrates the hand-cast film. The substance is characterized by a milky, cloudy, and transparent appearance. Figure 3.12 B depicts the freeze-dried film composed of HPMC. The material is white in color and exhibits a porous texture. Similarly, the freeze-dried film produced from PVA (Figure 3.12 C) is white and characterized by a high density of pores. The drying time of the freeze-dried films is 12 hours in the freeze dryer. However, it should be noted that these conditions are fundamentally different to the drying time of the other film formulations, and thus, a direct comparison of the drying times is not possible.

### 3.3.4. Film Properties

#### 3.3.4.1. *Mucoadhesion*<sup>1</sup>

The bacteria were embedded into mucoadhesive films designed to extend their residence time at the place of application. A key factor for mucoadhesive interactions is the electrostatic interaction with the negatively charged mucins. Mucoadhesion in the oral cavity was modelled and quantified by measuring the adhesive energy between the films and mucin-coated surfaces both for large and small surface areas.



**Figure 3.13.** **A:** Mucoadhesion was evaluated on a macroscale using a tensile tester. The interaction between the sample and a mucin-coated slide was recorded.  $n=3$  with standard deviation. **B:** Mucoadhesion was evaluated on the microscale using an atomic force microscope (AFM) at ambient conditions. The interaction between the sample and a mucin-coated cantilever was recorded. **C** The macroscale testing normalized to the contact area ( $1 \text{ cm}^2$ ) **D** The microscale testing in AFM was normalized by the contact area of the cantilever estimated from the tip indentation,  $n=3$  with standard deviation.

Two different set-ups were used. between the films and mucin-coated surfaces both for large and small surface areas. Two different set-ups were used.

Figure 3.13A summarizes the adhesion energy data. For the large surface area experiments ( $1 \text{ cm}^2$ ), a tensile test set-up was used. The data indicated that the adhesion energy between the mucin layer and the HPMC-PVA polymer film ( $1.28 \times 10^{-4} \text{ J}$ ) differed only minimally from that between mucin and the foamed PVA film ( $1.45 \times 10^{-4} \text{ J}$ ). As a reference, the interaction between the films and a clean microscope

slide was also measured. The interaction between glass and the HPMC-PVA film was  $3.94 \times 10^{-12}$  J, while the interaction between glass and the foamed PVA film was  $1.76 \times 10^{-11}$  J.

Interactions on a smaller surface area were measured using atomic force microscopy (AFM) with a mucin-coated tip. As shown in Figure 3.13B, the interactions on this scale were significantly weaker. The energy values for the HPMC-PVA film and the foamed PVA film were  $3.63 \times 10^{-14}$  J and  $1.69 \times 10^{-14}$  J, respectively. An uncoated cantilever was used as a reference, but the interactions were so minimal that they could not be quantitatively evaluated. In order to allow a comparison between the different scales, the contact area of the cantilever with the sample was calculated using equation 1. Equation 1 was adapted from the supporting information of Schmitz et al.<sup>[148]</sup> It is  $1.33 \times 10^{-12}$  cm<sup>2</sup> for the HPMC and PVA films and  $1.42 \times 10^{-10}$  cm<sup>2</sup> for the foamed PVA film. The penetration depth of the cantilever into the polymer film was previously estimated using JPK software enabling extraction from the measured data. The mucoadhesion was adapted to the area (1 cm<sup>2</sup>) for better comparison (Figure 3.13C, D).

$$Area = Radius\ Cantilever^2 - (Radius\ Cantilever - Penetration\ Depth)^2 \quad \text{Equation 1}$$

Mucoadhesion is a critical factor for ensuring that bacteria remain in the oral cavity long enough to exert their probiotic effects. The results demonstrate that both HPMC-PVA and foamed PVA films exhibit attractive forces higher than the reference reflecting potential mucoadhesion, with energy values ( $1.28 \times 10^{-4}$  J and  $1.45 \times 10^{-4}$  J, respectively) indicating strong interactions with the negatively charged mucins. This indicates that either formulation could be employed effectively in oral applications. It is noteworthy that the discrepancies between the large and small surface area measurements suggest that the strength of mucoadhesion may exhibit variability depending on the scale of interaction. On a larger scale, there may be a larger number of interactions than on a smaller scale.<sup>[63,64,72,102]</sup> This was demonstrated by the surface normalization, especially for the foamed PVA film but also for the HPMC-PVA films the values were in a similar range. Observed discrepancies may be due to different contact pressures for the different sized samples. This could not be changed due to the

different equipment used. The results of both tests demonstrated a notable discrepancy from the reference value in the absence of mucin.

### **3.3.4.2. Mucoadhesion Additional Film Formulations**

In addition to the foamed PVA film and the polymer film made from HPMC - PVA, the mucoadhesion of the freeze-dried films was evaluated. Figure 3.14 A presents the mucoadhesion values obtained through macroscale testing using a tensile tester, as described in the previous section. The mucoadhesion value for the HPMC film is  $3.49 \times 10^{-5}$  J, while the PVA film exhibits a value of  $9.63 \times 10^{-5}$  J. In the absence of a mucin coating, the interaction between the glass and the HPMC film was observed to be  $8.10 \times 10^{-16}$  J, the value of the PVA film was found to be  $3.61 \times 10^{-14}$  J.

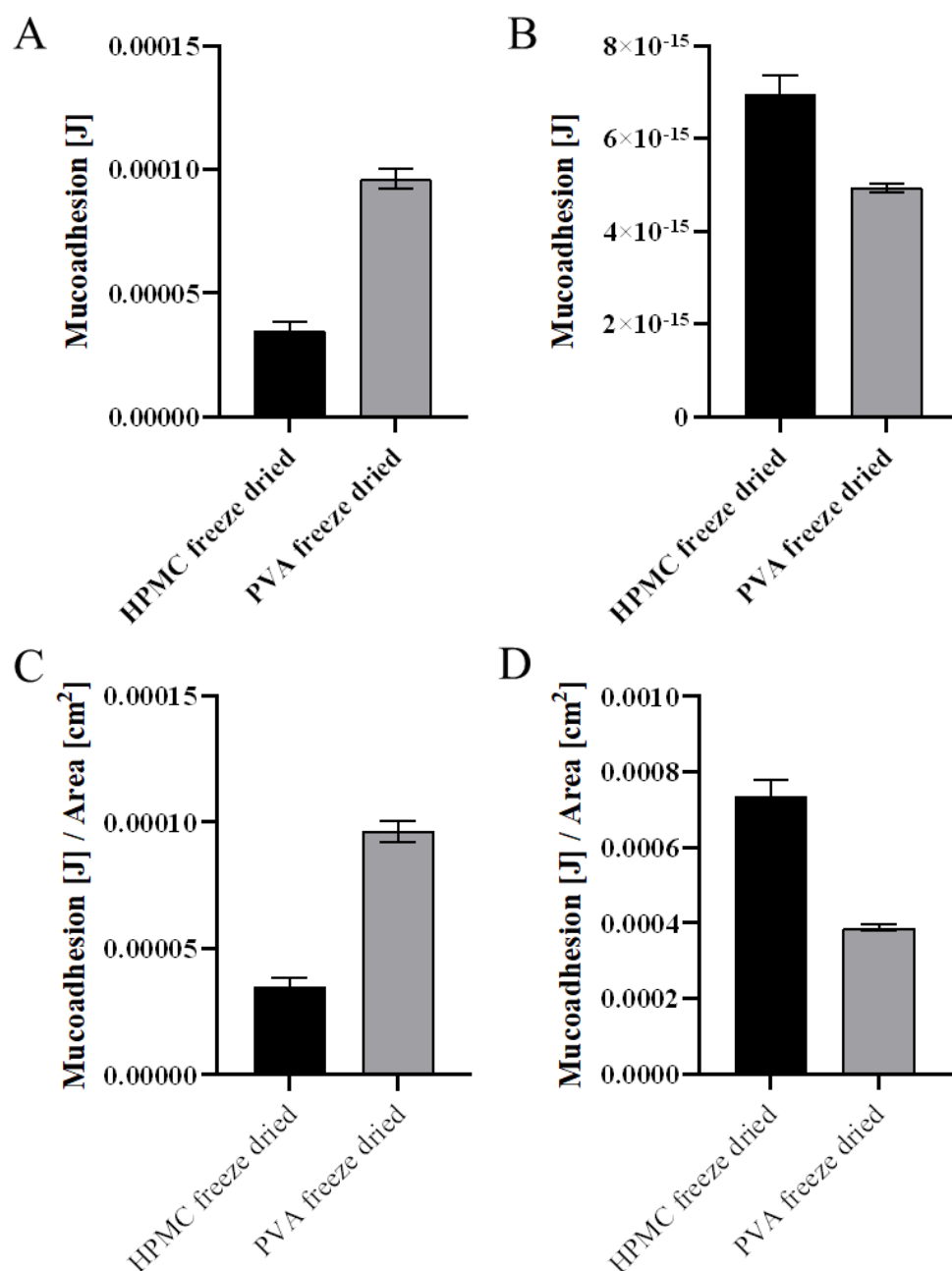


**Figure 3.14.** **A:** Mucoadhesion was evaluated on a macroscale using a tensile tester. The interaction between the sample and a mucin-coated slide was recorded.  $n=3$  with standard deviation. **B:** Mucoadhesion was evaluated on a microscale using an AFM. The interaction between the sample and a mucin-coated cantilever was recorded. **C:** The macroscale testing normalized to the contact area ( $1 \text{ cm}^2$ ) **D:** The area of the microscale testing in AFM was adapted to the area of the macroscale test ( $1 \text{ cm}^2$ )  $n=3$  with standard deviation.

Figure 3.14 B illustrates the results from microscale mucoadhesion testing performed using AFM. The HPMC film shows a mucoadhesion of  $6.957 \times 10^{-15} \text{ J}$ , and the PVA

film demonstrates a value of  $4.945 \times 10^{-15}$  J. Given that the hand-cast film made of HPMC-PVA has precisely the same composition as the one produced with the electromotive film casting device, there was no need to test the mucoadhesion again at this point.

Similar to the mucoadhesion testing performed on the HPMC - PVA and foamed PVA films, the area for the microscale test was calculated based on the area used in the tensile tester test ( $1 \text{ cm}^2$ ). Equation 1 was applied to calculate the cantilever's contact area, and the penetration depth was determined using JPK software. For the freeze-dried HPMC film, this resulted in a contact area of  $9.4405 \times 10^{-12} \text{ cm}^2$ , with a corresponding mucoadhesion value of  $7.36931 \times 10^{-4}$  J. For the freeze-dried PVA film, the contact area was calculated to be  $1.27684 \times 10^{-11} \text{ cm}^2$ , yielding a mucoadhesion value of  $3.87284 \times 10^{-4}$  J (Figure 3.14 C & D).

Normalization to the same area shows that mucoadhesion is stronger when measured with the AFM, consistent with previous results for the HPMC & PVA film and the foamed PVA film. As the cantilever was coated with the same mucins as the slide used for the tensile test, this difference in adhesion is likely due to the distinct experimental setups and measurement devices.

Both films also demonstrated increased adhesion compared to samples tested without mucin, suggesting that the presence of mucin enhances retention time of the bacteria in the oral cavity.

### **3.3.4.3. Flexibility<sup>1</sup>**

The flexibility of both the HPMC+PVA film and the foamed PVA film was determined via the folding endurance test. As previously documented in the literature, films intended for oral administration must demonstrate the capacity to withstand 300 folds in the same location (Figure 3.15).<sup>[71]</sup>

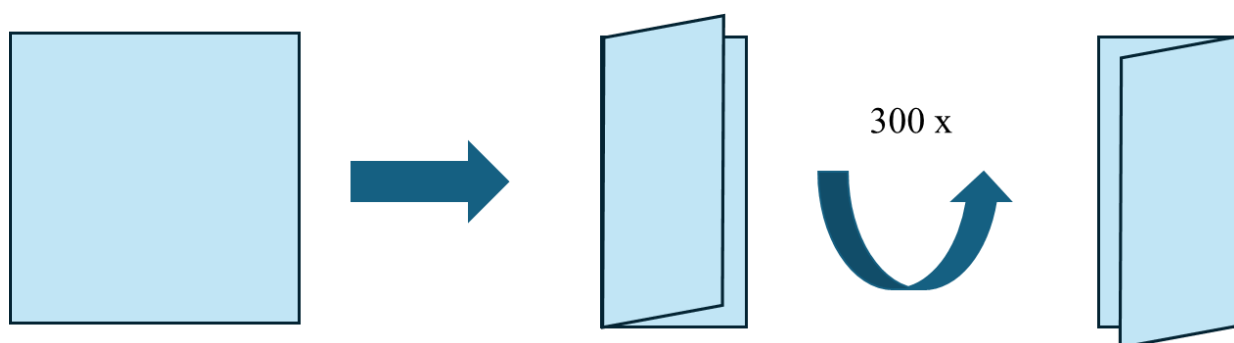


**Figure 3.15.** Schematic illustration of the flexibility test by folding the polymer films by 180° for 300 times. Both films demonstrated the capacity to withstand 300 cycles of folding without exhibiting any discernible breaks or tears.

#### **3.3.4.4. Flexibility Additional Film Formulations**

The other film formulations made from the hand-drawn HPMC - PVA film and the two freeze-dried films made from HPMC and PVA were also tested for flexibility using folding endurance. All three formulations passed the flexibility test and could be folded 300 times without any visible cracks appearing.

#### **3.3.4.5. Tensile strength<sup>1</sup>**

Tear resistance represents a pivotal parameter in the deployment of oral films, as these materials must exhibit an adequate tensile strength to withstand use within the oral cavity.<sup>[71]</sup> The tensile strength of the films was evaluated using a tensile test set-up, in which loaded and unloaded films were analyzed for both bacteria. The tensile strength was calculated using equation 2.

Figure 3.16A presents the tensile strength of the HPMC-PVA films, with and without bacterial loading. The tensile strength of the pure film was 69 Pa, while films loaded with *L. rhamnosus* (50 mg) and *L. reuteri* (50 mg) exhibited tensile strengths of 596 Pa and 522 Pa, respectively. The incorporation of microencapsulated bacteria (100 mg) resulted in a notable alteration in the tensile strength. As illustrated in Figure 3.16B, the tensile strength for *L. rhamnosus* decreased to 35 Pa, and for *L. reuteri*, it decreased to 53 Pa. The foamed PVA films, with and without bacterial loading, exhibited the lowest tensile strength. No significant differences in tensile strength were observed based on the bacterial loading. Figure 3.16C illustrates that the tensile

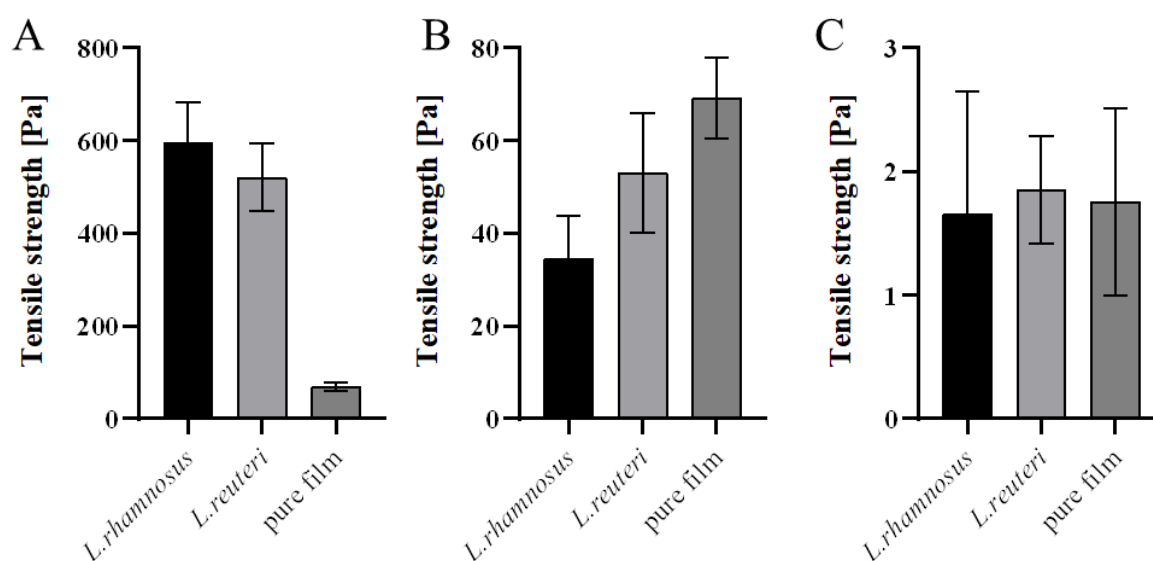


**Figure 3.16. A:** Tensile strength of polymer films made of HPMC and PVA with and without *L. rhamnosus* and *L. reuteri* **B:** Tensile strength of polymer films made of HPMC and PVA with and without microencapsulated bacteria. **C:** Tensile strength of polymer films made of foamed PVA with and without microencapsulated bacteria. n=5 with standard deviation.

strength of the pure foamed film was 1.8 Pa, while the tensile strengths of films loaded with microencapsulated *L. rhamnosus* and *L. reuteri* were 1.7 Pa and 1.9 Pa, respectively.

The elevated tensile strength of films containing non-encapsulated bacteria can be ascribed to the intrinsic structural characteristics of the bacteria. The rod-shaped bacterial cells form chains,<sup>[149]</sup> thereby enhancing the stability of the polymer matrix. In contrast, the microencapsulated bacteria, encased in a polymer shell composed of Eudragit EPO and RL 30D, are unable to provide the same degree of organization and thus stabilization of the polymer film. The structure of the microcapsules appears to



diminish tensile strength. The foamed PVA films exhibited the lowest tensile strength, which is likely due to the presence of pores, including those at the outer edges, which serve as weak points with a higher likelihood of tearing. The incorporation of microencapsulated bacteria did not result in a notable impact on tensile strength in these foamed systems, as the bacteria were predominantly confined to the pores and did not contribute directly to the polymer matrix.

The data on tensile strength offer crucial insights into the mechanical robustness of the films. The tensile strength of pure HPMC-PVA films was found to be sufficient (69.2 Pa). However, the addition of non-encapsulated bacteria resulted in a significant increase in tensile strength, reaching 596.4 Pa and 521.8 Pa for *L. rhamnosus* and *L. reuteri*, respectively. This is presumably due to the structural characteristics of the bacteria, which form chains within the polymer matrix, thereby reinforcing the film.<sup>[150–152]</sup> In contrast, films with microencapsulated bacteria demonstrated a reduction in tensile strength, which is likely attributable to the disruption of the ability of the bacteria to form chains due to the encapsulation process, thereby reducing structural integrity.

The foamed PVA films, despite offering advantages in terms of bacterial loading, exhibited the lowest tensile strength (1.8 Pa for the pure film). The presence of pores weakens the structure, resulting in films that are more prone to tearing. These films may be better suited for applications where large bacterial loadings are needed.

### **3.3.4.6. Tensile Strength Additional Film Formulations**

The tensile strength of all film formulations was tested prior to embedding the bacteria. The tensile strength of the HPMC and PVA films produced using the film casting device was 69.23 Pa, while the hand-cast films exhibited a higher tensile strength of 95.45 Pa (Figure 3.17).

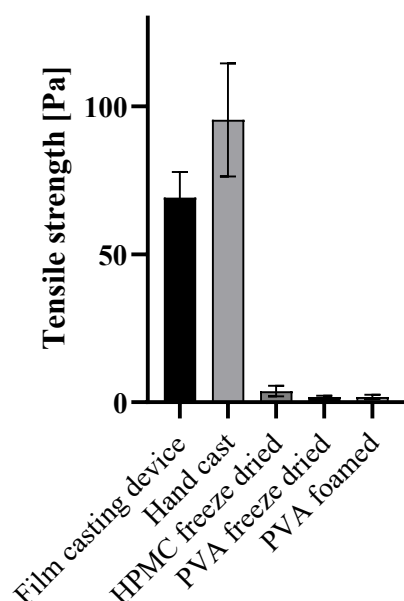


**Figure 3.17.** Tensile strength of the different polymer film formulations without *L. rhamnosus* and *L. reuteri*. n=5 with standard deviation.

In contrast, the tensile strengths of the freeze-dried and foamed PVA films were significantly lower. The freeze-dried HPMC film had a tensile strength of 3.74 Pa, the freeze-dried PVA film 1.79 Pa, and the foamed PVA film 1.75 Pa. The reduced tensile strength in the freeze-dried and foamed films can be attributed to the presence of numerous pores, which create weak points that make the films more prone to tearing. In comparison, the hand-cast films demonstrated higher tear resistance, likely due to their greater thickness.

#### 3.3.4.7. Dissolution<sup>1</sup>

The SEM images allowed to illustrate the release of bacteria in all tested formulations. The fastest release occurred from the HPMC and PVA polymer films containing pure *L. reuteri* (Figure 3.18 A) and *L. rhamnosus* (Figure 3.18 B). At the outset, no free bacteria are discernible. However, after 30 minutes, the predominant observation is that of free bacteria, with minimal non-washed away polymer residues. This trend persists over time, and by 120 minutes, only free bacteria remain visible.

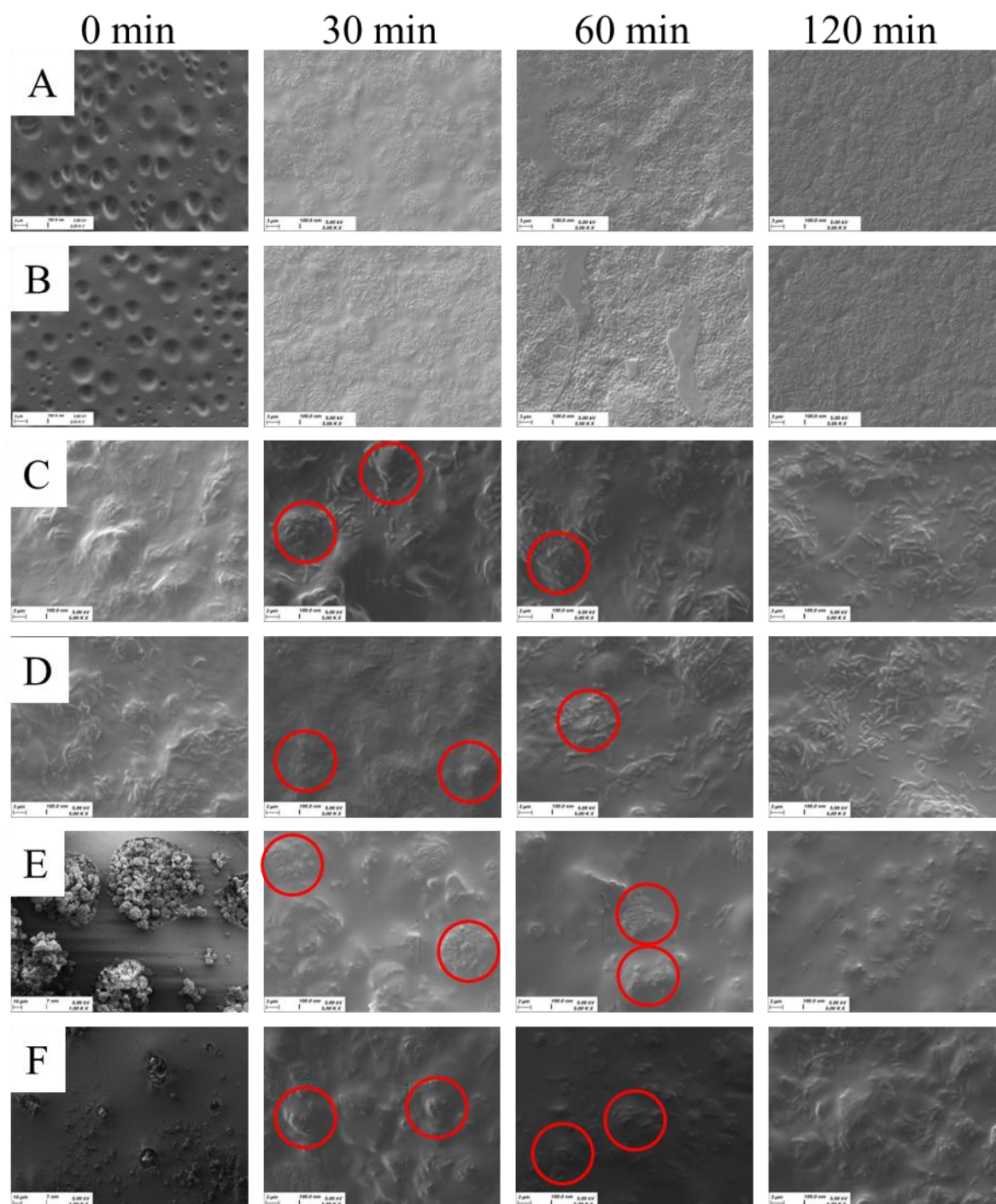


**Figure 3.18.** Series of SEM micrographs illustrating the dissolution of polymer films on 1.5% agarose gel patches at 36 °C and 100% relative humidity. Samples were imaged after different incubation times at 0 min, 30 min, 60 min and 120 min. A: HPMC & PVA film + *L. reuteri*, B: HPMC & PVA film + *L. rhamnosus*, C: HPMC & PVA film + microencapsulated *L. reuteri*, D: HPMC & PVA film + *L. rhamnosus*, E: foamed PVA film + microencapsulated *L. reuteri*, F: foamed PVA film + microencapsulated *L. rhamnosus*. The remaining microencapsulated structure is indicated by red circles.

The SEM images illustrate the release of bacteria in all tested formulations. The fastest release occurred from the HPMC and PVA polymer films containing pure *L. reuteri*

(Figure 3.18 A) and *L. rhamnosus* (Figure 3.18 B). At the outset, no free bacteria are discernible. However, after 30 minutes, the predominant observation is that of free bacteria, with minimal polymer residues. This trend persists over time, and by 120 minutes, only free bacteria remain visible.

In contrast, the release of bacteria from the HPMC and PVA films containing microencapsulated *L. reuteri* (Figure 3.18 C) and *L. rhamnosus* (Figure 3.18 D) occurred in a more gradual manner. After 30 min, rod-shaped bacteria began to be released, while the microencapsulation structures (red circles) remained visible. With the passage of time, the encapsulation structure diminishes, and by 60 min a greater number of bacteria were released. After 120 min, the encapsulation structures were no longer discernible, and only free rod-shaped bacteria were observed.

The slowest rate of bacterial release was observed in the foamed PVA films. At the designated time point, the film pores were observed to be filled with microencapsulated *L. reuteri* (Figure 3.18 E) or *L. rhamnosus* (Figure 3.18 F). After 30 min, the microencapsulation structures remained clearly visible (red circles), with only a few free rod-shaped bacteria observed. At this point, the dissolution of the PVA film was evident. After 60 min, dissolution progresses further, releasing more rod-shaped bacteria and reducing the microencapsulation structures. By 120 min, primarily free bacteria and remnants of the encapsulation remain visible.

SEM imaging of the dissolution profiles provides a visual confirmation of the release dynamics. The HPMC-PVA films exhibited the most rapid release of bacteria, with free *L. reuteri* and *L. rhamnosus* observed after 30 min and complete release by 120 min. This rapid dissolution may be advantageous for applications that necessitate expeditious bacterial delivery. In contrast, the gradual release from films containing microencapsulated bacteria allows for more precise control of bacterial delivery, which may prolong the therapeutic effect. The slowest release was observed with foamed PVA films, which retained microencapsulated bacteria within their pores even after 60 min. This indicates that foamed PVA films are more suitable for slow-release applications, offering a sustained release of probiotics over time. This is particularly due to the high loading and the higher polymer content of the film. The combination of

microencapsulation and film embedding thus also demonstrated to enable control over the release kinetics.

### 3.3.4.8. Initial Dissolution testing

In the initial dissolution test, diverse film formulations were applied to a 1.5% agarose patch at 36 °C and 100% relative humidity. The dissolution times are presented in Figure 3.19. The film composed of HPMC and PVA, produced using the film applicator, exhibited dissolution within a seven-minute timeframe, whereas the thicker, hand-drawn film made from the same material required 12.5 minutes to dissolve. Formulations with large pores and, consequently, larger surface areas exhibited the fastest dissolution times. The foamed PVA film dissolved in two minutes, the freeze dried HPMC film in one minute, and the freeze dried PVA film in five minutes.

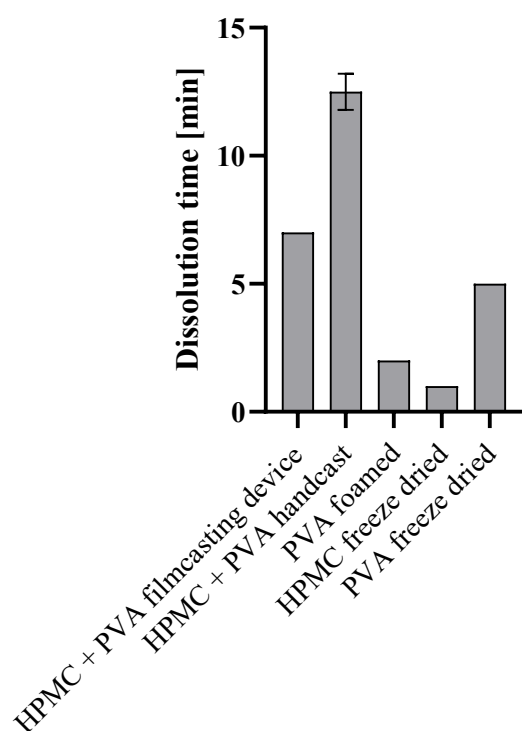


**Figure 3.19.** The dissolution time of the various film formulations was observed on a patch of 1.5% agarose at 100% relative humidity and 36 °C. n=3 with standard deviation

This initial test indicates that the non-porous films exhibit longer dissolution times. The HPMC-PVA film produced with the film applicator was chosen for in vivo testing due to its dissolution time and the sustained viability of the embedded bacteria.

### **3.3.4.9. *Dissolution of HPMC-PVA film on tooth enamel***

The final formulation selected was evaluated for its dissolution behavior in the oral cavity. A film of HPMC and PVA, produced using the film applicator, was attached to rehydrated bovine enamel using MilliQ water and fixed to an enamel splint with two-component silicone. The samples were incubated in the mouth of a volunteer for 30 minutes. After incubation, the samples were examined unsputtered in a low vacuum using SEM at a magnification of 50x.

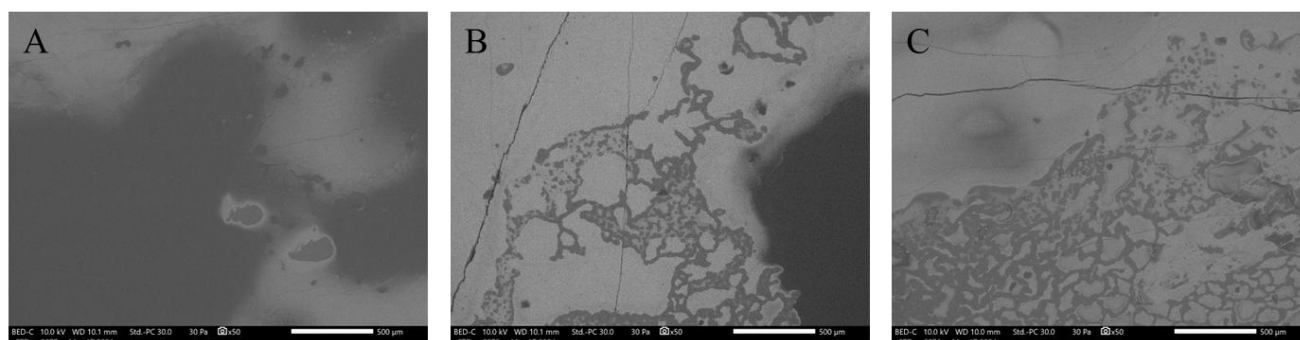


**Figure 3.20.** SEM micrographs of bovine tooth enamel samples with pure polymer film (HPMC-PVA) after incubation for **A:** 10 min, **B:** 20 min and **C:** 30 min in oral cavity of one volunteer.

Figure 3.20 depicts the SEM images of the enamel samples following 10 (Figure 3.20 A), 20 (Figure 3.20 B) and 30 (Figure 3.20 C) minutes of incubation. After 10 minutes, a considerable quantity of darker polymer film residues are visible, covering the tooth enamel. With the passage of time, after 20 minutes, there are fewer polymer residues visible, and after 30 minutes, even fewer darker residues of the polymer film are visible against the lighter background of the enamel. This indicates that the polymer film has almost completely dissolved, thereby releasing bacteria. This can be also observed when bacterial films are dissolved on an agarose patch, resulting in continuous bacterial release (see Figure 3.18).

### **3.4. Conclusion<sup>1</sup>**

This study successfully demonstrated the potential of polymer films for the delivery of *L. rhamnosus* and *L. reuteri* in oral cavity applications. Both HPMC-PVA and foamed PVA films demonstrated efficacy in supporting bacterial viability and adhesion while maintaining adequate mechanical properties. In particular, the fact that the foamed PVA film circumvents the drying process precludes a further reduction in activity. Spray drying was demonstrated to be a mild encapsulation technique, preserving high bacterial survival rates with minimal thermal stress, particularly when used in conjunction with a three-way nozzle as shown previously.<sup>[59]</sup> However, the incorporation of microencapsulated bacteria into the polymer film out of HPMC and PVA resulted in a decrease in bacterial activity.

The mucoadhesion testing demonstrated that both films exhibited sufficient interaction with mucins, thereby ensuring prolonged residence in the oral cavity, which is a critical factor for the efficacy of the therapeutic treatment.

Additionally, the study illuminated the distinctive advantages and limitations of the two film types. The HPMC-PVA films exhibited rapid bacterial release and robust tensile properties, rendering them well-suited for applications necessitating expeditious probiotic delivery. In contrast, the thicker, porous structure of foamed PVA films permitted higher bacterial loading and more controlled, sustained release, although this was at the expense of tensile strength and structural stability.

#### **3.4.1. Selection of Polymer Film**

The most promising films were subjected to further testing in order to evaluate a number of key characteristics, including bacterial viability, mechanical properties and dissolution characteristics.

All films exhibited mucoadhesion, as evidenced by interactions measured with and without the mucin-coated cantilever or glass slide, with values differing between macroscale and microscale assessments. The HPMC-PVA film displayed the optimal

mucoadhesive performance, exhibiting the second-highest value on the macroscale and the highest value on the microscale. All films exhibited satisfactory flexibility, rendering them appropriate for utilization within the oral cavity.

Tensile strength is a crucial attribute for polymer film applications. The non-porous HPMC-PVA films, produced via electromotive film casting or hand casting techniques, exhibited the most robust tensile strength. The thickness of the film was identified as a critical factor, with the thicker, hand-drawn films displaying superior strength. In contrast, the freeze-dried HPMC and PVA films and the foamed PVA films exhibited markedly reduced tensile resistance, which is likely attributable to the formation of pores due to the production process.

The initial dissolution of the placebo films was analyzed in a controlled incubator setup. Films with larger surface areas due to porosity exhibited the fastest dissolution, followed by films produced using the electromotive film-casting device. In contrast, the thicker, hand-cast films demonstrated the slowest dissolution. In general, the HPMC-PVA films demonstrated superior mechanical properties. Given the bioactivity of both microencapsulated and pure embedded bacteria, the HPMC-PVA polymer film, produced with the electromotive film casting device, was selected for further development. To this end, in vivo dissolution tests conducted in this chapter confirmed dissolution within the target time of 30 minutes.



## **4. Microencapsulation of *L. rhamnosus* and *L. reuteri* and incorporation inside mucoadhesive polymer films**

Parts of this chapter have been previously prepared for publication. The corresponding sections are indicated with footnote 2.

### **Development of Mucoadhesive Polymer Films as a Delivery System for Microencapsulated *Lactobacillus reuteri* – Strategies to Improve Bacterial Viability**

Charlotte Eckermann<sup>1</sup>, Constanze Lasch<sup>2</sup>, Sangeun Lee<sup>3,4</sup>, Andriy Luzhetskyy<sup>2,4</sup>, Marc Schneider<sup>1</sup>

<sup>1</sup>Department of Pharmacy, Biopharmaceutics and Pharmaceutical Technology, PharmaScienceHub, Saarland University, 66123 Saarbrücken, Germany

<sup>2</sup>Department of Pharmacy, Pharmaceutical Biotechnology, PharmaScienceHub, Saarland University, 66123 Saarbrücken, Germany

<sup>3</sup>Pharmaceutical Materials and Processing, Department of Pharmacy, Saarland University, Campus C4 1, 66123 Saarbrücken, Germany

<sup>4</sup>Helmholtz Institute for Pharmaceutical Research Saarland (HIPS), Helmholtz Center for Infection Research (HZI), 66123 Saarbrücken, Germany

## 4.1. Introduction

In order to facilitate the applicability of *L. rhamnosus* and *L. reuteri*, these bacteria are embedded in previously developed polymer films. This process is conducted with both the pure and microencapsulated forms of the bacteria. Chapter 3.9 discussed the activities of the bacteria embedded in the HPMC-PVA polymer films. In this chapter, we will discuss additional ways in which the bacteria have been embedded.

Spray-drying is emerging as a widely used technique for microencapsulation, known for its gentle and rapid drying process coupled with high survival rates for bacteria.<sup>[35,39]</sup> Variations in structural results can be achieved through the use of both two-way and three-way nozzles<sup>[38,45–47]</sup>. In the former, a branching of pathways facilitates the simultaneous flow of drying gas and spray dispersion, resulting in microencapsulation in which bacteria are embedded in a matrix. Conversely, the three-way nozzle has inner and outer feeds for the spray dispersions and an outer feed for the drying gas. At the tip of the nozzle, the convergence of the two liquids creates the microencapsulation. This microencapsulation strategy aims to shield bacteria and ensure controlled release and local behaviour<sup>[39]</sup>. In particular, Eudragit® E and RL serve as viable options that have demonstrated efficacy in achieving the desired results at the pH levels found in the oral cavity.<sup>[55]</sup> In addition, Eudragit® RL facilitates mucoadhesion, enhancing the adherence of microencapsulated entities and thus prolonging the local residence time<sup>[58,153]</sup> which is often limited in current therapies.

In addition to encapsulation in a mucoadhesive polymer, the residence time of probiotic bacteria in the oral cavity can be further prolonged using mucoadhesive films.<sup>[63–66]</sup> Mucoadhesion can result from different interactions such as Van der Waals forces, hydrogen bonds, ionic interactions, or chain entanglements. It is important that the negatively charged nature of mucins generates electrostatic interactions<sup>[65,66,69,71–75]</sup>. For this purpose, different polymeric films composed of hydroxypropyl methylcellulose (HPMC) and/or polyvinyl alcohol (PVA) were prepared for embedding probiotics exploiting the specific interaction potentials of the polymers<sup>[71,76–78]</sup>. Spray-drying as well as film formation involves drying of the system which applies stress to the microorganisms reducing the viability dramatically.

The drying time has a major impact on the survival of the bacteria. A shorter drying time results in the microencapsulation not dissolving, thereby allowing the bacteria to become active once more due to the presence of water. The film dispersion lacks nutrients, which results in the death of the bacteria. A variety of methods for reducing the adverse effects of drying stress are currently being investigated. Films of varying thicknesses are manufactured, the drying time is modified through the utilization of disparate drying temperatures, the films undergo freeze-drying, foaming or drying in a vacuum.

The drying time plays a crucial role in the survival and functionality of *Lactobacillus* cells. The rapid drying time associated with spray drying can result in considerable thermal and oxidative stress, which may potentially damage cell membranes and proteins. Nevertheless, a shorter exposure time can assist in preserving some functionality, enabling cells to rehydrate rapidly without necessitating extensive recovery.<sup>[155,156]</sup> Conversely, freeze drying, with a considerably longer drying time, typically preserves cell integrity and enzyme activity by circumventing high temperatures. However, this prolonged dehydration can stress cell structure, resulting in a longer recovery period upon rehydration.<sup>[155,157,158]</sup> Optimizing drying time, temperature, and protective agents is crucial for maximizing cell viability in different *Lactobacillus* drying methods.

It is crucial to enhance the resilience of lactic acid bacteria, such as *L. reuteri* and *L. rhamnosus*, to drying processes for the successful utilization of these bacteria in probiotics and other industrial formulations. The resistance of bacteria to drying can be enhanced through the strategic manipulation of cultivation parameters, including the growth phase, pH, temperature, and exposure to stress conditions. It has been demonstrated that during the stationary phase, bacteria undergo metabolic shifts that enhance their resilience to environmental stresses.<sup>[81]</sup> Another approach is to manipulate the pH value during cultivation, which influences cell wall composition and enhances tolerance to osmotic fluctuations.<sup>[84–88]</sup>

For example, the cultivation of lactic acid bacteria at a slightly acidic pH and moderately elevated temperatures can enhance membrane resilience, as cells increase the proportion of unsaturated fatty acids to maintain fluidity during drying.<sup>[86,159]</sup>

The application of mild stress conditioning, such as osmotic or thermal preconditioning, has been demonstrated to enhance resilience by inducing the expression of protective proteins and the upregulation of genes associated with stress responses.<sup>[82,83,91,92]</sup> The adaptive response of *L. reuteri* and *L. rhamnosus* is mediated by key genes involved in the stabilization of proteins under stress, including those encoding heat shock proteins (e.g., groEL, dnaK),<sup>[160]</sup> and in the modification of membrane composition (e.g., cfa). Other crucial genes, including atpA, otsA, and otsB, are involved in maintaining pH homeostasis and the accumulation of protective solutes, which serve to safeguard cellular integrity during drying and rehydration.<sup>[83,89]</sup> Furthermore, the upregulation of phosphate transporters and acetoin production pathways contributes to pH stability, thereby enhancing cellular survival.<sup>[84–86,160]</sup>

These coordinated molecular and physiological adaptations are fundamental to the development of robust bacterial strains for probiotic formulations, as they facilitate the retention of high viability and functional efficacy in desiccated products. The implementation of growth-phase-dependent stress responses, in conjunction with the strategic activation of stress-related genes, represents a promising approach for enhancing the drying tolerance of lactic acid bacteria, thereby optimising their efficacy for industrial use.

We used *L. reuteri* and *L. rhamnosus* which were previously described to be a beneficial probiotics in the treatment of periodontitis.<sup>[24]</sup> Thus, the probiotic bacteria were formulated for application into the oral cavity and allow for colonisation. It was microencapsulated with Eudragit® EPO and RL30D via spray-drying for controlled release and mucoadhesion. These microencapsulated bacteria were then embedded in mucoadhesive polymer films for good application properties and prolonged retention in the oral cavity. The bacterial survival rates could further be improved by stressing the bacteria during cultivation and by the use of the optimal growth phase for formulation.

## **4.2. Methods**

In addition to the following described and for publication prepared work with *L. reuteri*, all methods outlined below were also conducted with the probiotic lactic acid bacterium *L. rhamnosus* following the same protocols.

To process the original bacterial powder of *L. reuteri* and *L. rhamnosus* the cryoprotectant matrix was removed by resuspending them in MilliQ water and subsequent centrifugation ( $5000 \times g$ ; 5 min). This was repeated three times.

### **4.2.1. Microencapsulation via Spray Drying<sup>2</sup>**

Microencapsulation of bacteria was conducted through spray-drying utilizing polymethacrylate derivatives, specifically a 1:1 mixture of Eudragit® EPO and Eudragit® RL30D, at a concentration of 10% total polymer content. The procedure was performed using a laboratory-scale Mini spray dryer (Büchi B290, Flawil, Switzerland) configured in two distinct setups. The incorporation of bacteria into a polymer matrix was facilitated using a two-way nozzle. To minimize the thermal stress on the bacteria, a three-way nozzle configuration was employed, which allows for more controlled temperature management. The polymer solutions, Eudragit® EPO and RL30D, were dispersed in water and fed into the outer feed, while the purified bacteria were introduced through the inner feed. The spray-drying process was optimized for reduced thermal impact by maintaining a low inlet temperature of 55 °C and an outlet temperature of 42 °C, with a system pressure of 1.5 bar. The flow rate was regulated at 1 mL/min, the rotameter was set to 60 mm, and the aspirator was operated at 100% capacity.

### **4.2.2. Morphology Analysis<sup>2</sup>**

The microencapsulation was evaluated using SEM, EVO HD15, Zeiss, Oberkochen, Germany. The microencapsulated bacteria were attached to SEM holders via adhesive carbon plates and followed by 100 s gold sputtering using a Quorum Q150R ES sputter coater (Quorum Technologies Ltd., East Grinstead, UK), for better conductivity. The images were captured at a voltage of 5 kV and a magnification of 5 kX.

The core-shell structure was analysed using CLSM. *L. reuteri* and *L. rhamnosus* was stained with Syto 9 (488 nm excitation, 525 nm emission), and Eudragit® S conjugated with BODIPY (561 nm excitation, 622 nm emission) was incorporated into the Eudragit® dispersion for visualization and analysis.

To prepare the conjugate, Eudragit® S100 (0.349 mmol of repeating unit) was dissolved in anhydrous DMSO (5 mg/mL), followed by the addition of EDC (2 equivalents, relative to a repeating unit of Eudragit® S100) and NHS (1.1 equivalents). The mixture was stirred at 21 °C for one hour, after which BODIPY-OH (0.1 equivalent) was added to the solution. Following an overnight reaction at 21 °C, the resulting solution was subjected to dialysis (3 kDa MWCO) in a solution of DMSO and H<sub>2</sub>O (750 mL, three times) in order to remove any residual free dye and side products. Subsequently, the purified polymer was lyophilised, resulting in a yield of 75.3%.

### **4.2.3. Microbiological Analysis<sup>2</sup>**

The viability of *L. reuteri* and *L. rhamnosus* was assessed via the plate count method. The microencapsulated bacteria were incubated in 0.9% NaCl solution at 37 °C for 45 min in order to dissolve the polymeric matrix or shell, respectively. Subsequently, the dispersion was diluted in 0.9% NaCl and plated on MRS agar. Following incubation at 36 °C and 5% CO<sub>2</sub> for 48 h, the number of colonies was determined in triplicates. The results obtained were converted to logarithmic values and the means and standard deviations were calculated.

### **4.2.4. Dissolution of Microencapsulated Bacteria and Polymer Film<sup>2</sup>**

The disintegration of microcapsules and polymer film were examined through incubation on a 1.5% agarose patch maintained at 36 °C and 100% relative humidity. In this procedure, the bacteria were applied to a polycarbonate membrane with 50 nm pore diameter and incubated for durations of 30, 60 and 120 min. Microscopic observation of dissolution was conducted using SEM, after complete drying following the procedure described above.

#### **4.2.5. Polymer Films Incorporating *L. reuteri*<sup>2</sup> and *L. rhamnosus* (Film Casting Device)**

Polymer films were produced using an electromotive film casting device (Coatmaster 510, Erichsen, Hemer, Germany). Aqueous solutions containing 1.5% hydroxypropyl methylcellulose (HPMC) and 1.5% polyvinyl alcohol (PVA) (18-88) were prepared, with glycerol incorporated as a plasticizer, constituting 20% of the total polymer mass. The solutions were sterilized via autoclaving. Microencapsulated *L. reuteri* and *L. rhamnosus*, sourced from either freeze-dried or liquid cultures, were then integrated into the solution through gentle mixing. This mixture was uniformly spread onto a Teflon foil using a squeegee (Erichsen, Hemer, Germany) with a slit width of 1000 µm. Subsequently, the films were dried at 37 °C in a ventilated drying chamber for a duration of approximately 1.5 h.

#### **4.2.6. Hand-cast Polymer Films**

The hand-cast polymer films were prepared similarly to the placebo films as described in Chapter 3. Both microencapsulated and non-encapsulated forms of *L. rhamnosus* and *L. reuteri* were incorporated into the polymer dispersion and gently mixed using pipetting.

#### **4.2.7. Drying at Different Temperatures**

To achieve varied drying times, films were dried either at room temperature or at 37 °C with forced ventilation. The polymer films were cast from HPMC-PVA and (microencapsulated) *L. rhamnosus* or *L. reuteri* using an electromotive film casting device, following previously established protocols, and subsequently dried under these differing conditions. Drying times and bacterial activity were then evaluated.

#### **4.2.8. Freeze-Dried Polymer Films**

Freeze-drying, recognized as a gentle drying process, was explored as an alternative method to enhance bacterial activity.

Two formulations were developed: one film containing 10% HPMC and another containing 10% HPMC with 20% glycerol, used as a plasticizer to ensure adequate flexibility. The autoclaved 10% polymer solution was carefully mixed with the (microencapsulated) bacteria by pipetting. The mixture was then cast onto a Teflon film using an electromotive film casting device and a squeegee with a 1000  $\mu\text{m}$  gap height. After casting, the films were frozen at  $-80\text{ }^{\circ}\text{C}$  and subsequently lyophilized until fully dry. Bacterial activity was assessed using the plate count method as described previously.

### **4.2.9. Foamed PVA Films with Incorporated Bacteria**

To further reduce drying time, faster water evaporation was explored, as seen with foamed PVA films (Chapter 3). This method included incorporating bacteria directly during the manufacturing process, as illustrated in Figure 4.1.



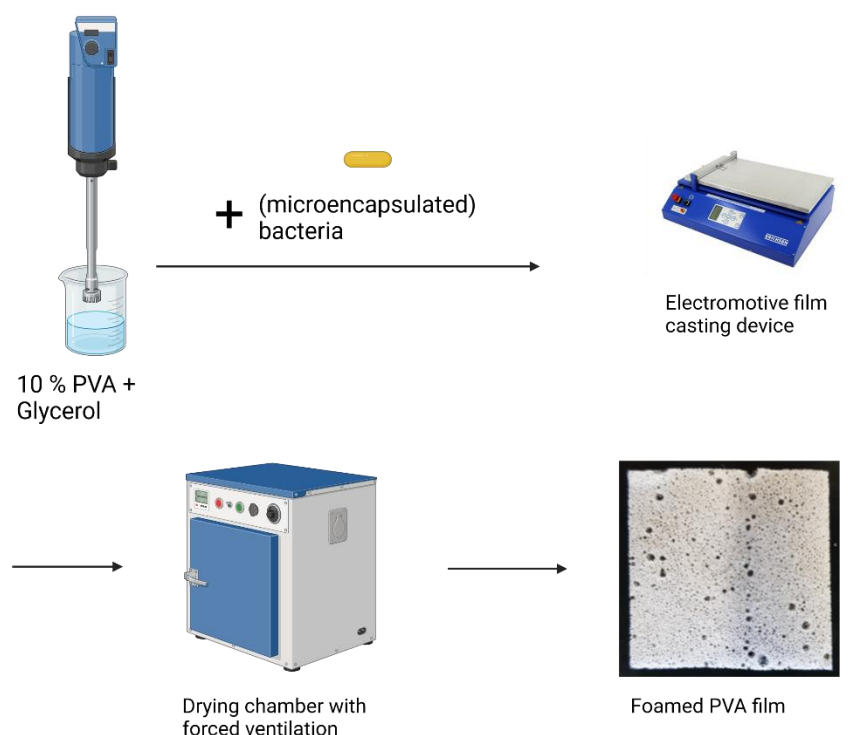


**Figure 4.1.** Schematic representation of the production of foamed PVA-films with incorporated probiotic bacteria.

First, a cooled 10% PVA solution, sterilized by autoclaving, was foamed using an Ultraturrax at maximum speed for 5 minutes. The (microencapsulated) bacteria in the stationary phase were then gently added by pipetting. The resulting dispersion was cast onto a Teflon film using an electromotive film casting device with a squeegee set to a 1000  $\mu\text{m}$  gap width. The film was dried at 37 °C with forced air circulation for 30 minutes, after which bacterial activity was assessed using the plate count method.

### 4.2.10. Foamed PVA Films with Bacteria filled Pores

The pores of the foamed PVA-films were filled with microencapsulated bacteria via vortexes, as described in section 3.2.4.4. The experiment was carried out with *L. rhamnosus* and *L. reuteri* microencapsulated via the two- and three-way nozzle. The activities were determined using the plate count method.

#### 4.2.11. Covered Polymer Films with Bacteria

To completely eliminate the stress of the film-drawing process on the bacteria, HPMC-PVA films—prepared as previously described—were coated with microencapsulated bacteria. To ensure a uniform distribution, the films were sprayed with bacterial powder using a DP4 Dry Powder Insufflator (Figure 4.2). The microencapsulated bacteria were weighed into the insufflator chamber and then dispersed onto the polymer film by applying compressed air via a syringe. Bacterial activity was subsequently assessed using the plate count method..



**Figure 4.2.** Schematic representation of the DP4 dry powder insufflator.

#### 4.2.12. Vacuum Dried Films

To accelerate drying, the polymer films were dried under vacuum conditions. HPMC-PVA films embedded with bacteria were prepared as previously described and then placed in a desiccator containing a dry granulate. The desiccator was fully evacuated to remove air, facilitating faster drying. Bacterial activity was quantified afterward using the plate count method.

#### 4.2.13. Cultivation of *L. reuteri* and *L. rhamnosus* in Liquid Culture<sup>2</sup>

Bacterial cultivation in liquid culture started by plating the bacteria on MRS Agar, followed by incubation at 36 °C and 5% CO<sub>2</sub> for 48 h. Colonies were picked and

transferred to MRS broth, undergoing incubation under aerobic conditions at 36 °C and 5% CO<sub>2</sub> for a 24-hour preculture. The 250 mL main culture (prewarmed MRS broth) was inoculated with 1 mL of preculture, and growth was monitored through measurement of OD 600. Following the determination of the growth curve, bacteria were cultivated until the late growth phase and stationary phase for survival comparison. Subsequently, bacteria were harvested by centrifugation (Figure 4.3) and incorporated into polymer films after microencapsulation, as described previously.

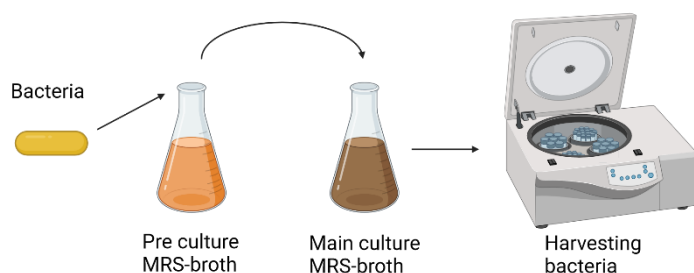


**Figure 4.3.** Schematic representation of bacterial cultivation.

### 4.2.14. Activation of Protection Mechanisms in Bacteria<sup>2</sup>

To enhance bacterial survival within polymer films, activation of various resistance mechanisms was pursued through two distinct test series. In each series, a preculture was established according to the mentioned procedure.

For cultivation under pH 5 conditions, the main culture, MRS broth pH 5, was inoculated from the preculture with 1 mL. The pH value of the medium was adjusted with concentrated hydrochloric acid, and its subsequent level was confirmed post-autoclaving. The flasks were subsequently incubated at 36 °C and 5% CO<sub>2</sub> until the stationary phase was attained, totalling a 16-hour incubation period.

In the salt shock treatment, the main culture, MRS broth pH 6.2, was inoculated with 1 mL of preculture. After a 6.5-hour incubation at OD 0.8, bacteria were centrifuged,

dispersed in MRS broth supplemented with 0.6 M NaCl, and incubated under standard conditions for a total duration of 16 h.

Upon reaching the stationary phase, bacteria were harvested through centrifugation, followed by microencapsulation achieved through spray-drying, followed by embedding in polymer films, as detailed previously.

### **4.2.15. Stability Testing**

The stability of HPMC-PVA films with embedded bacteria was subjected to analysis. In order to achieve this, pure bacteria and bacteria microencapsulated with the three-way nozzle were embedded in HPMC-PVA films using the film applicator. The samples were stored at room temperature (20 °C) and 4 °C, and the activity was determined after 0, 1, 4, 7, 14 and 20 days using the plate count method.

Additionally, the pure bacteria were embedded in HPMC-PVA polymer films, and their stability was tested at 4 °C after 0, 7, 14, 28, 42 and 58 days.

### 4.3. Results

#### 4.3.1. Survival of *L. reuteri* after Spray Drying<sup>2</sup>

*L. reuteri* was microencapsulated via spray-drying, utilizing Eudragit® EPO and RL30D polymers. The process employed both two-way and three-way nozzles, with each demonstrating effective bacterial survival rates. Notably, the three-way nozzle configuration resulted in enhanced viability of the microencapsulated *L. reuteri*, likely due to the reduced thermal stress and diminished mechanical shear forces compared to the two-way nozzle setup. This enhanced survival can be attributed to the polymer dispersion method, where the material is ejected through the outer spray channel, ensuring a lower internal temperature within the encapsulated particles, thereby

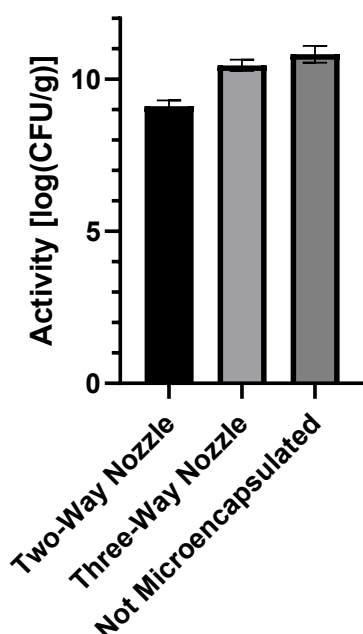


**Figure 4.5.** Viability of *L. reuteri* after microencapsulation using two- and three-way nozzles compared to freeze-dried reference bacteria prior to spray-drying. n=3, with standard deviation (SD).

offering additional protection to the bacteria. Overall, the survival of the untreated bacteria was 10.82 log(CFU/g) with a small SD of 0.27 log(CFU/g). The microencapsulation with the two-way nozzle led to a corrected activity (considering the additional mass of the polymer) of 9.113 log(CFU/g). The three-way nozzle showed a minor loss of activity of the bacteria with a value of 10.46 log(CFU/g) (Figure 4.5).

### 4.3.2. Survival of *L. rhamnosus* after Spray Drying

As with *L. reuteri*, the *L. rhamnosus* bacteria were microencapsulated via spray drying, utilizing both two- and three-way nozzles.

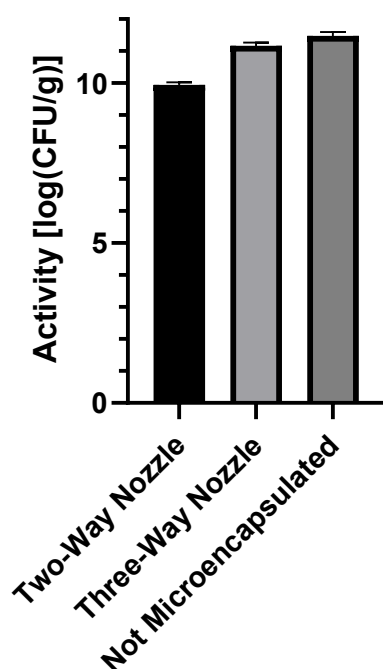


**Figure 4.6.** Viability of *L. rhamnosus* after microencapsulation using two- and three-way nozzles compared to freeze-dried reference bacteria prior to spray-drying. n=3, with standard deviation (SD).

The activities are illustrated in Figure 4.6. The freeze-dried *L. rhamnosus* exhibited an activity of 11.48 log(CFU/g), which exhibited only a slight decrease to 11.17 log(CFU/g) when microencapsulated using a three-way nozzle. The activity with microencapsulation via the two-way nozzle exhibits a slight decline, reaching 9.95 log(CFU/g).

### 4.3.3. Morphology of Microencapsulated *L. reuteri*<sup>2</sup>

The morphology was determined using microencapsulated *L. reuteri* as the microencapsulation of *L. rhamnosus* took place in exactly the same way and the bacteria behaved in the same way, no extra visualization was needed. The bacteria exhibited comparable properties, morphology, and dimensions, necessitating the execution of dissolution testing with one of the two bacteria.

As the intention of the process was the encapsulation of the probiotics into the polymer matrix SEM was used to analyse the morphology (Fig. 4.7). For both encapsulation approaches using the two-way and the three-way nozzle, no free bacteria were observed on the SEM samples. Spray-drying resulted mainly in spherical objects which smooth surfaces indicating the polymer being the outer layer of the objects. The fact that no free bacteria are visible points to the fact that all bacteria are incorporated demonstrating the effectiveness of the microencapsulation process. The different fine structure when spraying without polymer is depicted in Figure 4.7 C. It shows *L. reuteri* spray-dried without the addition of Eudragit® revealing round particles consisting of rod-shaped bacteria. The figure and the differences in the surface morphology demonstrate that the presence of the polymers led to the smooth surfaces surrounding the probiotics by a polymer layer.

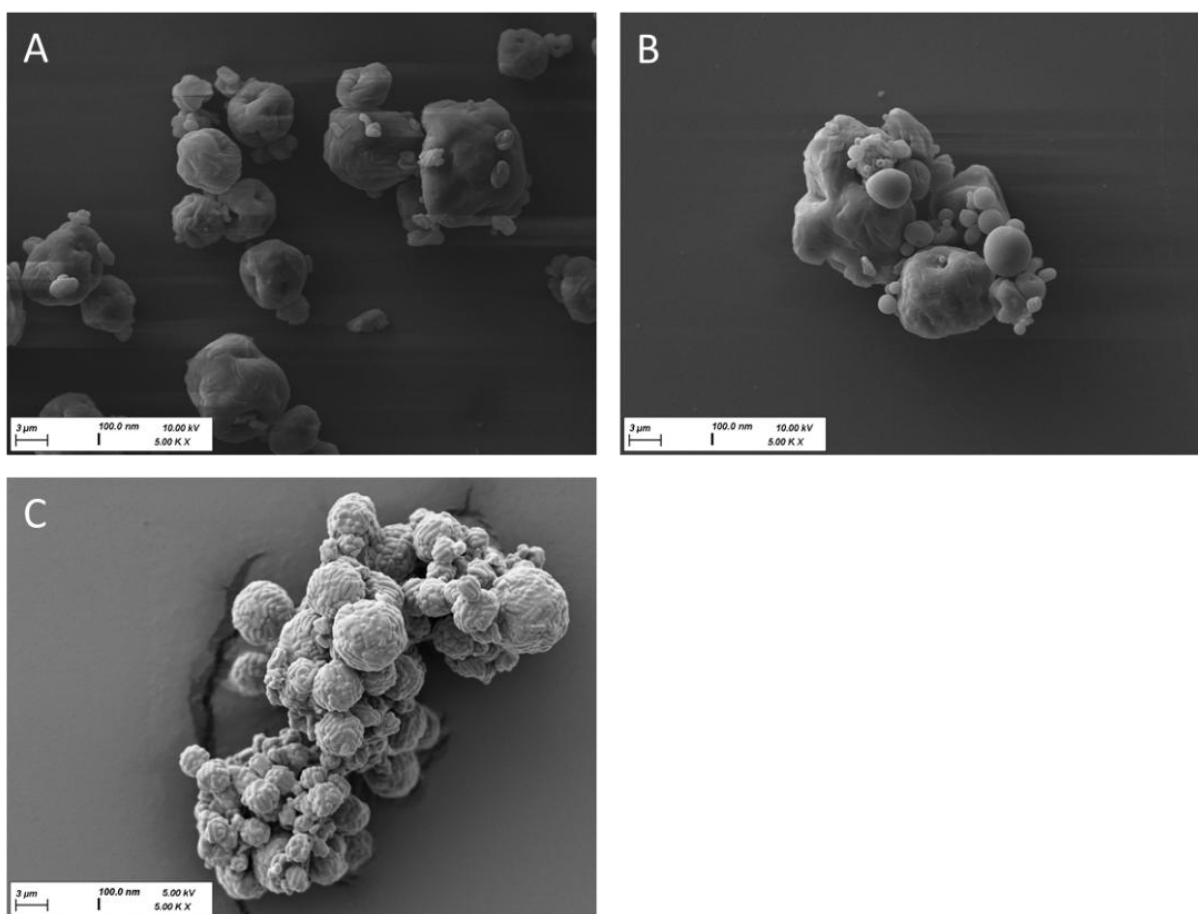


**Figure 4.7.** SEM images A) *L. reuteri* microencapsulated via two-way nozzle; B) *L. reuteri* microencapsulated via three-way nozzle. C) For comparison, *L. reuteri* was spray-dried without Eudragit® EPO and RL30D.

Following the success of microencapsulation in both experimental setups and the observed high survival during spray-drying using the three-way nozzle, it was used for subsequent investigations.

### 4.3.4. Investigation of Core-Shell Structure<sup>2</sup>

In order to investigate the internal structure of the spray-dried objects, the microorganisms were stained with Syto 9, a green-fluorescent dye that is able to stain living cells.

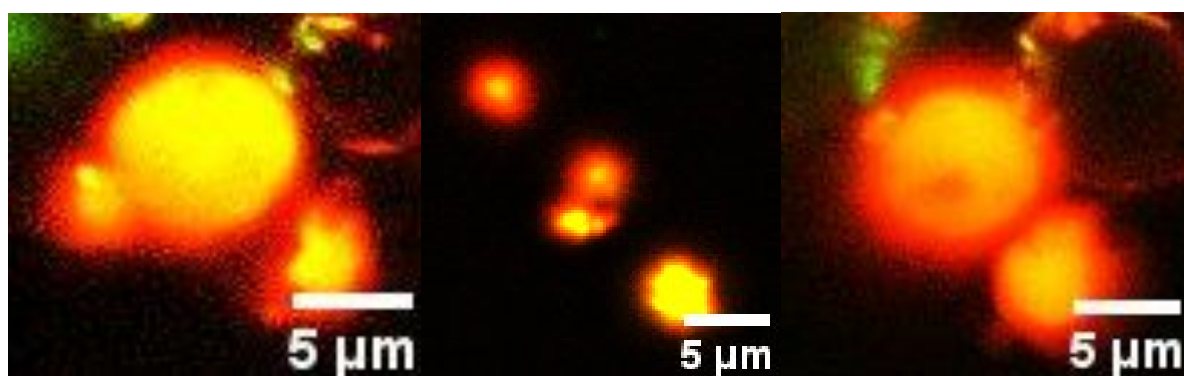


**Figure 4.8.** CLSM images show *L. reuteri* stained with SYTO 9 and microencapsulated with Eudragit® EPO, RL & S, labelled with BODIPY, and RL30D. Three distinct samples were subjected to analysis, and the data from the channels were merged. n=3

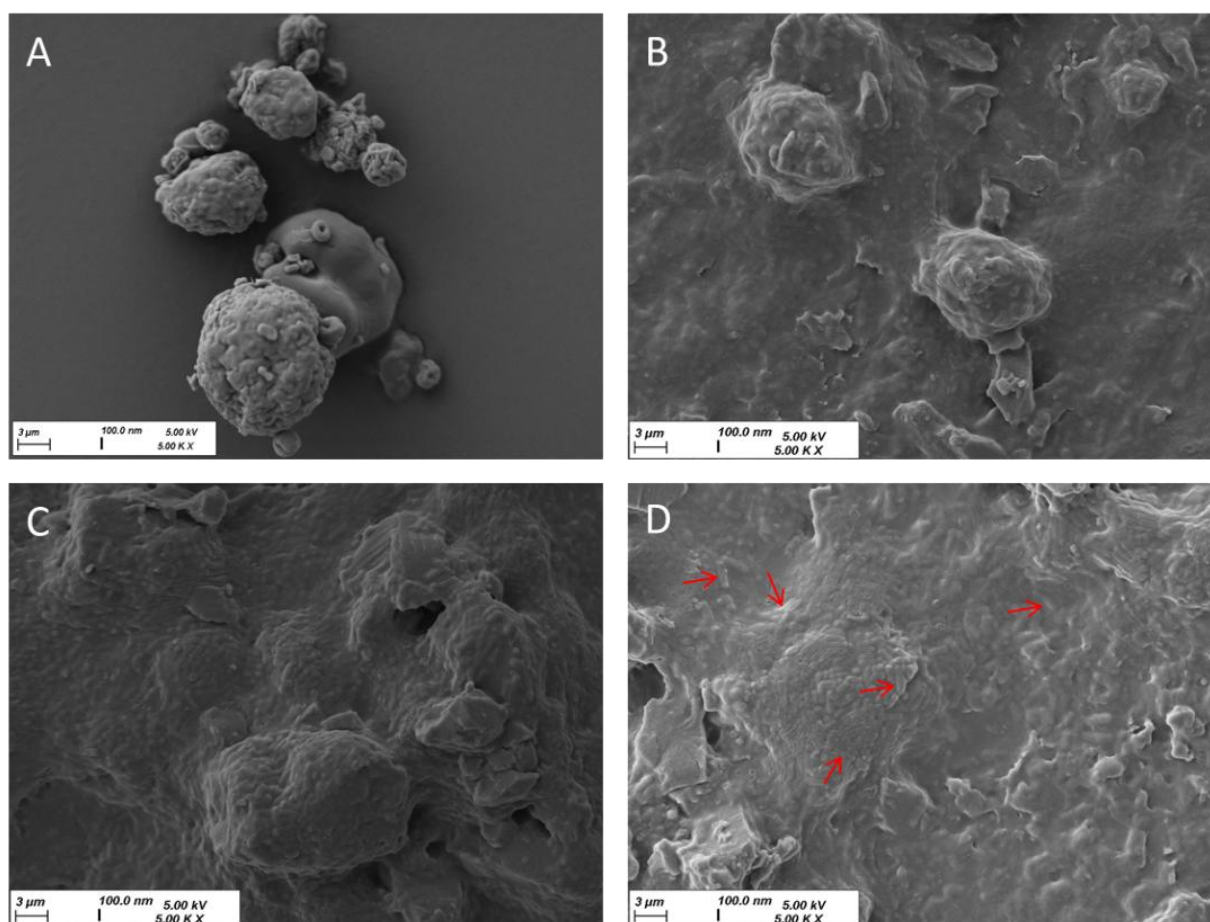
Figure 4.8 illustrates the formation of a core-shell structure, wherein the bacteria stained with Syto 9 (in green) are encapsulated by Eudragit® EPO, RL30D and S conjugated with BODIPY (in red) as a dye. The particles exhibit a red shell on the exterior, while the interior displays the stained bacteria colocalized with the Eudragit® S-BODIPY (red signal) leading to the yellow colour in the merged images.

### 4.3.5. Dissolution of Microencapsulated *L. reuteri*<sup>2</sup> (Three-Way-Nozzle)

SEM images from Figure 4.9 demonstrate that particle dissolution begins after only 30 min being exposed to 100% air humidity, resulting in the presence of identifiable free bacteria. The particles start to dissolve and free rod shaped bacteria are detectable in the dissolved polymer matrix together with particulate structures (Fig. 4.9 B, C). After



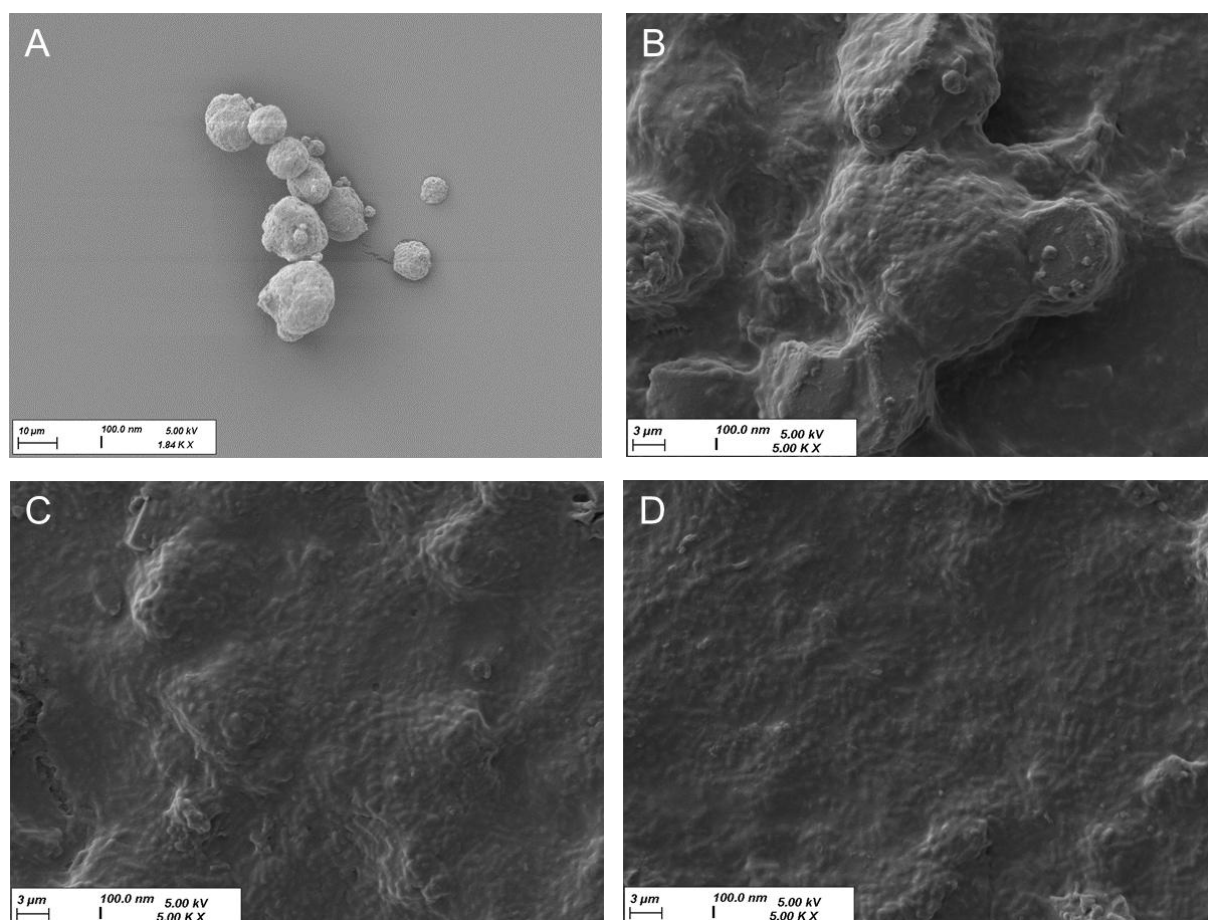
120 min, the dissolution process has led to a residual polymer film with free bacteria. The bacteria can be identified by their rod-shaped structure, which is slightly elevated from the background. In order to identify them more easily, some of the bacteria are marked with red arrows in Figure 4.9 C. The transformation of the two compounds from particles to films is expected as the polymer cannot leave the place of disintegration due to the interface-bound dissolution process. Thus, the change in morphology is what is expected and indicating the successful initiation of the release process.



**Figure 4.9.** Series of SEM micrographs illustrating the dissolution of microencapsulated *L. reuteri* on 1.5% agarose gel patches at 36 °C and 100% relative humidity. The bacteria were microencapsulated via the three-way nozzle. Samples were imaged after different incubation times A: 0 minutes, B: 30 minutes, C: 60 minutes, and D: 120 minutes. The arrows exemplify free, individual bacteria visible on the film.

#### 4.3.6. Dissolution of Microencapsulated *L. reuteri* (Three-Way Nozzle)

The dissolution of microencapsulated bacteria from the two-way nozzle was assessed using a 1.5% agarose gel patch incubated at 36 °C and 100% relative humidity, following the methodology previously used for microcapsules produced with the three-way nozzle.



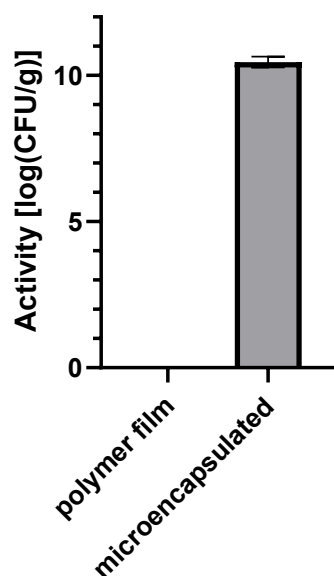
**Figure 4.10.** Dissolution of microencapsulated *L. reuteri*. The bacteria were microencapsulated via the two-way nozzle. Series of SEM micrographs illustrating the dissolution of microencapsulated *L. reuteri* (Two-way nozzle) on 1.5% agarose gel patches at 36 °C and 100% relative humidity. Samples were imaged after different incubation times **A**: 0 minutes, **B**: 30 minutes, **C**: 60 minutes, and **D**: 120 minutes.

Figure 4.10 A shows the microcapsules at the initial time point, where no free, rod-shaped bacteria are visible, but particles encased in a uniform polymer layer are observed. Figure 4.10 B illustrates the beginning of particle dissolution after 30 minutes, with initial free bacteria identified by their rod-like shape. Dissolution

progresses further, and by 60 minutes (Figure 4.10 C), remaining particles appear wavy, with many free, rod-shaped bacteria present. At 120 minutes (Figure 4.10 D), only free, rod-shaped bacteria and polymer residues are visible, with no remaining particles detected.

### 4.3.7. Survival Embedding *L. reuteri* inside Polymer Films<sup>2</sup>

Following the successful preparation of microencapsulated *L. reuteri*, the probiotic bacteria were incorporated into polymeric films, allowing for direct application to the site of action in the oral cavity. After spray-drying the microencapsulated bacteria, they were directly mixed with the polymer dispersion and then cast using an electronic film casting device. The drying time was approximately 1.5 hours at 37 °C and with forced ventilation.



**Figure 4.11.** Assessment of *L. reuteri* survival embedded within polymer films subsequent to microencapsulation (three-way nozzle) in comparison to only spray-dried bacteria. n=3, with standard deviation (SD).

The results indicate that the bacteria did not survive the embedding process in the polymer films after being microencapsulated directly from the lyophilized powder after purification (Fig 4.11). With the respective dilution step for plating (1:100) no living

microorganisms could be identified although the starting values after microencapsulation were high (10.82 log(CFU/g)).

### 4.3.8. Survival Embedding *L. rhamnosus* inside Polymer Films

In the case of *L. rhamnosus*, the microencapsulated bacteria were also embedded in an HPMC-PVA polymer film using a three-way nozzle. Similarly, the methodology employed was consistent with that utilized for the films comprising *L. reuteri*.

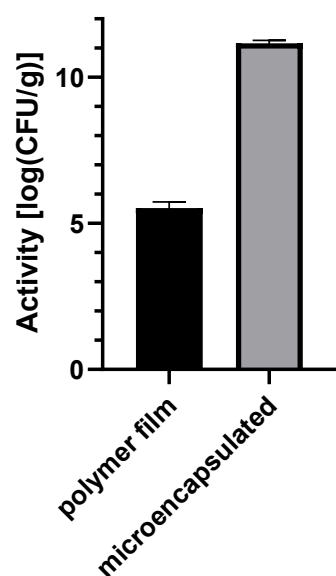


**Figure 4.12.** Assessment of *L. rhamnosus* survival embedded within polymer films subsequent to microencapsulation (three-way nozzle) in comparison to only spray-dried bacteria. n=3, with standard deviation (SD).

Figure 4.12 illustrates the activity of the microencapsulated *L. rhamnosus* before and after embedding. Following microencapsulation, the bacteria exhibited an activity level of 11.17 log(CFU/g), which subsequently decreased to 5.52 log(CFU/g) following the production of the film.

### 4.3.9. Survival Bacteria inside Hand-Cast Polymer Films

A straightforward method for producing robust films involves manual casting. Due to their higher mass, these films require an extended drying time of 12 hours at 37 °C with forced air circulation.

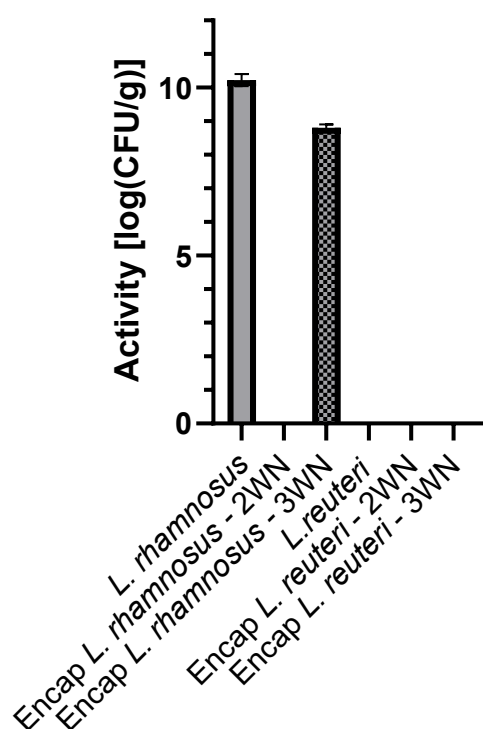


**Figure 4.13.** Assessment of *L. reuteri* and *L. rhamnosus* survival embedded within hand-cast polymer films out of HPMC-PVA. Activity of microencapsulated bacteria can be found in 4.3.1 and 4.3.2 and is stated in the text.  $n=3$ , with standard deviation (SD).

*L. reuteri* exhibited no detectable activity even at a low dilution of 1:100. Pure *L. rhamnosus* (Figure 4.13) within the film showed only a slight reduction in activity, with 10.23 log(CFU/g) compared to the initial 11.48 log(CFU/g). Microencapsulated bacteria produced with the two-way nozzle showed no activity, whereas those from the three-way nozzle retained an activity of 8.80 log(CFU/g), compared to the initial 11.17 log(CFU/g). This finding indicates that the three-way nozzle was the most effective method for preserving the activity in this case.

### 4.3.10. Survival Probiotic Polymer Films at Different Drying Conditions

The activity of microencapsulated *L. reuteri* and *L. rhamnosus* is strongly influenced by their incorporation into films following microencapsulation, as previously demonstrated. Figure 4.14 A presents the activities of these bacteria after embedding in an HPMC-PVA film and drying at room temperature without forced air circulation, a process that required 5 hours for complete drying. Unlike *L. reuteri*, *L. rhamnosus* retained activity post-embedding. Specifically, *L. rhamnosus* microencapsulated with the two-way nozzle showed an activity of 5.10 log(CFU/g), while those microencapsulated with the three-way nozzle exhibited an activity of 5.52 log(CFU/g).

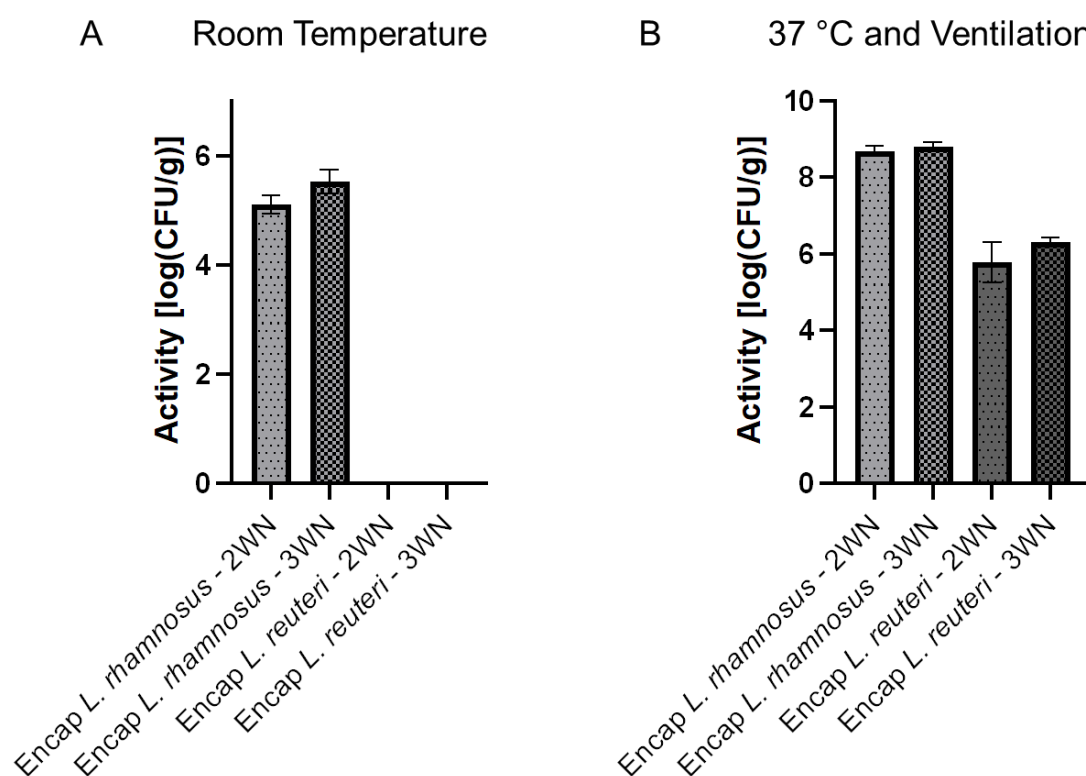


**Figure 4.14.** Assessment of *L. reuteri* and *L. rhamnosus* survival embedded within polymer films subsequent to microencapsulation **A**: polymer film dried at room temperature **B**: polymer film dried at 37 °C with forced ventilation n=3, with standard deviation (SD).

The drying process was optimized by drying the films at 37 °C with forced air circulation, reducing the drying time to 1.5 hours and enhancing bacterial activity (Figure 4.14 B). *L. rhamnosus* displayed activities of 8.70 log(CFU/g) for the two-way

nozzle and 8.81 log(CFU/g) for the three-way nozzle. *L. reuteri* also retained activity within the polymer films, showing 5.78 log(CFU/g) after microencapsulation with the two-way nozzle and 6.31 log(CFU/g) with the three-way nozzle. The bacteria used in this experiment originated from a freeze-dried starting product.

## Freeze-Dried Polymer Films

Freeze-drying, a widely used and gentle drying technique, was employed to develop two formulations: one containing 10% HPMC and the other 10% PVA, each supplemented with 20% glycerol (of the total polymer content). The osmolarity of these polymer dispersions was measured, yielding 0.278 osmol/kg for the HPMC dispersion and 0.308 osmol/kg for the PVA dispersion. These values approach isotonic conditions for bacteria, indicating minimal risk of osmotic stress.

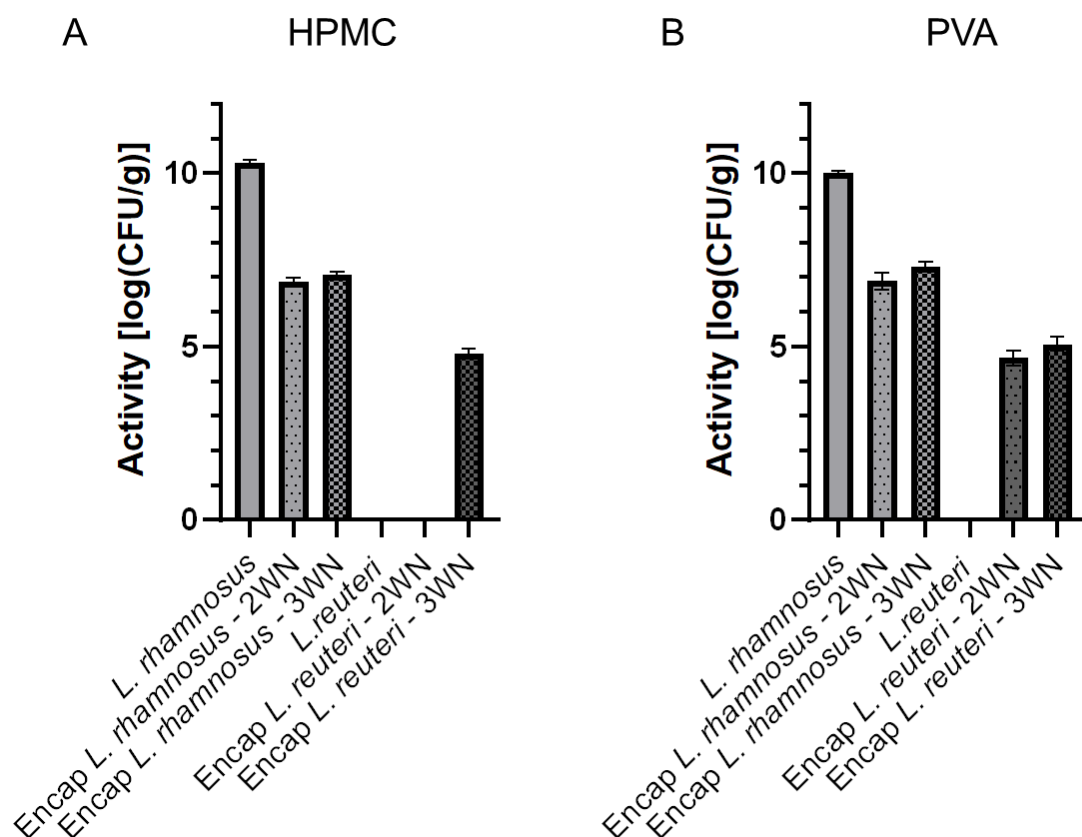


**Figure 4.15.** Assessment of (microencapsulated) *L. reuteri* and *L. rhamnosus* survival embedded within freeze-dried polymer films **A:** Polymer film out of HPMC **B:** polymer film out of PVA. n=3, with standard deviation (SD).

Bacterial activity was further enhanced through freeze-drying. For *L. rhamnosus* in the freeze-dried HPMC film (Figure 4.15 A), activity levels reached 10.32 log(CFU/g) in the pure form. After microencapsulation with the two-way nozzle, activity was 6.88 log(CFU/g), and with the three-way nozzle, slightly higher at 7.08 log(CFU/g). *L. reuteri* survival in the freeze-dried HPMC film was not observed for the pure bacteria or for those microencapsulated with the two-way nozzle, with no detectable activity even at a dilution of 1:100. However, an activity of 4.80 log(CFU/g) was observed for bacteria microencapsulated with the three-way nozzle and embedded in the freeze-dried HPMC film.

A similar trend was observed for bacteria embedded in the freeze-dried PVA film (Figure 4. 15 B). Pure *L. rhamnosus* displayed an activity of 10.00 log(CFU/g), while the two-way nozzle microencapsulated bacteria showed an activity of 6.89 log(CFU/g), and the three-way nozzle microencapsulated bacteria exhibited an activity of 7.32 log(CFU/g). *L. reuteri* showed slightly improved survival in the freeze-dried PVA film compared to the HPMC film. Although no activity was detected for pure *L. reuteri*, microencapsulated bacteria retained detectable activity: 4.67 log(CFU/g) with the two-way nozzle and 5.08 log(CFU/g) with the three-way nozzle. In this context, microencapsulation technology can be regarded as having certain advantages.

### **4.3.12. Foamed PVA Films with Incorporated Bacteria**

The drying time was further reduced to 30 minutes at 37 °C with forced air circulation by using foamed PVA films. Unlike the previously described method (Chapter 3), this formulation involved directly incorporating the bacteria into the film, achieving a faster drying process. Both pure bacteria and microencapsulated bacteria with the three-way nozzle were incorporated into the foamed PVA films. Given the consistently lower activity of the bacteria microencapsulated with the two-way nozzle in the preceding experiments, this formulation was not subjected to further testing.



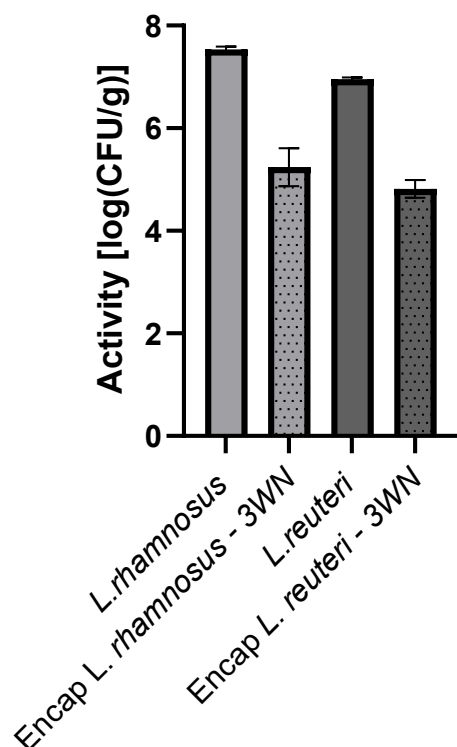


**Figure 4.16.** Assessment of (microencapsulated) *L. reuteri* and *L. rhamnosus* survival embedded within foamed PVA. n=3, with standard deviation (SD).

The activity of *L. rhamnosus* in the foamed PVA films was 7.54 log(CFU/g) for the pure form and 5.24 log(CFU/g) for the microencapsulated form. For *L. reuteri*, the activity was 6.96 log(CFU/g) in the pure form and 4.82 log(CFU/g) after microencapsulation, as shown in figure 4.16.

#### 4.3.13. Foamed PVA Films with Bacteria filled in Pores

The microencapsulated bacteria that were loaded into the pores of the foamed PVA films showed no changes in activity. The microencapsulation of the bacteria was not affected by the loading via the vortex.

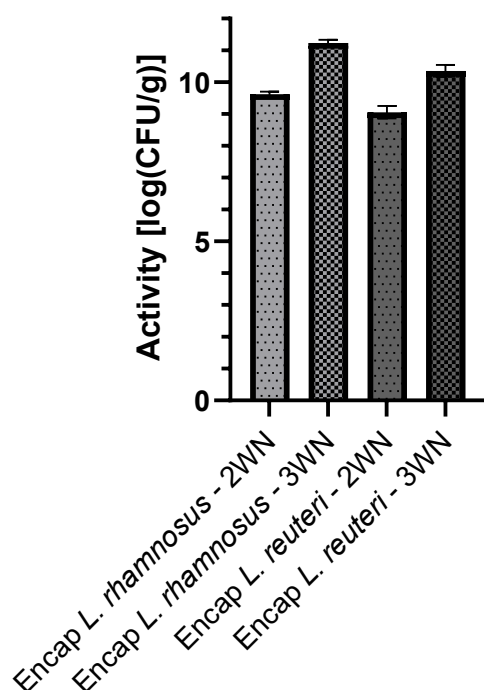


**Figure 4.17.** Assessment of microencapsulated *L. reuteri* and *L. rhamnosus* survival embedded inside pores of foamed PVA-films.  $n=3$ , with standard deviation (SD).

The activities are shown in Figure 4.17. *L. rhamnosus* microencapsulated with the two-substance nozzle shows an activity of 9.62 log(CFU/g) and after microencapsulation with the three-substance nozzle and embedding in the pores of the film 11.24 log(CFU/g). The microencapsulated *L. reuteri* also showed no reduction in activity after embedding in the foamed PVA film. After microencapsulation of the two-way nozzle 9.10 log(CFU/g) and after microencapsulation with the three-way nozzle 10.36 log(CFU/g). The activities directly after microencapsulation can be found in chapters 4.5.1 and 4.5.2.

#### 4.3.14. Polymer Films with Covered Bacteria

To eliminate the need for a drying process, HPMC-PVA polymer films were coated directly with microencapsulated bacteria. This was achieved by loading a DP4 Dry Powder Insufflator with microencapsulated bacteria and evenly dusting the film with the powder, using a syringe for application. To improve powder adhesion, the film was pre-moistened with MilliQ water and allowed to dry. Notably, the spraying process preserved bacterial viability, with *L. rhamnosus* showing an activity of 9.95 log(CFU/g)

when microencapsulated with the two-way nozzle, and 11.17 log(CFU/g) with the three-way nozzle, shown in Figure 4.18. *L. reuteri* demonstrated activities of 9.19 log(CFU/g) with the two-way nozzle and 10.12 log(CFU/g) with the three-way nozzle (Figure 4.18).

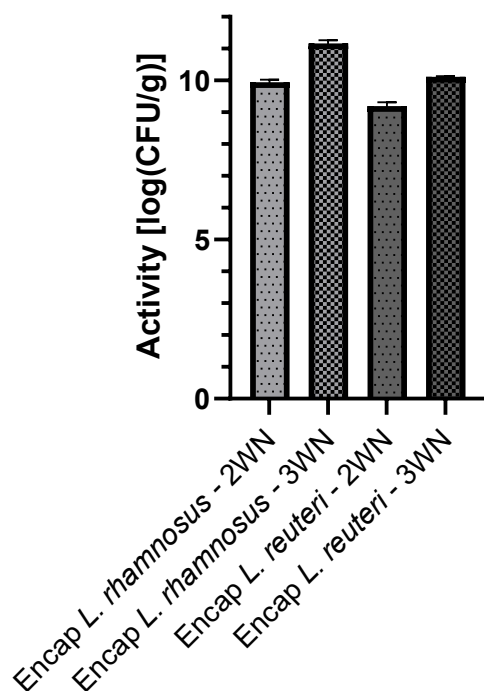


**Figure 4.18.** Assessment of microencapsulated *L. reuteri* and *L. rhamnosus* survival sprayed on top of HPMC-PVA films. n=3, with standard deviation (SD).

However, a limitation of this approach is the poor adhesion of the bacterial coating to the polymer films, which could affect product stability and bacterial retention. This trade-off between preserving bacterial viability and achieving stable film adhesion suggests that further optimization is needed to enhance the adhesion without compromising bacterial activity, in an appropriate amount.

### 4.3.15. Vacuum-Dried Polymer Films

Another approach to accelerate the drying process involves reducing ambient pressure. For this method, HPMC-PVA films were placed in a fully evacuated desiccator containing dry granules immediately after casting. The drying time remained constant at 1.5 hours. Figure 4.19 shows that under these conditions, *L. rhamnosus*

retained a high activity level of 10.44 log(CFU/g) in its pure form, though activity decreased to 4.21 log(CFU/g) after microencapsulation. In contrast, *L. reuteri* showed no detectable activity in either its pure or microencapsulated state after film casting and vacuum drying.

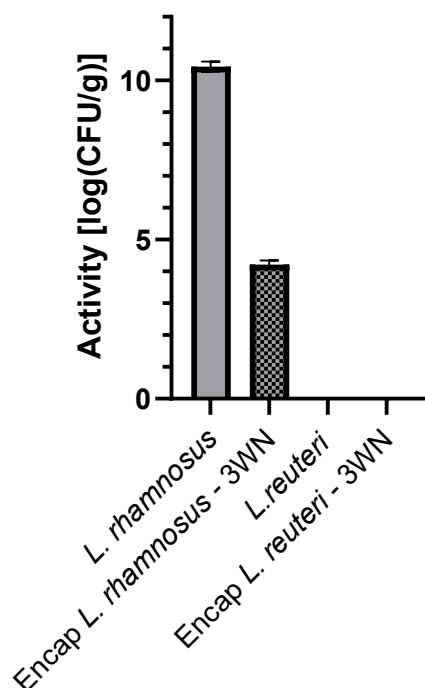


**Figure 4.19.** Assessment of (microencapsulated) *L. reuteri* and *L. rhamnosus* survival embedded within HPMC-PVA films, dried in vacuum. n=3, with standard deviation (SD).

### 4.3.16. Liquid Cultivation and Determination of Growth Curve (*L. reuteri*)<sup>2</sup>

To understand the factors influencing bacterial survival the effect of the status of bacterial growth was investigated. To improve the survivability of bacteria within films, liquid cultures were produced and the different growth phases were identified. To ensure uniform growth of all bacteria and prevent potential damage coming from the original freeze-drying process for commercial distribution.

The growth curve (Fig 4.20 A) illustrates the achievement of the stationary phase after 16 h. In subsequent experiments, *L. reuteri* was microencapsulated in the late growth

phase after 11 h to ensure adequate biomass development. Additionally, in the stationary phase after 16 h of incubation, microencapsulation was conducted through spray-drying.

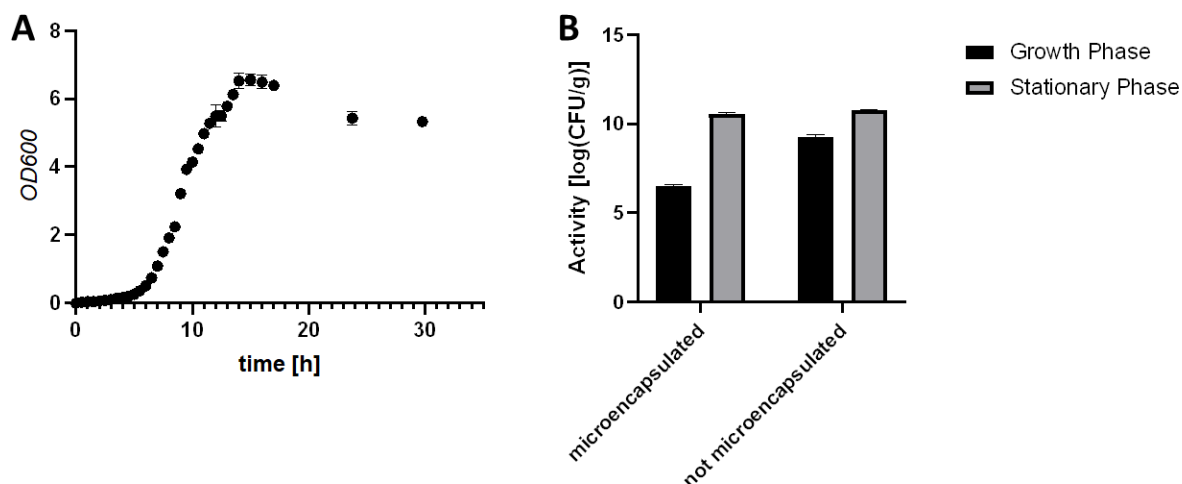


**Figure 4.20. A.** *L. reuteri* growth curve, incubated at 36 °C and 5% CO<sub>2</sub>; n=3 with standard deviation **B.** Survival of *L. reuteri* was recorded before and after microencapsulation in the growth phase (11 h) and stationary phase (16 h); n=3 with standard deviation.

Figure 4.20 B depicts that the survival of spray-dried bacteria decreases during the growth phase but remains unaffected using bacteria taken from the stationary phase. The microcapsules obtained were then incorporated into polymer films, and their survival was evaluated. No bacterial survival was observed post-embedding from bacteria of the growth phase into the polymer films. This outcome was, in some sense, predictable as the activity was already challenged during spray-drying in contrast to the bacteria spray-dried from the stationary phase (Fig 4.21). An improved activity was observed for the bacteria processed from the stationary phase. A bacterial activity after microencapsulation (10.54 log(CFU/g) and film formation with 4.76 log(CFU/g) could be observed.

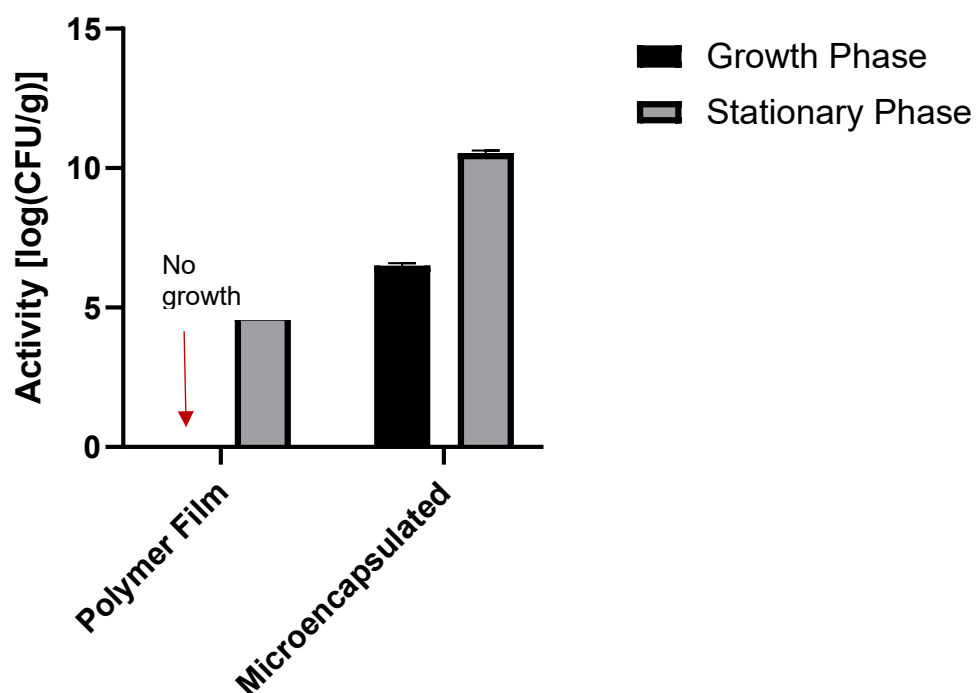


**Figure 4.21.** Survival of microencapsulated *L. reuteri* was assessed during the growth phase (11 h) and stationary phase (16 h), both before and after embedded in polymer films. n=3 with standard deviation.

#### 4.3.17. Liquid Cultivation and Determination of Growth Curve (*L. rhamnosus*)

In addition to the for publication prepared data from *L. reuteri*, all experiments were also conducted with *L. rhamnosus*. Precisely the same methodology was employed in each case.

The growth curve of *L. rhamnosus* was analyzed by measuring optical density at 600 nm, showing that the bacteria reached the stationary phase after 17 h (Figure 4.22 A).

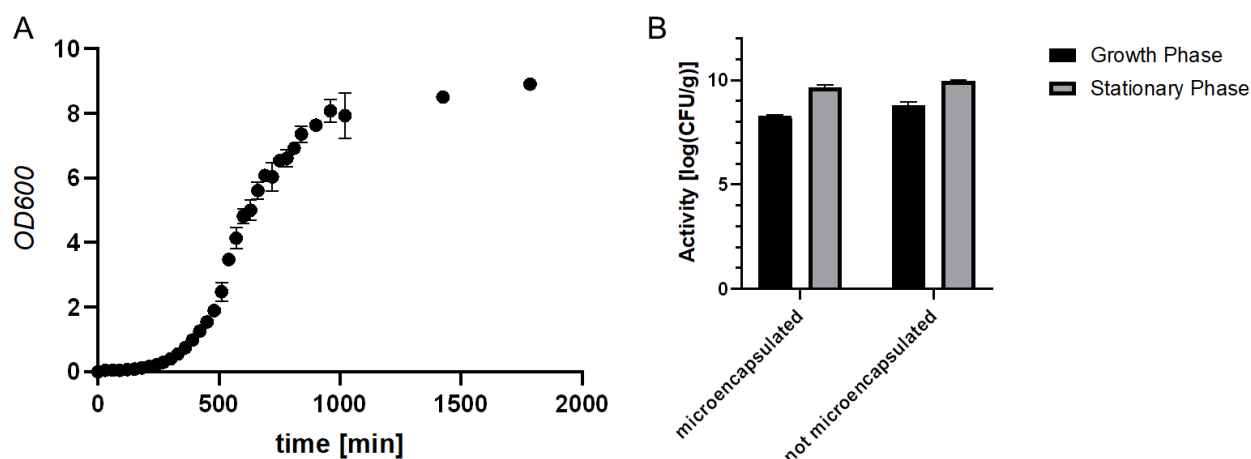


**Figure 4.22. A.** *L. rhamnosus* growth curve, incubated at 36 °C and 5% CO<sub>2</sub>; n=3 with standard deviation **B.** Survival of *L. rhamnosus* was recorded before and after microencapsulation in the growth phase (12 h) and stationary phase (17 h); n=3 with standard deviation.

*L. rhamnosus* cultures grown in MRS Bouillon were microencapsulated at different growth stages, and activity levels were measured before and after encapsulation. Microencapsulation was done after 12 hours, marking the late growth phase, and after 17 hours, at the stationary phase. In the late growth phase, bacterial activity was 8.79 log(CFU/g) before microencapsulation, decreasing only slightly to 8.28 log(CFU/g) after encapsulation with the three-way nozzle. In the stationary phase, *L. rhamnosus* maintained robust activity, with initial counts of 9.96 log(CFU/g) dropping minimally to 9.66 log(CFU/g) post-encapsulation.

After microencapsulation, the bacteria were embedded in HPMC-PVA polymer films (Figure 4.23). Notably, activity during the growth phase showed a significant reduction, with bacterial counts declining to 4.58 log(CFU/g) due to film casting, indicating that bacteria in the growth phase are more sensitive to the embedding process. Conversely, in the stationary phase, bacteria exhibited reduced sensitivity to film casting, retaining an activity of 9.17 log(CFU/g) after embedding.

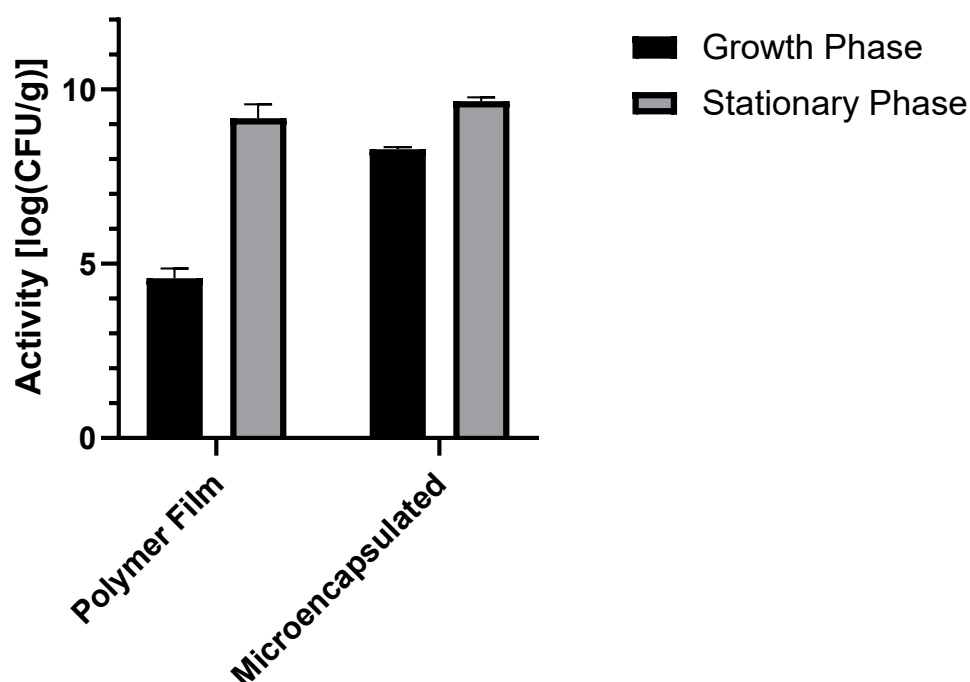


**Figure 4.23.** Survival of microencapsulated *L. rhamnosus* was assessed during the growth phase (12 h) and stationary phase (17 h), both before and after embedded in polymer films. n=3 with standard deviation.

#### 4.3.18. Microencapsulating after Cultivation under Osmotic Stress and Film Formation (*L. reuteri*)<sup>2</sup>

The growth phase had a slight impact on the activity of the treated bacteria, prompting the investigation of other parameters that might influence bacterial survival. Harsh osmotic conditions were chosen to challenge and stimulate *L. reuteri*.

The survival of *L. reuteri* after cultivation with the addition of 0.6 M NaCl was analyzed after spray-drying and embedding in polymer films. Spray-drying had only a slight effect on the activity (9.79 log(CFU/g)) with a standard deviation of 0.03 log(CFU/g). This represents a loss of 0.75 log(CFU/g). The activity was reduced by embedding the bacteria in the polymer film (to 4.31 log(CFU/g)) as shown in Figure 4.24. This reflects a slight deterioration compared to bacteria cultured in pure MRS broth and embedded in the polymer film with an activity of 4.76 log(CFU/g) (Fig 7).



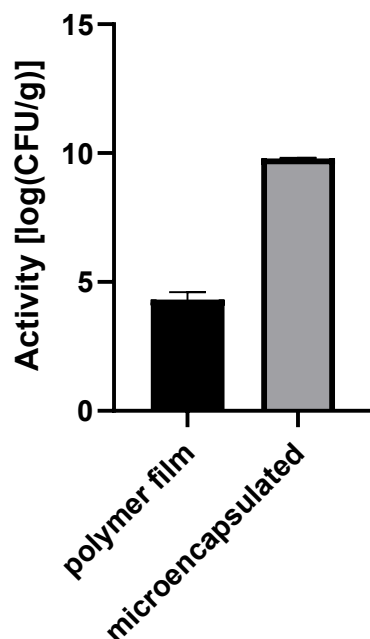


**Figure 4.24.** Survival of *L. reuteri* after microencapsulation and embedding in polymer films, following prior cultivation in MRS broth supplemented with 0.6M NaCl for 16 h. n=3 with standard deviation.

#### 4.3.19. Microencapsulation after Cultivation under Osmotic Stress and Film Formation (*L. rhamnosus*)

Given that the activity of *L. rhamnosus* was also most effectively preserved in the stationary phase, further research was conducted with bacteria in this phase. Furthermore, the impact of various cultivation conditions on the activity of *L. rhamnosus* was examined. To this end, the bacteria were harvested from an OD600 of 0.8, the main culture, and subsequently cultivated in a hyperosmolar medium with the addition of 0.6 M NaCl until the stationary phase was reached.

Following microencapsulation, an activity of 9.25 log(CFU/g) was achieved, while subsequent film embedding resulted in an activity of 3.51 log(CFU/g) (Figure 4.25). This indicates a decline in bacterial activity resulting from the addition of NaCl, particularly following the embedding of the bacteria in polymer films.

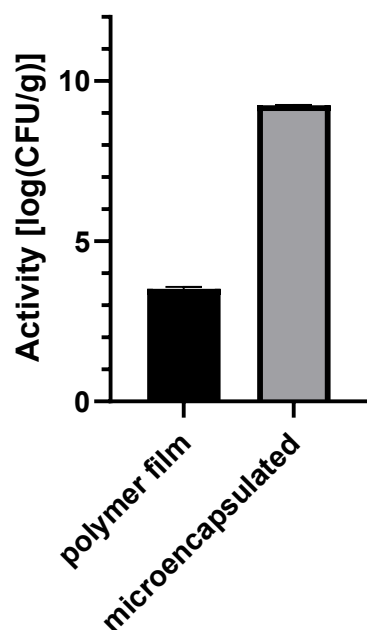


**Figure 4.25.** Survival of *L. rhamnosus* after microencapsulation and embedding in polymer films, following prior cultivation in MRS broth supplemented with 0.6M NaCl for 17 h. n=3 with standard deviation.

#### 4.3.20. Microencapsulation after Cultivation under Acidic Conditions and Film Formation (*L. reuteri*)<sup>2</sup>

In order to stimulate the activation of further metabolic pathways, the bacteria were cultivated in MRS broth at pH 5 following a preculture at pH 6.2.

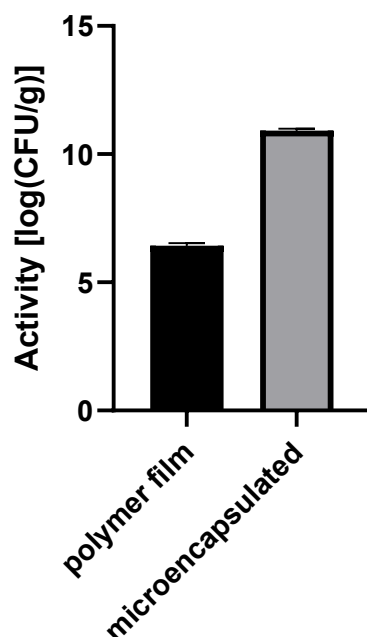


**Figure 4.26.** Survival of *L. reuteri* after microencapsulation and embedding in polymer films, following prior cultivation at pH 5 for 16 h. n=3 with standard deviation.

Figure 4.26 shows the survival of *L. reuteri* after microencapsulation and additional embedding in the polymer film after cultivation at pH 5. Spray-drying did not affect survival as also observed for the osmotic shock (Fig. 4.23). This time, the embedding in the polymer films led to an improved survival with an activity of 6.43 log(CFU/g) compared to 4.76 log(CFU/g) after cultivation in pure MRS broth (Fig 7).

#### **4.3.21. Microencapsulation after Cultivation under Acidic Conditions and Film Formation (*L. rhamnosus*)**

*L. rhamnosus* was also cultivated at a pH of 5 to examine the effect of a more acidic environment on bacterial growth and viability. This variation in pH could potentially influence the growth rate, encapsulation efficiency, and survival during subsequent embedding in polymer films. Further analysis would involve comparing the growth curves, activity levels, and survival rates of *L. rhamnosus* cultivated at this lower pH to those grown under standard pH conditions.

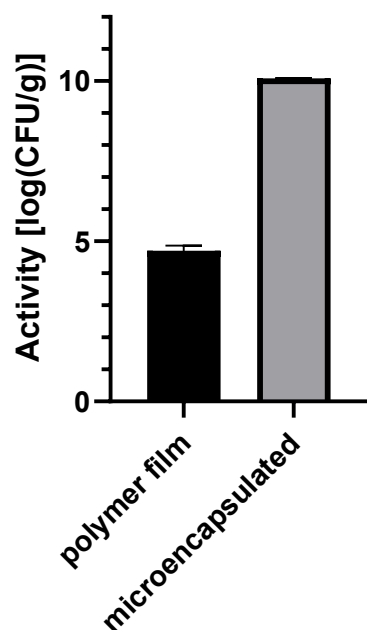


**Figure 4.27.** Survival of *L. rhamnosus* after microencapsulation and embedding in polymer films, following prior cultivation at pH 5 for 17 h. n=3 with standard deviation.

Following microencapsulation, the activity was observed to be marginally higher than that observed prior to encapsulation when cultivated in pure MRS bouillon, reaching 10.08 log(CFU/g). However, embedding the material in the polymer film resulted in a notable loss, with the activity reducing to 4.70 log(CFU/g) (Figure 4.27).

#### 4.3.22. Microencapsulation after Cultivation under Acidic Conditions and Osmotic Shock Followed by Film Formation<sup>2</sup>

The results of combining both methods (acidic conditions plus osmotic shock) to challenge the probiotics are shown in figure 4.28. The activity of the bacteria after microencapsulation had a small adverse effect (8.27 log(CFU/g)) when two methods to challenge *L. reuteri* were applied (pH 5 and 0.6 M NaCl).

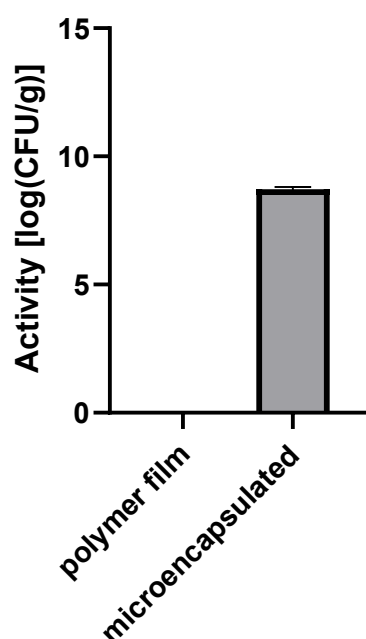


**Figure 4.28.** Survival of *L. reuteri* after microencapsulation and embedding in polymer films, following prior cultivation at pH 5 and addition of 0.6 M NaCl for 16 h. n=3 with standard deviation.

However, it is noteworthy that no bacterial activity was detectable after the extraction from the polymer films, indicating a huge loss of viability during the film processing stage in consequence of the combination of osmotic shock and the reduced pH.

#### 4.3.23. Microencapsulation after Cultivation under Acidic Conditions and Osmotic Shock Followed by Film Formation (*L. rhamnosus*)

The combination of both conditions (acidic conditions plus osmotic shock) did not yield the desired outcome with *L. rhamnosus*. Figure 4.29 illustrates that an activity of 7.82 log(CFU/g) is still achieved following microencapsulation. However, no activity can be detected after embedding in the HPMC-PVA film.

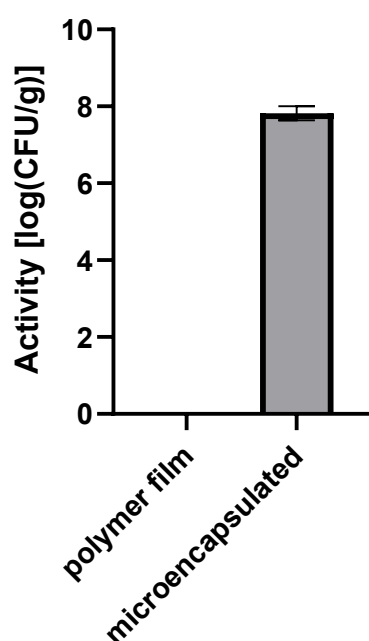


**Figure 4.29.** Survival of *L. rhamnosus* after microencapsulation (three-way nozzle) and embedding in polymer films, following prior cultivation at pH 5 and addition of 0.6 M NaCl for 17 h. n=3 with standard deviation.

#### 4.3.24. Dissolution of Polymer Film Containing Microencapsulated *L. reuteri*<sup>2</sup>

The release of bacteria and thus the control about availability at the site of action was a key idea of the current work allowing to differentiate from other formulation approaches such as lozenges. The films release bacteria directly onto the mucosa, as opposed to the lozenges, which release bacteria into the saliva. This allows them to adhere more effectively to the mucosa. The release of bacteria from

microencapsulation and polymer films was analyzed by incubating the samples on agarose patches at 36 °C and 100% relative humidity, which was also the temperature and humidity used for the microencapsulation dissolution. In this experiment, polymer films containing microencapsulated *L. reuteri* cultivated at pH 5 were the selected material, as it has been demonstrated that this combination exhibits the highest activity. The dissolution was evaluated through the analysis of SEM images.

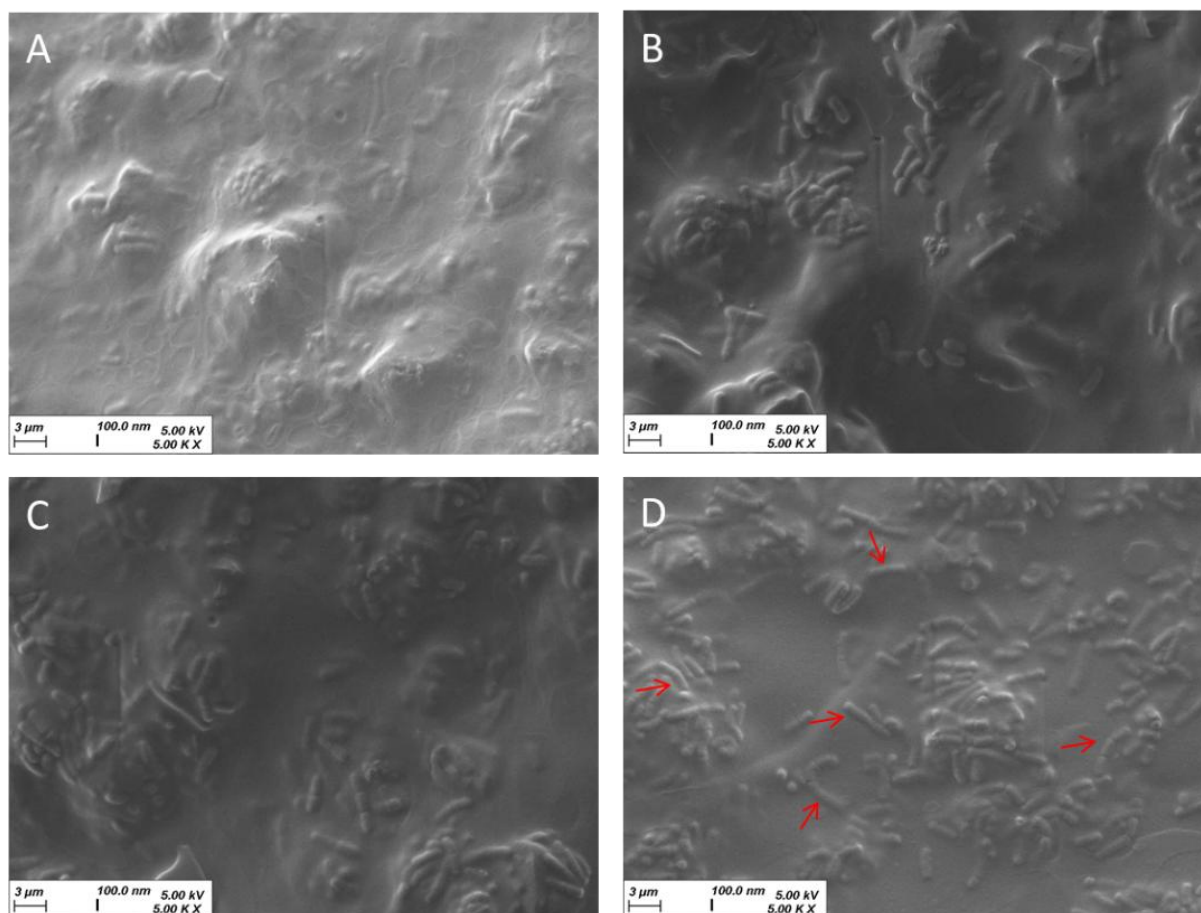


**Figure 4.30.** Series of SEM micrographs illustrating the dissolution of polymer films (HPMC & PVA) containing microencapsulated *L. reuteri* on 1.5% agarose gel patches at 36 °C and 100% relative humidity. Samples were imaged after different incubation times **A**: 0 minutes, **B**: 30 minutes, **C**: 60 minutes, and **D**: 120 minutes.

Figure 4.30 A depicts the microencapsulated particles embedded in the polymer film, as well as individual free, rod-shaped bacteria at time 0 minutes. After 30 minutes (Figure 4.30 B), an increase in the number of free bacteria is observed. This trend persists for 60 minutes, as illustrated in Figure 4.30 C, with an increasing number of released bacteria. By 120 minutes (Figure 4.30 D), only free, rod-shaped *L. reuteri* can

be observed, and the microencapsulation structure has completely dissolved. Therefore, it can be concluded that *L. reuteri* shall gradually release in the oral cavity over a period of 120 minutes.

### **4.3.25. Dissolution of Polymer Film Containing Microencapsulated *L. rhamnosus***

Further details regarding the dissolution of the films can be found in chapter 3.5.5.

### **4.3.26. Stability**

The stability of the HPMC-PVA films containing the bacteria microencapsulated using the three-way nozzle was evaluated. The samples were stored at room temperature (20 °C) and 4 °C, and the activity was analyzed after 0, 1, 4, 7, 14 and 20 days. Additionally, the films comprising the pure bacteria obtained from the stationary phase were subjected to examination. To this end, the films were stored at 4 °C, and the activity was analyzed after 0, 7, 14, 28, 42 and 58 days. The films containing the pure bacteria were no longer tested at room temperature, as the activity of the microencapsulated bacteria could no longer be detected after 4 or 14 days. In order to facilitate comparison, the relative values of the activities were calculated and plotted on the graphs as a function of the initial value.

Figure 4.31 A demonstrates the stability of microencapsulated *L. rhamnosus* and *L. reuteri* under different storage conditions. For *L. rhamnosus*, microencapsulation provided good survival rates at room temperature, maintaining 94.02% of initial activity through the seventh day. However, after 14 days, no detectable activity remained. In contrast, storage at 4 °C preserved bacterial activity much longer; after 20 days, activity was still measurable at 72.30% of the initial value, with 94.78% remaining after seven days. *L. reuteri* showed similar patterns, with no detectable activity after four days at room temperature, but a notable preservation at 4 °C, where activity was 92.28% after seven days and 75.12% after 20 days.



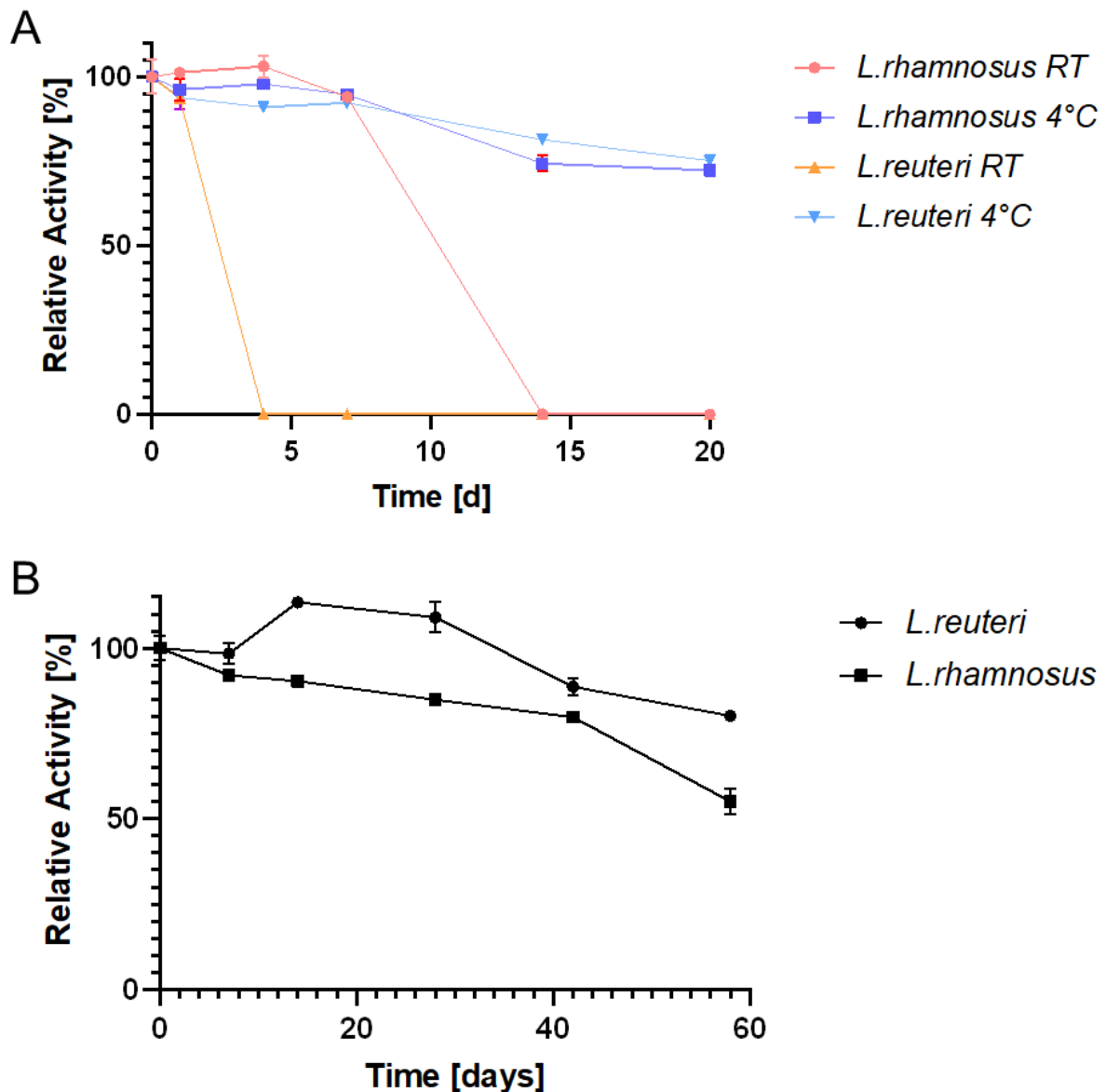


**Figure 4.31.** Stability of embedded bacteria in HPMC-PVA films. **A.** microencapsulated bacteria at RT and 4 °C; 0, 1, 4, 7, 14 & 20 days **B.** pure bacteria at 4 °C; 0, 7, 14, 28, 42 & 58 days. n=3 with standard deviation

Figure 4.31 B illustrates the stability of *L. rhamnosus* and *L. reuteri* stored as pure bacteria embedded in HPMC-PVA films at 4°C. For *L. rhamnosus*, activity remained at 90.33% for 14 days, though this decreased to 55.02% after 58 days. *L. reuteri* exhibited higher stability, retaining full activity for up to 28 days, with a reduction to 80.20% after 58 days.

These results indicate that lower temperatures (4 °C) significantly enhance the stability of both microencapsulated and pure bacteria in HPMC-PVA films, particularly for *L.*

*reuteri*, which exhibits larger resilience over extended storage. Microencapsulation also appears beneficial for maintaining bacterial viability, although prolonged stability is best achieved with cooler storage conditions. This insight is crucial for applications requiring long-term stability, where refrigeration and potentially microencapsulation can markedly improve bacterial survival.

### 4.4. Discussion<sup>2</sup>

The successful microencapsulation of *L. reuteri* was achieved using Eudragit® EPO and RL30D polymers. In this process, the bacteria were coated with a polymer layer, which was confirmed by SEM examination performed with both two- and three-way nozzles. The analysis revealed the presence of particles with a smooth and uniform surface, which can be attributed to the properties of the Eudragit® polymers (Fig. 2). The morphology of the particles within the core-shell structure can be observed by labelling the polymer layers with BODIPY and the encapsulated bacteria with Syto 9 using fluorescence imaging with a CLSM. The shell's coloration is distinctly visible, while in the core, the Syto 9 coloration of the bacteria is colocalized with BODIPY used for the polymer staining. This could be attributed to the higher intensity of BODIPY or the accumulation of some polymer inside the particles but clearly supports the successful incorporation of the microorganisms into the microparticles.

Microencapsulating *L. reuteri* did not show a strong impact on the bacterial activity. The values of 10.46 log(CFU/g) were observed when utilising the three-way nozzle and freeze-dried bacteria. Further, the microencapsulation process resulted in a delayed release, as evidenced by the dissolution process over time of the microencapsulated bacteria on an agarose patch (Fig. 4). After 120 min, the particles were found to be completely disintegrated, with only free bacteria and polymer residues remaining. The delayed release will allow the bacteria to gradually colonise the oral mucosa and tooth enamel. When using Eudragit® EPO, the pH value of the oral cavity, which is typically around 7, is exploited.<sup>[56]</sup> This results in the swelling of the material and the indirect release of the bacteria. Eudragit® RL30D is described to also swell at pH 7 inducing a less dense polymer network and pore formation.<sup>[56]</sup> The release of the bacteria might happen along those pores. Furthermore, Eudragit® RL30D is expected

to exhibit delayed release and mucoadhesive properties due to the positive charge of the quaternary ammonium group, which enables it to interact with negatively charged mucins.<sup>[56–58,153]</sup> As with the particles, dissolution of the polymer films was observed over a 120-minute period. Figure 4.30 illustrates that as the microcapsules undergo dissolution over time, an increasing number of bacteria were released, and the particle structures break down. After 120 minutes, no residual polymer film is discernible. The SEM images demonstrate the simultaneous dissolution of the polymer film and microencapsulation, with the release of bacteria. This delayed release mechanism provides support for the colonisation of the bacteria as previously described.

In contrast to the results for microencapsulation, no observable activity was detected following the introduction of *L. reuteri* into polymer films of HPMC and PVA. This may be attributed to damage caused by earlier freeze-drying processes of the freeze-dried bacteria that were used initially.<sup>[146]</sup> We could show that the growth phase can have an impact on the survival of the bacteria. The growth phase during which the bacteria were harvested and freeze-dried is also uncertain. This might also influence the subsequent activity following film pulling. While spray-drying has a shorter drying time, the comparatively longer duration of 1.5 h during film pulling leads to slower changes in the water concentration, which could be excessively harsh. Preliminary results indicated that an increase in drying time resulted in a corresponding increase in the mortality of bacteria. When polymer films were subjected to drying at 21 °C in the absence of forced ventilation, the process was observed to take approximately five hours, resulting in a complete loss of *L. reuteri* activity. To circumvent the damage caused by prior freeze-drying, liquid cultures were employed. A growth curve was documented to identify different growth phases. During the log phase and the stationary phase, different metabolic pathways of the bacteria are active, resulting in varying responses to external influences.<sup>[81]</sup> The distinct properties of the bacteria in different growth phases will be leveraged to analyze the influence on the activity after microencapsulation and film growth.<sup>[86,88]</sup>

*L. reuteri* was microencapsulated using spray-drying at various stages, including the growth and stationary phases, and then embedded in films. It should be noted that, although microencapsulation has an impact on the observed viability (6.50

log(CFU/g)), the microcapsules obtained during the growth phase failed to survive the embedding process. Conversely, *L. reuteri* from the stationary phase also demonstrated no decline in viability during spray-drying (10.54 log(CFU/g)) and exhibited an activity level of 4.76 log(CFU/g) even after filming (Fig. 6B & 7). As previously documented in literature, bacteria harvested in the stationary phase exhibit enhanced resistance to drying processes.<sup>[81]</sup> Our formulation has corroborated this observation indicating a potential way for a film formation process embedding viable *L. reuteri*.

In order to enhance the osmotic resilience of the bacteria to the drying process, two distinct methodologies and their combination were subjected to testing. Firstly, 0.6 M NaCl was added to the medium of the main culture to obtain a hypertonic medium. Another strategy involved the use of acidified MRS broth at pH 5. It was previously demonstrated that this can activate various metabolic pathways, resulting in alterations to the composition of the cell membrane.<sup>[146]</sup> The viability of *L. reuteri* was not affected by the microencapsulation process (Fig. 8 & 9). The activity values of the bacteria after spray-drying and cultivation with 0.6 M NaCl were 9.79 log(CFU/g), while those of the ones cultivated at pH 5 were 10.92 log(CFU/g). These values were compared to those ones where bacteria were cultivated in pure MRS broth, which yielded 10.54 log(CFU/g). Following encapsulation within polymer films, the bacteria displayed activity in both cultivation scenarios, with a small change in activity observed following treatment with 0.6 M NaCl, 4.31 log(CFU/g), and increased activity, 6.43 log(CFU/g), observed particularly after cultivation at pH 5. It has been demonstrated that the diverse cultivation conditions have induced bacterial resistance to the film-forming process.<sup>[83,91–93]</sup> Conversely, the combination of both methods appears to be excessively harsh, resulting in a further reduction in activity following microencapsulation and embedding *L. reuteri* into the HPMC-PVA films.

### **4.4.1. Discussion *L. rhamnosus* and *L. reuteri* and Different Film Preparation Methods**

This study explores the impact of various film preparation methods, drying times, and microencapsulation on the viability of *L. reuteri* and *L. rhamnosus* under different

conditions. The comparative analysis between microencapsulated and pure bacterial forms highlights the protective benefits of microencapsulation, particularly with Eudragit® EPO and RL30D polymers, in safeguarding bacterial activity through spray-drying and embedding processes.

### **4.4.1.1. Film Preparation Methods and Drying Times**

Several film preparation methods were tested, including hand and electromotive film casting, freeze-drying, foamed PVA films, and polymer film coated with microencapsulated bacteria. Spray-drying was the microencapsulation technique, comparing two-way and three-way nozzle configurations, which influenced bacterial survival. The three-way nozzle, in particular, offered enhanced bacterial viability by reducing thermal and mechanical stress.<sup>[51–53,116]</sup> The temperature of a spray-dried particle decreases from the exterior to the interior. As the bacteria are sprayed through the inner feed, they are subjected to a reduced temperature load.

Drying times played a significant role in bacterial survival. Rapid drying (1.5 hours at 37 °C with forced ventilation) generally led to higher activity retention than longer drying periods (12 hours for thicker, manually cast films). The use of foamed PVA films, which required only 30 minutes of drying, also demonstrated the retention of viable bacteria, thereby illustrating that shortened drying times can facilitate the preservation of bacterial viability.<sup>[155]</sup> Despite the rapid drying time, the survival of the bacteria was slightly lower than with the HPMC-PVA films and the drying time of 1.5 hours. This could be attributed to the higher concentration of PVA with which the bacteria come into contact. PVA exhibits self-emulsifying properties, which are essential for the formation of the foamed films but can destroy the cell membrane of the bacteria.<sup>[144,161]</sup> Freeze-drying, a gentle method<sup>[122]</sup>, was also found to be partially effective in maintaining bacterial activity. In this case, *L. rhamnosus* exhibited higher activity than *L. reuteri*. No difference was observed between the HPMC and the PVA films. Nevertheless, the efficacy of vacuum drying was found to be constrained, even when the drying time was maintained at 1.5 hours, particularly in preserving bacterial viability, particularly for *L. reuteri*, which exhibited no observable activity.

#### **4.4.1.2. Activity and Stability of Bacteria**

Activity levels were particularly affected by microencapsulation, which generally reduced bacterial viability compared to pure bacteria under various conditions. In particular, there was a difference between microencapsulation using the two-way nozzle and the three-way nozzle. As was the case after microencapsulation, the activity of the three-way nozzle without embedding in the films was higher than that of the bacteria microencapsulated using the two-way nozzle. Therefore, the focus was primarily on the three-way nozzle and not all tests were performed with both types of microencapsulation. The higher activity is due to the lower damage to the bacteria. The temperature load the bacteria are exposed to during microencapsulation is lower. They are also better protected by a thicker polymer layer around the particles.<sup>[50,53,54]</sup> This can be seen in the SEM images by the smoother surface, due to the polymethacrylates covering the surface of the particles.

The storage conditions significantly influenced bacterial stability, with refrigerated storage preserving over 70% of initial activity for up to 20 days (*L. reuteri*), while room temperature storage resulted in a rapid activity decline. These results demonstrate the benefits of low-temperature storage and microencapsulation in prolonging bacterial shelf life.

#### **4.4.1.3. Differences Between Microencapsulation and Pure Bacteria**

Microencapsulation was identified as a critical factor influencing the survival of bacteria during drying, embedding, and storage. SEM images corroborated that microencapsulation had successfully incorporated bacteria within a protective polymer matrix, yielding smooth, spherical particles devoid of any visible free bacteria, thereby attesting to the efficacy of the encapsulation process. This protective layer prevents degradation and facilitated a controlled release<sup>[32,35]</sup>, as evidenced by the dissolution tests. Furthermore, the Eudragit RL30D also causes mucoadhesion through interaction between the positive charge and the negatively charged mucin on the oral mucosa.<sup>[162–164]</sup>

The incorporation of pure bacteria into polymer films resulted in elevated activity levels. However, this approach negates the advantageous outcomes of microencapsulation, including mucoadhesion and especially controlled release. Pure *L. rhamnosus* retained activity more effectively, suggesting species-specific differences in sensitivity to drying and embedding processes.

#### **4.4.1.4. Differences Between *L. rhamnosus* and *L. reuteri***

Throughout the work, *L. rhamnosus* consistently showed higher survival rates than *L. reuteri*, particularly in polymer films and after longer drying processes. Freeze-dried *L. rhamnosus* embedded in HPMC-PVA films retained high activity levels, whereas *L. reuteri* showed a marked loss. Under acidic and osmotic stress, *L. rhamnosus* retained less activity following microencapsulation and embedding, in contrast to the beneficial effect on *L. reuteri*. Additionally, growth phase influenced survival, with bacteria harvested in the stationary phase exhibiting improved post-encapsulation and embedding activity. It has been demonstrated that disparate metabolic pathways and byproducts appear to be critical for the survival of drying processes in bacteria.<sup>[82,107,165,166]</sup>

In conclusion, microencapsulation, nozzle selection, drying conditions, and storage significantly impact the survival of *L. reuteri* and *L. rhamnosus*. *L. rhamnosus* proved more resilient under diverse conditions, indicating its suitability for formulations requiring extended shelf life and exposure to challenging environments. The insights gained here are essential for optimizing the formulation and storage of probiotic films aimed at maintaining bacterial viability for therapeutic oral applications.

## **4.5. Conclusion<sup>2</sup>**

In summary, the effectiveness of encapsulating *L. reuteri* has been affirmed through our experimentation. The bacteria exhibit a continuous polymer coating, as evidenced by SEM analysis and robustness indicated by no diminishment in their activity. This encapsulation and polymer film ensures a delayed release of the bacteria, extending

over a period of 120 min, thereby facilitating controlled delivery. Further processing of *L. reuteri* to embed the microencapsulated bacteria into HPMC/PVA polymer films revealed the sensitivity of *L. reuteri* to this procedure. Under standard conditions and direct transfer no survival of the bacteria in the polymer film was found. Nevertheless, some additional culturing conditions allowed to harvest viable *L. reuteri* from the polymer films. Cultivation of the bacteria in MRS broth, till the stationary phase, has been found to enhance their activity within mucoadhesive polymer films. Additionally, a reduction in pH to 5 further augments this activity, underscoring the potential for optimizing bacterial performance in such delivery systems.

In conclusion, it can be confirmed that the encapsulation of *L. reuteri* is effective. SEM analysis confirmed the presence of a polymer coating, yielding particles with smooth surfaces. The microencapsulation process enabled a delayed release of the bacteria, evident by their dissolution on agarose after 120 min, leaving behind only free bacteria and residual polymer. This extended release was validated by observing disintegration on agarose patches over the same duration.

Eudragit® EPO, exploiting the oral cavity's pH of 7, facilitated postponed release, while Eudragit® RL30D exhibited mucoadhesive properties due to its positive charge interacting with negatively charged mucins. However, introducing bacteria into polymer films resulted in undetectable activity, possibly due to damages incurred during prior freeze-drying processes.

To mitigate damage, liquid cultures were utilized, and growth curves were documented to understand bacterial behaviour across different growth phases post encapsulation. Microencapsulation during the growth phase compromised viability during embedding, whereas bacteria from the stationary phase maintained viability post encapsulation, with no decrease observed even after filming.

Osmotic resilience was enhanced by supplementing 0.6 M NaCl during cultivation or cultivating under pH 5 conditions. Microencapsulation did not affect *L. reuteri* viability, and post-encapsulation, the bacteria exhibited activity under both cultivation scenarios. Notably, activity remained unchanged after treatment with 0.6 M NaCl, while cultivation



at pH 5 significantly increased activity, suggesting induced bacterial resistance to the film-forming process under diverse cultivation conditions.

## 5. Biological Testing

Parts of this chapter have been previously prepared for publication. The corresponding sections are indicated with footnote 1.

# Probiotic-Embedded Polymer Films for Oral Health: Development, Characterization, and Therapeutic Potential

Charlotte Eckermann<sup>1</sup>, Florian Schäfer<sup>2</sup>, Marc Thiel<sup>3</sup>, Agnes-Valencia Weiss<sup>1</sup>, Christian Motz<sup>2</sup>, Karen Lienkamp<sup>3</sup>, Matthias Hannig<sup>4</sup>, Marc Schneider<sup>1\*</sup>

<sup>1</sup>Department of Pharmacy, Biopharmaceutics and Pharmaceutical Technology, PharmaScienceHub, Saarland University, 66123 Saarbrücken, Germany

<sup>2</sup>Chair of Materials Science and Methods, Department of Materials and Engineering, Science, Saarland University, 66123 Saarbrücken, Germany

<sup>3</sup>Chair of Polymer Materials, Department of Materials Science and Engineering, Saarland University, 66123 Saarbrücken, Germany

<sup>4</sup>Clinic of Operative Dentistry, Periodontology and Preventive Dentistry, Saarland University, 66421 Homburg, Germany

## 5.1. Introduction

It is essential that the probiotic bacteria present in the formulation are released and adhere to the surfaces in the oral cavity in order for them to exert their effect.

The colonization and adherence of *Lactobacilli*, in this particular case *L. reuteri* and *L. rhamnosus*, in the oral cavity has been the subject of considerable research interest, given the potential probiotic benefits that they may offer in oral health. Probiotics are defined as live microorganisms that confer health benefits to the host when administered in adequate amounts. They are widely recognized for their role in gastrointestinal health and have more recently been explored for applications in the oral cavity.<sup>[167–169]</sup> The principal mechanism through which lactobacilli exert beneficial effects in the oral environment is competitive inhibition, whereby they compete with pathogenic bacteria for adhesion sites on mucosal surfaces and dental biofilms. This competitive inhibition can result in a reduction in the levels of cariogenic bacteria, such as *Streptococcus mutans*, which are implicated in tooth decay and periodontal pathogens.<sup>[167,170]</sup>

It is essential that these probiotic bacteria adhere to the oral surfaces in order for them to confer long-term benefits. It has been demonstrated that while strains such as *L. rhamnosus* are capable of adhering to saliva-coated surfaces and exerting temporary anti-cariogenic effects, they do not establish a permanent colonization of the oral cavity in the majority of individuals.<sup>[169,171]</sup> To achieve these effects, an adequate dose is essential. For example, LGG has been demonstrated to be effective in quantities of approximately  $5 \times 10^6$  CFU/ml, administered three times daily, as evidenced by short-term intervention studies.<sup>[169]</sup> This dosage enables LGG to exert a transient influence on the oral microbiota, potentially reducing the prevalence of pathogenic bacteria during the course of active administration. However, it does not typically result in the establishment of a permanent colonization.<sup>[171]</sup>

The transient colonization of *Lactobacilli* and the specific dosages needed for potential benefits are areas of ongoing research, particularly with a view to understanding the balance that is required to support oral health without encouraging acidogenic strains

that might lower oral pH and contribute to enamel demineralization. Therefore, while the use of Lactobacilli as probiotics in oral health is a promising avenue of research, further evidence is required to substantiate its efficacy in managing or preventing oral diseases.<sup>[168,170]</sup>

### 5.2. Methods<sup>1</sup>

The initial testing of the concentration of bacteria per film involved the incorporation of 50, 100 and 150 mg of microencapsulated bacteria (equivalent to 108 mg of dry mass) into each film. The selection of microencapsulated bacteria was based on their higher loading capacity, which is attributed to the polymers utilized in the encapsulation process. The films were fixed to rehydrated bovine enamel samples and agitated for a period of two hours in a solution of 2 mL of MilliQ® water at 37 °C, which corresponds to the average volume of saliva present in the oral cavity.<sup>[172]</sup> This test was conducted *in vitro* to obviate the need for unnecessary exposure of volunteers. Following the incubation period, the enamel samples were washed with MilliQ® water and stained with Syto 9 (3 µL/mL,  $\lambda$  = 488 nm excitation,  $\lambda$  = 525 nm emission) for 15 min. The bacteria were visualized and quantified using confocal laser scanning microscopy (LSM710, AxioObserver, Carl Zeiss AG, Oberkochen, Germany) using the EC Plan-Neofluar 100x/1.3 Oil objective, with 14 CLSM images (8100 µm<sup>2</sup> per image) analyzed per sample. Images were extracted using the Zeiss ZEN blue software with no further processing. Bacterial counts were performed manually. The amount of pure bacteria incorporated into the films was adjusted to match the bacterial content of the corresponding microencapsulated samples.

For biological testing, the film samples were applied to bovine tooth enamel and incubated in the oral cavity of volunteers for 8 h. The volunteers provided written consent for participating in the trials. Bovine enamel samples were rehydrated in demineralized water for 24 h, then fixed onto dental splints using a two-component silicone.<sup>[173]</sup> The films were attached to the enamel, with untreated enamel used as a control on the opposite side of the mouth. Only one type of film sample was tested per subject at a time. The study was conducted with two volunteers. After 8 h of incubation, the samples were rinsed with Milli-Q® water and stained with Syto 9 (3 µL/mL,  $\lambda$  = 488

nm excitation,  $\lambda = 525$  nm emission) for 15 min. The samples were subsequently analyzed using CLSM. Per sample 14 CLSM images ( $8100 \mu\text{m}^2$  per image) were analyzed for quantification of the bacteria.

## 5.3. Results and Discussion<sup>1</sup>

### 5.3.1. Influence of Bacterial Concentration<sup>1</sup>

Various concentrations of microencapsulated bacteria were incorporated into the polymer films to determine the optimal bacterial loading. The goal was to produce a stable film with the highest possible bacterial content.

For both *L. rhamnosus* and *L. reuteri*, an increase in the quantity of microencapsulated bacteria from 50 mg to 100 mg and 150 mg per film resulted in a corresponding rise in the number of adhered bacteria per enamel piece, as shown in Figure 5.1. The film containing 150 mg of bacteria exhibited the highest bacterial adhesion; however, its structural stability was insufficient.

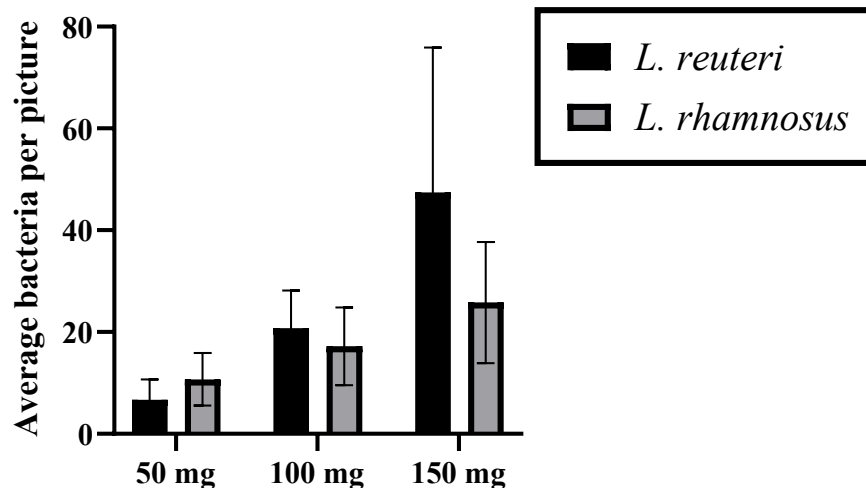


**Figure 5.1.** Adherence of microencapsulated *L. rhamnosus* and *L. reuteri* incorporated in different concentrations in polymer films (HPMC - PVA). (tested in MilliQ-water on shaker) n=3 with standard deviation.

During the manufacturing process, the film could not be harvested in a single piece from the Teflon foil, rendering it unsuitable for further tear resistance testing. Consequently, subsequent experiments were conducted using films containing 100 mg of microencapsulated bacteria, which provided an appropriate balance between

bacterial incorporation and film stability. These films were also employed for the subsequent tests. The mass of bacteria in the polymer films containing pure cultures was adjusted to achieve the desired result, with 50 mg (dry mass) of bacteria per polymer film (108 mg dry mass) utilized.

### **5.3.2. Incubation in Oral Cavity<sup>1</sup>**

#### **5.3.2.1. *Pure Polymer Film<sup>1</sup>***

To assess the effect of the polymer film on bacterial adhesion under real conditions, the pure polymer film out of HPMC and PVA was incubated in the oral cavity of two volunteers for eight hours, independently of the influence of bacterial loading. The bacteria were imaged using CLSM.

After the incubation period, a trend for reduced number of bacteria were observed adhering to the polymer-coated samples compared to the enamel samples (Figure 5.2 A) and the uncoated reference samples (Figure 5.2 B) in both test subjects. All adherent bacteria exhibited a coccoid morphology. The quantification presented in Figure 5.2C supports the conclusion that a reduced number of bacteria adhered to the enamel samples with the films applied before in vivo exposure.

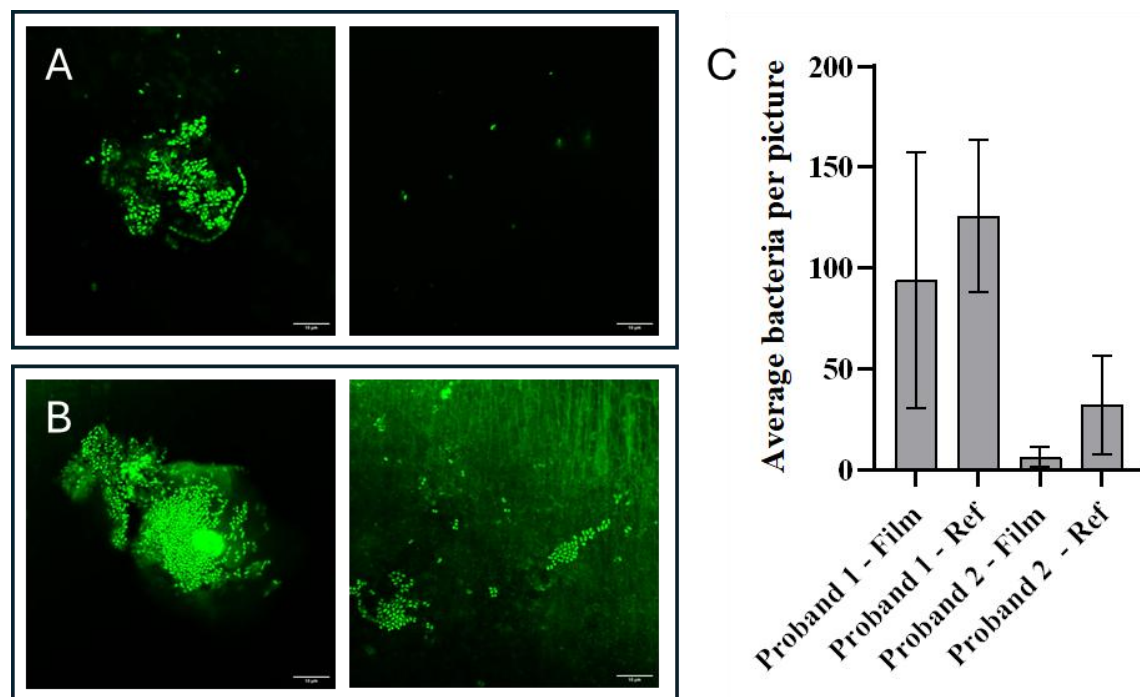


**Figure 5.2.** Adherence of bacteria from the oral cavity to tooth enamel, after incubation for 8 h in the oral cavity. Samples coated with pure polymer film (A) or without polymer film (B). Adhered bacteria counted (C). Incubation in oral cavity of two volunteers. n=3 with standard deviation.

#### 5.3.2.2. *Polymer Film Containing Microencapsulated Bacteria<sup>1</sup>*

The polymer film containing microencapsulated bacteria was incubated in the oral cavity of two volunteers for eight hours, following the same procedure as that used for the pure polymer film. The samples were analyzed with the help of CLSM, as described before.

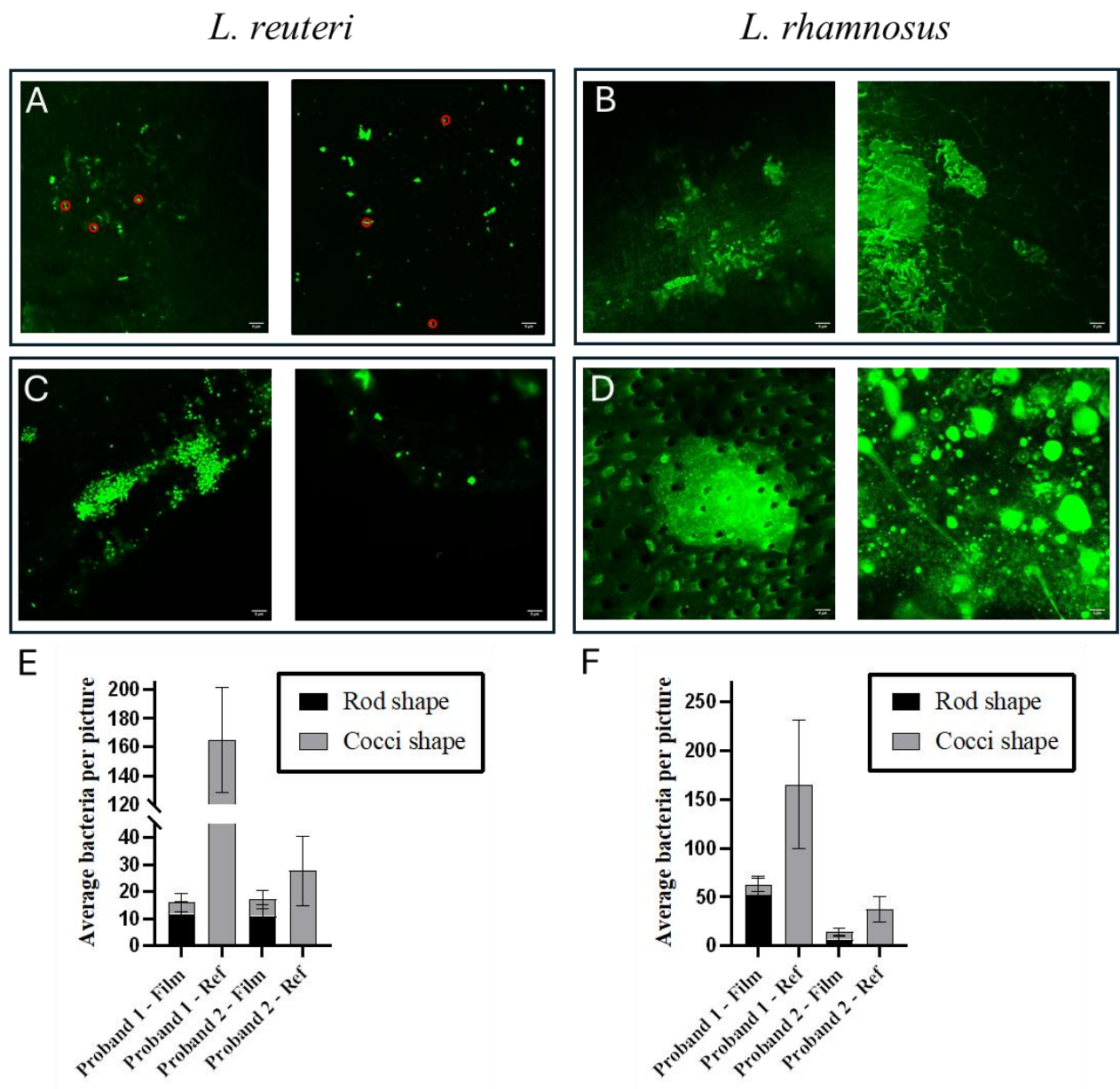


**Figure 5.3.** Adherence of bacteria from the oral cavity to tooth enamel after incubation in the oral cavity for 8 h. Samples coated with polymer film (HPMC-PVA) + microencapsulated bacteria (**A & C**) or without polymer film (**B & D**). Bacteria counted, adhered and classified by morphology (**E & F**). Incubation in oral cavity of two volunteers. n=3 with standard deviation.

Figure 5.3 A illustrates two examples of enamel samples coated with polymer films containing *L. reuteri*, demonstrating the presence of both cocci and rod-shaped bacteria, with selected rods highlighted by red circles for clarity. In contrast, the reference sample (Figure 5.3 C) exhibited only cocci. Bacterial quantification (Figure 5.3 E) indicates that rod-shaped bacteria were able to adhere to the enamel in both test subjects when the polymer film was applied, while the number of adhered cocci was reduced.



A comparable pattern was observed for the polymer film containing microencapsulated *L. rhamnosus*. The enamel samples coated with the film exhibited the presence of both rod-shaped and cocci bacteria (Figure 5.3 B), whereas the reference samples displayed only cocci (Figure 5.3 D). The bacterial count (Figure 5.3 F) provides further evidence to support these findings, indicating that rod-shaped bacteria adhered exclusively in the presence of the polymer film, while the number of cocci was diminished.

### **5.3.2.3. Polymer Film Containing Pure Bacteria<sup>1</sup>**

In addition to testing the polymer film with microencapsulated bacteria, a polymer film containing non-encapsulated bacteria was also applied to tooth enamel and evaluated. As with the preceding films, the film was incubated for eight hours in the oral cavities of two volunteers, and bacterial visualization was performed using CLSM.

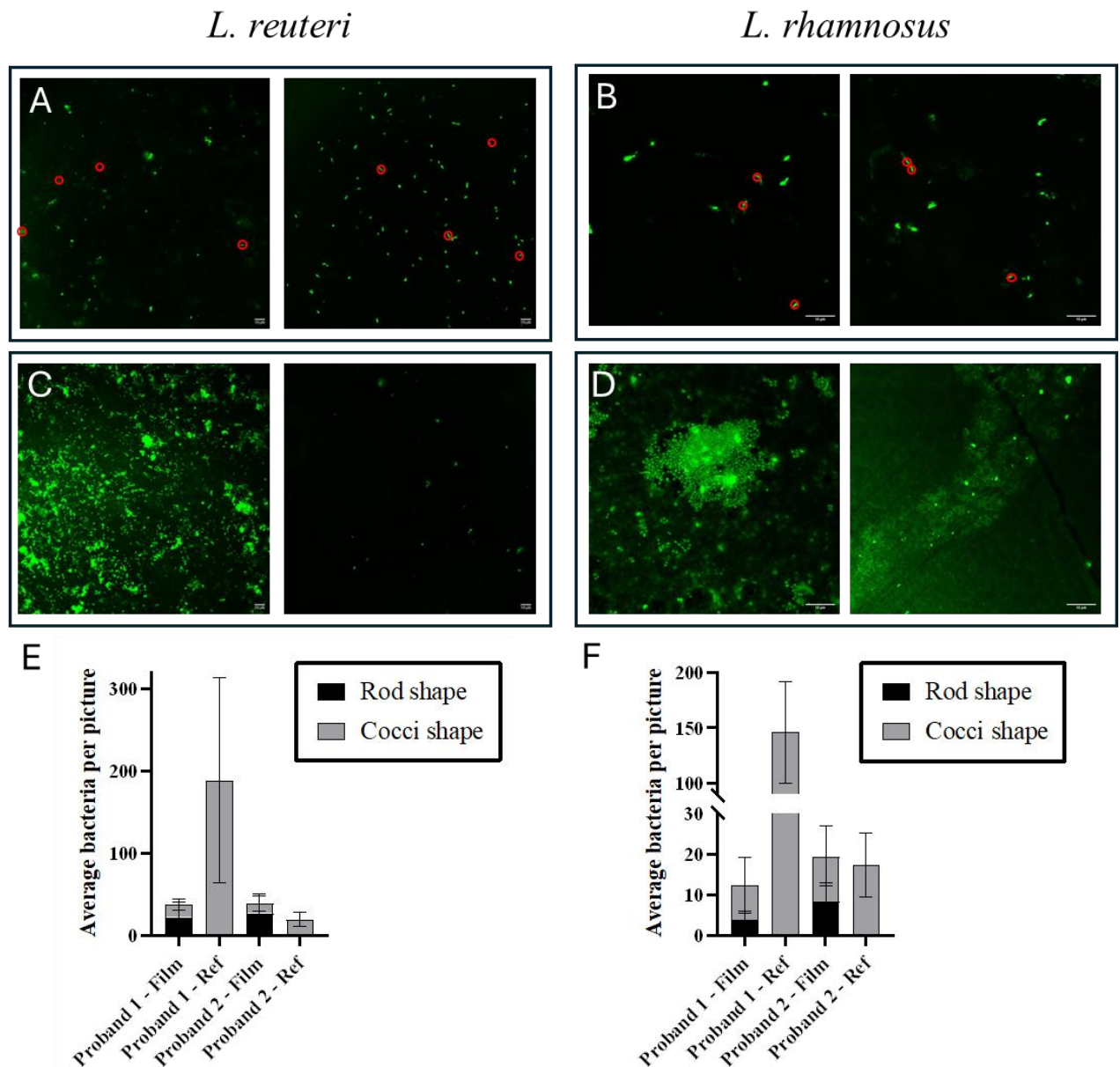


**Figure 5.4.** Adherence of bacteria from the oral cavity to tooth enamel after incubation in the oral cavity for 8 h. Samples coated with polymer film (HPMC-PVA) + pure bacteria (**A** & **C**) or without polymer film (**B** & **D**). Bacteria counted, adhered and classified by morphology (**E** & **F**). Incubation in oral cavity of two volunteers. n=3 with standard deviation.

Figure 5.4 A illustrates two enamel samples coated with polymer films containing *L. reuteri*, demonstrating the presence of both cocci and rod-shaped bacteria. Selected rods are indicated with red circles for enhanced visibility. In contrast, the corresponding reference sample (Figure 5.4 C) exhibited only cocci. Figure 5.4 E illustrates the bacterial quantification, which demonstrates that rod-shaped bacteria successfully adhered to the enamel in both test subjects when the polymer film was applied.

Conversely, the number of cocci was reduced when the probiotic bacteria were present. This is particularly evident in proband one, but proband two also shows a reduction in cocci. However, this is clearly less due to the lower total amount.

A comparable pattern was observed with the polymer film containing non-encapsulated *L. rhamnosus*. The enamel samples coated with the film exhibited the presence of both rods and cocci (Figure 5.4 B), whereas the reference samples displayed only cocci (Figure 5.4 D). The bacterial count (Figure 5.4 F) corroborates these findings, indicating that rod-shaped bacteria exhibited exclusive adherence in the presence of the polymer film, while the number of cocci was significantly diminished.

### **5.3.2.4. Increased Loading with Microencapsulated Bacteria<sup>1</sup>**

One strategy to increase bacterial loading involved utilizing a foamed PVA film, where the film's pores were loaded with bacteria. The pores were then sealed with a polymer film composed of PVA and HPMC. This was achieved by partly dissolving the film in water and subsequently fixing it to the underlying foamed film.

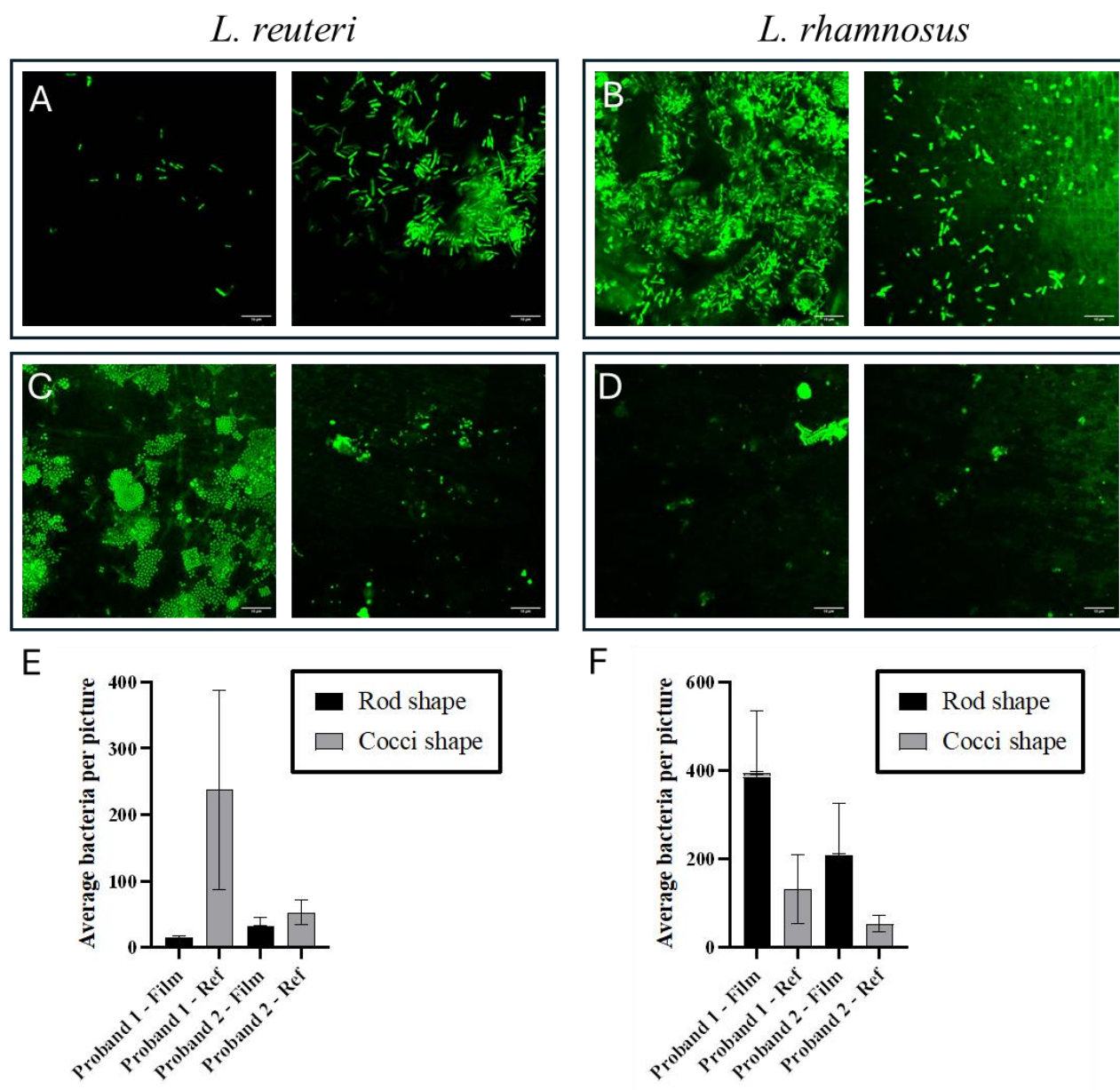


**Figure 5.5.** Adherence of oral cavity bacteria to tooth enamel after incubation for 8 h in the oral cavity. Samples coated with foamed PVA film + microencapsulated bacteria (**A & B**) or without polymer film (**C & D**). Bacteria counted, adhered and categorized by shape (**E & F**). Incubation in oral cavity of two volunteers. n=3 with standard deviation.

As with previous films, this formulation was incubated in the oral cavities of two test subjects for eight hours, and the bacteria were visualized using CLSM. Figure 5.5 A presents two examples of enamel samples coated with polymer films containing *L. reuteri*, where rod-shaped bacteria are predominantly visible. The reference sample (Figure 5.5 C) showed the presence of cocci. Bacterial quantification (Figure 5.5 E)

confirms that rod-shaped bacteria successfully adhered to the enamel in both test subjects, while the number of adhered cocci was almost completely suppressed.

A similar trend was observed for the polymer film containing microencapsulated *L. rhamnosus*. On the enamel samples coated with this film, the majority of adhered bacteria were rods (Figure 5.5 B), whereas only cocci were detected in the reference sample (Figure 5.5 D). The bacterial enumeration (Figure 5.5 F) corroborates these findings, showing that rod-shaped bacteria adhered only to the samples with the polymer film, while the number of cocci was reduced. Furthermore, *L. rhamnosus* demonstrated superior adhesion properties compared to *L. reuteri*, as evidenced by a higher prevalence of rod-shaped bacteria adhering to the tooth enamel.

Compared to applications using the HPMC-PVA polymer films, the number of adhering bacteria (*L. reuteri* and *L. rhamnosus*) was higher with the foamed PVA films. The increased bacterial loading in the polymer films led to enhanced adherence within the oral cavity.

The biological analysis highlights the potential of these films for oral cavity applications. Both polymer films containing microencapsulated and non-encapsulated bacteria effectively facilitated the adhesion of rod-shaped bacteria (*L. rhamnosus* and *L. reuteri*) to enamel samples, as shown by CLSM. Importantly, the presence of the polymer film significantly reduced the adhesion of cocci bacteria, which are commonly associated with periodontitis.<sup>[5,9,24]</sup> This suggests that the films not only deliver probiotics but also potentially inhibit the colonization of harmful bacteria.

The increased bacterial loading in foamed PVA films further enhanced bacterial adhesion within the oral cavity.

### **5.4. Summary**

The objective of this study was to investigate the incorporation of varying concentrations of microencapsulated bacteria (*L. rhamnosus* and *L. reuteri*) into polymer films to optimize bacterial loading for oral cavity applications. Films containing

150 mg of bacteria exhibited the highest levels of bacterial adhesion, but they lacked the requisite structural stability. Consequently, 100 mg films were selected as an optimal balance between bacterial content and structural stability.

In vivo experiments demonstrated that pure polymer films (HPMC-PVA) exhibited a reduction in bacterial adhesion compared to uncoated enamel samples. Films containing microencapsulated bacteria facilitated the adhesion of rod-shaped bacteria (*L. rhamnosus* and *L. reuteri*) while simultaneously reducing the adhesion of cocci, which are commonly associated with periodontitis. This outcome was observed consistently across polymer films containing both encapsulated and non-encapsulated bacteria.

The incorporation of foam into foamed PVA films resulted in enhanced bacterial loading via pore incorporation, which was observed to facilitate superior bacterial adhesion compared to traditional polymer films. Confirmation of the effective delivery of probiotics was obtained through CLSM analysis, which also demonstrated the inhibition of harmful cocci colonization and enhancement of beneficial bacteria adhesion. *L. rhamnosus* exhibited superior adhesion compared to *L. reuteri*.

The dual benefits of polymer films with encapsulated probiotics were thus revealed: the delivery of beneficial bacteria and the potential inhibition of harmful bacterial growth. These findings highlight the potential of such films for oral health applications.

## 6. Bioprinting

### 6.1. Introduction

3D bioprinting, a subfield of additive manufacturing, has emerged as a transformative technology in biomedical engineering and microbiology. It enables the precise spatial arrangement of cells, biomaterials, and other biologically relevant compounds to construct tissue analogs, organoids, and complex cellular systems. This technique primarily uses "bioinks," composed of cells and supportive materials, to create structures layer by layer.<sup>[127,128,130]</sup>

One of the primary advantages of 3D bioprinting is its capacity for high spatial precision and customization, enabling the creation of constructs tailored to specific experimental or clinical needs. The ability to build intricate, patient-specific models holds promise for advancing personalized medicine. Moreover, this technology facilitates the reduction of animal models by offering physiologically relevant in vitro systems for research. However, challenges remain, including optimizing bioinks to support cell viability and function, achieving structural integrity in the constructs, and addressing the limited availability of suitable materials. Despite these limitations, the potential for scalable production and the development of intricate biological systems continues to drive innovation in the field.<sup>[127,128]</sup>

3D bioprinting spans a wide array of fields, from regenerative medicine and drug testing to microbiology and food science. In microbiological contexts, it facilitates the study of bacterial behaviors, including biofilm formation and host-microbe interactions.

Probiotics, beneficial microorganisms that confer health advantages when ingested in sufficient amounts, are increasingly recognized for their role in modulating gut health, immune response, and metabolic functions. However, their viability, controlled delivery, and integration into host environments remain challenging in therapeutic applications. Bioprinting offers a unique approach to address these challenges, allowing for the creation of customized, structured microbial environments that can potentially improve probiotic stability, function, and bioavailability.<sup>[130]</sup>

Bioink composition is critical in microbial bioprinting. Hydrogels composed of alginate and gelatin are employed due to their biocompatibility, tunable mechanical properties, and suitability for printing living cells.<sup>[130]</sup> Alginate, a naturally occurring polysaccharide derived from brown algae, forms hydrogels upon ionic crosslinking with divalent cations such as calcium. This material provides structural stability and creates a supportive matrix for cells. However, alginate lacks intrinsic cell-adhesive properties, which limits its biological functionality.<sup>[174–176]</sup> To address this, alginate is often combined with gelatin, a collagen-derived polymer. Gelatin enhances the bioink's biological activity by supporting cell attachment, proliferation, and migration. Its thermo-reversible gelation properties allow for easy processing during bioprinting. Together, alginate and gelatin provide a balance between mechanical stability and biological functionality, making them ideal for bioprinting of bacterial cells.<sup>[127]</sup> The combination of alginate and gelatin offers a balance between mechanical stability and biological functionality, making it ideal for bioprinting living materials.

Lactic acid bacteria (LAB) represent an exciting focus in microbial bioprinting due to their roles in food fermentation and probiotic applications. Embedding LAB within hydrogels offers numerous advantages, including the ability to study fermentation processes, evaluate microbial interactions, and develop advanced delivery systems for probiotics. LAB-embedded hydrogels maintain high cell viability and metabolic activity, enabling controlled release and sustained performance in both research and industrial applications. and functional foods by tailoring microbial compositions to specific health needs.<sup>[128,130]</sup>

In conclusion, 3D bioprinting represents a revolutionary tool at the intersection of biology and engineering. The use of alginate and gelatin-based bioinks has proven effective in constructing bacterial systems, with a growing interest in lactic acid bacteria for both biomedical and food science applications. Continued research into optimizing bioink compositions and refining printing techniques will expand the utility of this technology, paving the way for innovative applications in science and industry.



## 6.2. Methods

### 6.2.1. Formulation

Gelatin (Bloom 300, type A, Sigma-Aldrich, Germany) (3% (w/w)) and sodium alginate (W202503, Sigma-Aldrich, Germany) (2% (w/w)) were dissolved in MilliQ water by stirring at 60-70 °C. The prepared solutions were sterile-filtered using a 0.45 µm pore size filter. For inoculation, the hydrogel was heated to 70 °C to avoid premature solidification and filled into two sterile glass vials. *L. rhamnosus* and *L. reuteri* grown to stationary phase (100 µL per vial) were inoculated into 5 mL of bioink each. The dispersion was gently mixed and the bioink was filled into syringes and transferred to sterile cartridges. The bioink was then incubated at 21 °C for 4 hours until the hydrogel solidified.

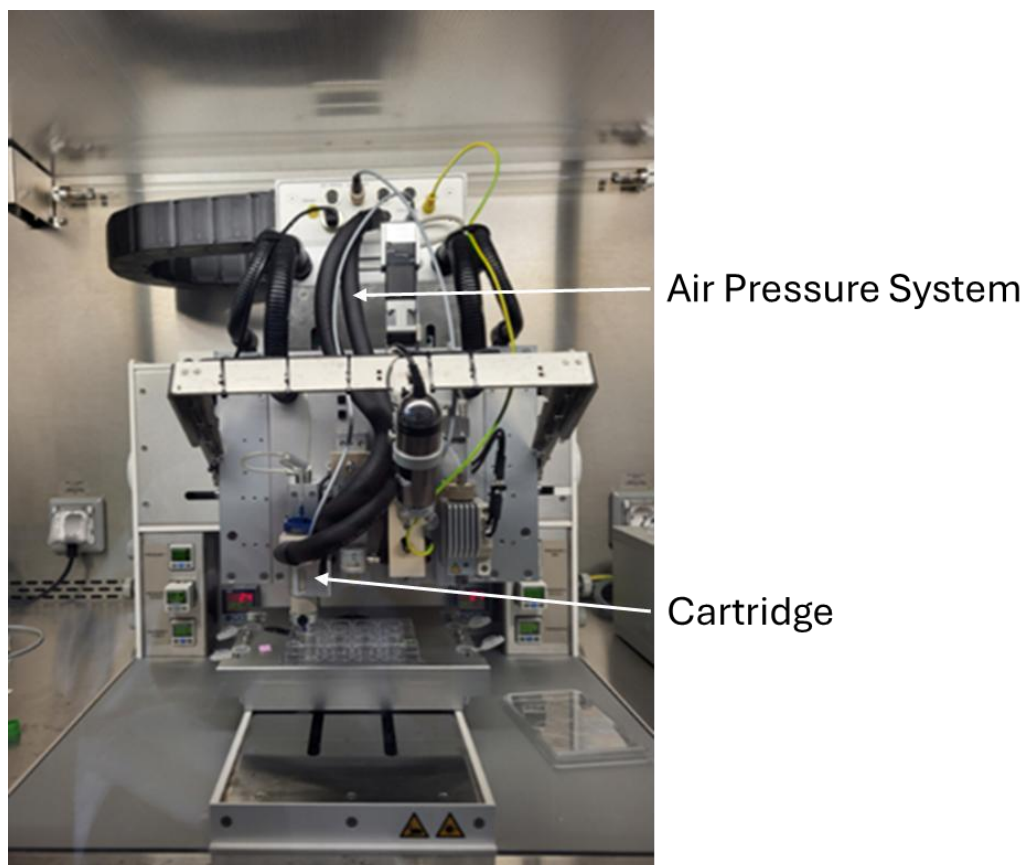


**Figure 6.1.** 3D Bioprinter RegenHU

## Bioprinting

The bioink was printed using a 3D bioprinter (3D Discovery, RegenHu, Villaz ST-Pierre, Switzerland (Figure 6.1)). A 25G needle was attached to the cartridge, which was connected to an air pressure system to allow controlled filament extrusion. A round patch or a grid consisting of four layers was designed using the bioprinter's proprietary software (BIOCAD™) and then printed. Air pressure settings were optimized for each bioink to ensure consistent flow during printing. All experiments were performed in biological triplicates. The printed patches were crosslinked by immersion in a sterile 100 mM  $\text{CaCl}_2$  solution for 15 minutes (Figure 6.2). For activity analysis, the cross-linked patches were dissolved in 110 mM EDTA solution and assessed using the plate count method as previously described. The patches were subjected to either immediate analysis following printing or prior to this, freeze-drying or drying at 37 °C with forced ventilation.

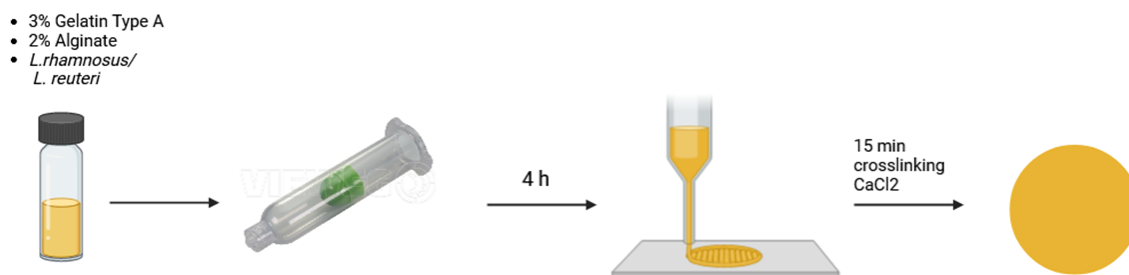


**Figure 6.2.** Schematic representation of the production of bioprinted patches with incorporated probiotic bacteria.

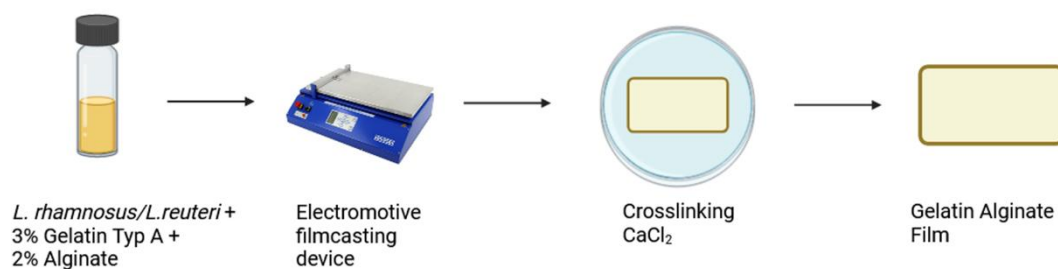


**Figure 6.3.** Schematic representation of the production of films out of bioink with the electromotive film casting device.

To ensure comparability with the film applicator, the formulation was also processed with the aforementioned device. The bioink was prepared as previously described and drawn onto a Teflon film using the film applicator and a squeegee (1000  $\mu\text{m}$  gap height). This process is illustrated in Figure 6.3. The resulting film was crosslinked with  $\text{CaCl}_2$ , and the activity was determined after dissolution using the plate count method.

### 6.2.2. Surface Morphology

For fixation, 3% glutaraldehyde in PBS was added to the patches and incubated for 2 hours at room temperature. The fixative was then carefully removed. Dehydration was performed using a graded ethanol series (30%, 40%, 50%, 60%, 70%, 80%, 90%, 96%, and 100%) with 400  $\mu\text{L}$  applied for 10 minutes at each step. Two additional 100% ethanol steps were included for complete dehydration. Samples were air-dried in a hood overnight. The dried prints were mounted on SEM sample holders using adhesive carbon tabs, gold sputtered for 100 seconds and analyzed using a SEM.

### 6.2.3. Dissolution

The release of *L. rhamnosus* and *L. reuteri* was determined over a period of 60 minutes. To this end, the patches were incubated in 2 mL of MilliQ water containing trypsin at 37 °C with gentle shaking. Subsequently, samples were taken at 10, 30 and 60 minutes, and the activity was determined using the plate count method.

## 6.3. Results and Discussion

### 6.3.1. Formulation

Hydrogels composed of gelatin and sodium alginate, together with *L. rhamnosus* or *L. reuteri* from the stationary phase, were successfully printed using a 3D bioprinter. The constructs were printed in five layers and cross-linked with  $\text{CaCl}_2$ , resulting in solid, rubber-like patches with a milky white appearance (Figure 6.4).

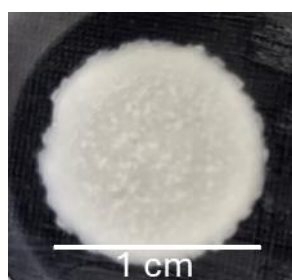


**Figure 6.4.** Bioprinted Gelatin – Alginate patch containing *L. rhamnosus*.

### 6.3.2. Surface Morphology

The surface morphology of the patches was analyzed using SEM. Prior to imaging, the patches were fully dehydrated and sputter-coated with gold. Figure 6.5 illustrates the patches, where *L. rhamnosus* (A) and *L. reuteri* (B) are evenly distributed across the surface. The presence of rod-shaped bacteria is clearly discernible.

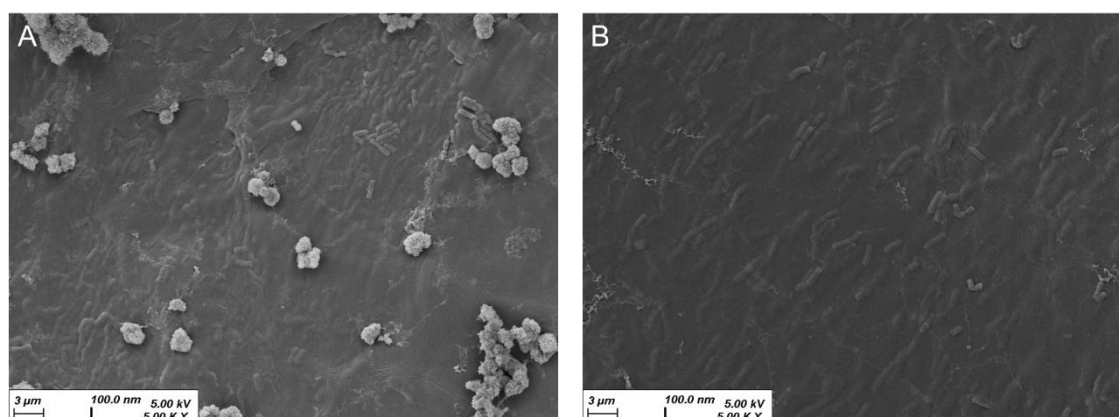


**Figure 6.5.** Bioprinted Gelatin – Alginate patch containing **A:** *L. rhamnosus* **B:** *L. reuteri*, imaged via SEM

### 6.3.3. Activity

The activity of the patches was evaluated immediately following the bioprinting process (Figure 6.6 A). Only pure bacteria were utilized, as microencapsulation would have been susceptible to dissolution in the aqueous environment of the patches. The bioprinting process did not affect the activity of *L. rhamnosus*, with values of 11.42 log(CFU/g) prior to printing and 11.80 log(CFU/g) following the procedure. Similarly, *L. reuteri* demonstrated no notable decline in activity, with values of 11.43 log(CFU/g) prior to and 11.57 log(CFU/g) following bioprinting. The observed variations in the values can be attributed to the presence of living bacteria and natural variations.

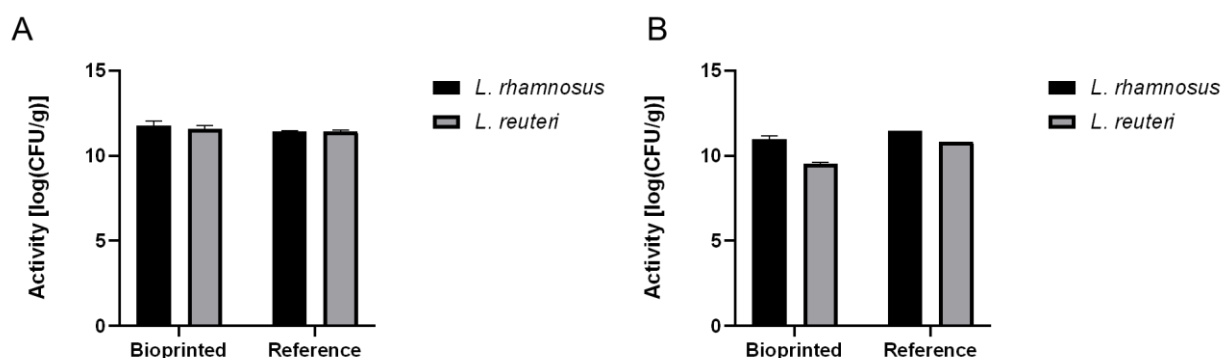


**Figure 6.6.** Assessment of *L. reuteri* and *L. rhamnosus* survival embedded within 3D bioprinted patches **A:** after printing; **B:** freeze-dried patch. n=3, with standard deviation (SD).

Once the patches had been completely dried at 37 °C with forced air circulation for five hours, no bacterial activity was detectable, even at a dilution of 1:100. In contrast, freeze-drying was demonstrated to be a more gentle drying method. Following freeze-drying, pure *L. rhamnosus* retained an activity of 11.47 log(CFU/g), which decreased slightly to 11.00 log(CFU/g) when incorporated into the patch. In the case of *L. reuteri*, the level of activity decreased from 10.82 log(CFU/g) in its pure form to 9.54 log(CFU/g) following incorporation into the patch and subsequent freeze-drying (Figure 6.6 B).

The bacteria demonstrate enhanced survival following freeze-drying when exposed to the printed patch composed of alginate and gelatin as compared to films composed of HPMC and PVA. This phenomenon may be attributed to the distinct structural

characteristics of the respective matrix substances, which serve to stabilize the bacteria.

The bioprinting process did not adversely affect bacterial viability, as shown by the negligible changes in activity for both *L. rhamnosus* and *L. reuteri* immediately after bioprinting. This highlights the gentle nature of bioprinting as a fabrication method. However, the drying method significantly influenced bacterial activity. While drying at 37 °C with forced air circulation led to a complete loss of bacterial activity, freeze-drying proved to be a more viable method, with only a slight reduction in activity for both bacterial strains. This underscores the critical role of the drying process in preserving bacterial viability, making freeze-drying the preferred method.

### 6.3.4. Release

The release of bacteria from the patches was evaluated at 37 °C with gentle shaking, utilizing MilliQ water supplemented with 0.5% trypsin to simulate the oral environment. The release was monitored over a 60-minute period. It is noteworthy that the patches remained intact throughout the observation period, exhibiting no signs of dissolution even after 24 hours.

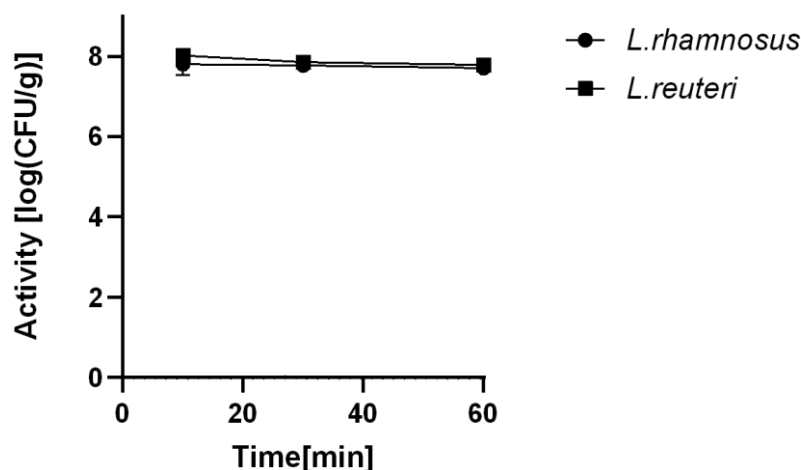


**Figure 6.7.** Assessment of *L. reuteri* and *L. rhamnosus* release from 3D-bioprinted patches over a period of 60 minutes, with samples taken at 10, 30 and 60 minutes. n=3, with standard deviation (SD).

Following a 10-minute period, the activity of *L. rhamnosus* in the surrounding medium was observed to be 7.81 log(CFU/g), which remained stable for the subsequent 30-minute interval (7.77 log(CFU/g)) and the following 60-minute period (7.71 log(CFU/g)). A comparable pattern was observed for *L. reuteri*, with activity levels of 8.02 log(CFU/g) at 10 minutes, 7.85 log(CFU/g) at 30 minutes, and 7.80 log(CFU/g) at 60 minutes. (Figure 6.7).

The consistent bacterial activity, in addition to the intact structure of the patches, indicates that the release mechanism is likely to involve the detachment of bacteria from the surface of the patch, rather than the dissolution of the patch material. Furthermore, the bacteria do not diffuse out through the pores. This is because an increase in the activity of the bacteria in the surrounding medium over time would be indicated by diffusion. It is important to note that the patches were not washed after the printing and crosslinking processes.

### 6.3.5. Bioprinted Grid

To facilitate enhanced bacterial release, the surface area of the patch was increased by printing it in a grid pattern. The resulting structure, as illustrated in Figure 6.8, is a uniform, milky, and cloudy grid. This design should optimize the release mechanism by providing a larger exposed surface area.

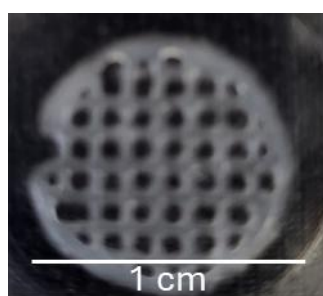


**Figure 6.8.** Bioprinted Gelatin – Alginate grid containing *L. rhamnosus*.

#### 6.3.5.1. Surface Morphology

The surface morphology of the grid-structured patches was also investigated. Figure 6.9 A and C illustrate the grid containing *L. rhamnosus*, while Figure 6.9 B and D depict

the grid containing *L. reuteri*. As with the previously printed patches, rod-shaped bacteria embedded within the gelatin-alginate matrix are clearly discernible on the surface.

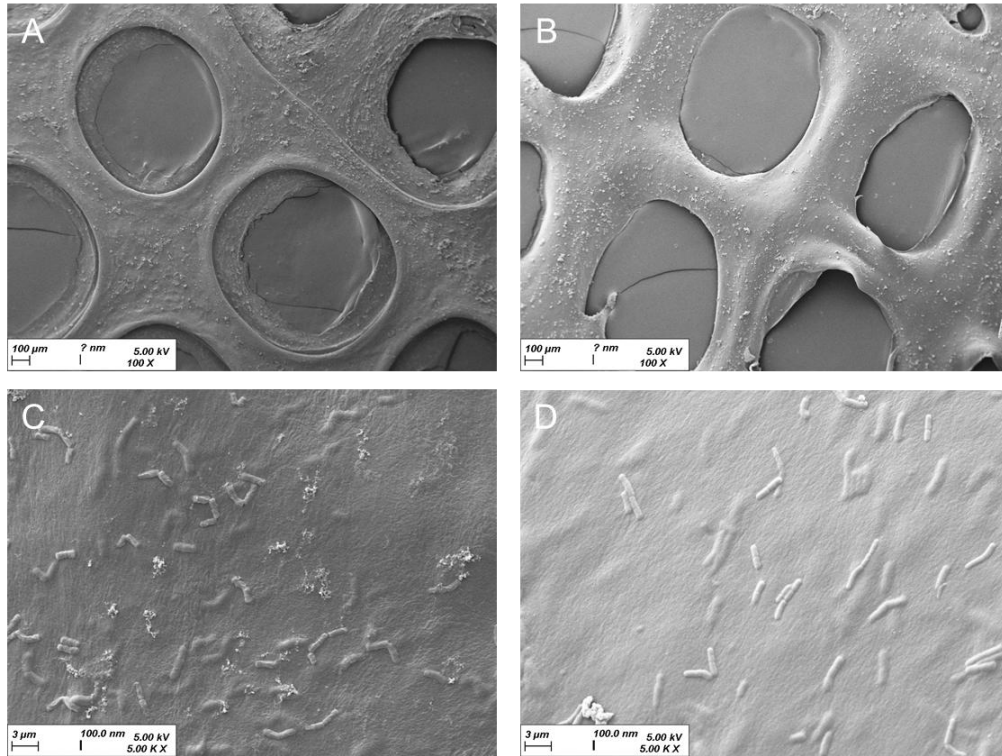


**Figure 6.9.** Bioprinted Gelatin – Alginate grid containing **A & C:** *L. rhamnosus* **B & D:** *L. reuteri*, imaged via SEM

### 6.3.5.2. Activity

The activities of the bacteria in the grid-structured patches were evaluated, demonstrating only minor reductions (Figure 6.10). The activity of *L. rhamnosus* was observed to decline from 11.42 log(CFU/g) following the cultivation process to 10.74 log(CFU/g) subsequent to the bioprinting procedure. Similarly, *L. reuteri* exhibited a negligible decline in activity, from 11.43 log(CFU/g) following cultivation to 10.31 log(CFU/g) post-bioprinting. These findings suggest that the bioprinting process exerts a minimal influence on bacterial viability.



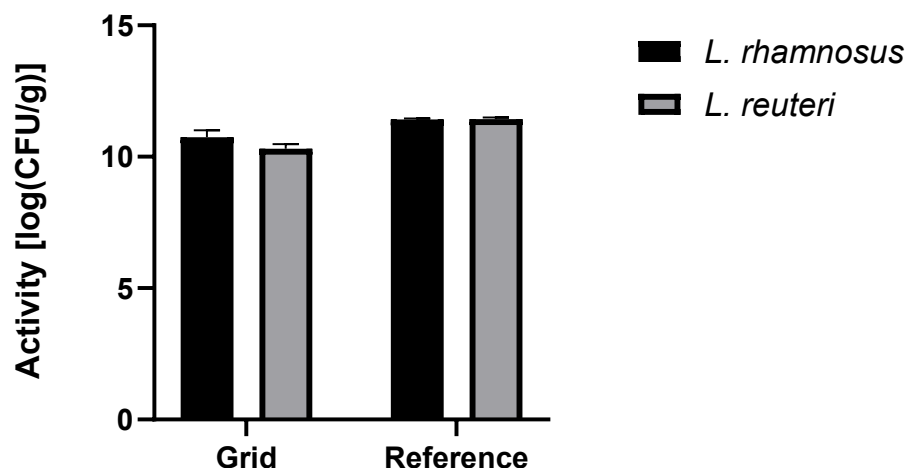


**Figure 6.10.** Assessment of *L. reuteri* and *L. rhamnosus* survival embedded within 3D-bioprinted grid. n=3, with standard deviation (SD).

#### 6.3.5.3. Release

The release of bacteria from grid-structured patches was analyzed using the same methodology as that employed for solid patches. A comparable release pattern was identified. For *L. rhamnosus*, the bacterial activity in the surrounding medium was observed to be 7.95 log(CFU/g) after 10 minutes, 8.04 log(CFU/g) after 30 minutes, and 7.97 log(CFU/g) after 60 minutes. Similarly, for *L. reuteri*, the activity levels were 7.75 log(CFU/g) at 10 minutes, 7.75 log(CFU/g) at 30 minutes, and 7.52 log(CFU/g) at 60 minutes (Figure 6.11).

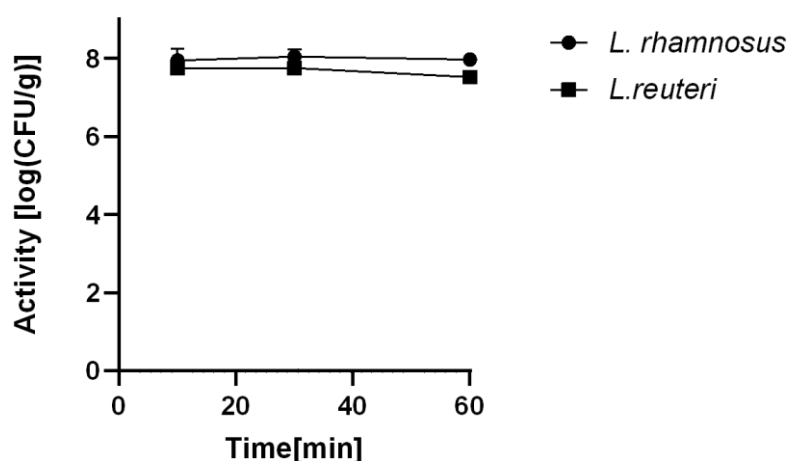


**Figure 6.11.** Assessment of *L. reuteri* and *L. rhamnosus* from 3D-bioprinted grids over a period of 60 minutes, with samples taken at 10, 30 and 60 minutes. n=3, with standard deviation (SD).

The observation of consistent activity over time provides further support for the hypothesis that bacteria are released directly from the surface of the patch. Despite the increased surface area afforded by the grid structure, no significant enhancement in bacterial activity was observed in comparison to the solid patches. To enhance bacterial release, a grid structure was introduced to increase the surface area of the patches. However, while the grid design provided a uniform and cloudy structure, it did not result in a significant increase in bacterial activity during release compared to solid patches. This may indicate that the release mechanism is primarily governed by the surface properties of the material rather than the total exposed surface area. Nevertheless, the grid-structured patches retained bacterial viability with minimal reductions in activity post-bioprinting, similar to the solid patches.

### **6.3.6. Bioprinting formulation – Filmcasting Device**

To facilitate a comparative analysis of the bioprinting process with electromotive film casting, the bioprinting formulation was also processed using an electromotive film casting device, with the resulting bacterial activities analyzed immediately after film casting (Figure 6.12). The activity of *L. rhamnosus* was 11.42 log(CFU/g) both before and after film pulling, while *L. reuteri* exhibited no reduction in activity, with values increasing slightly from 11.43 log(CFU/g) before to 11.68 log(CFU/g) after film pulling.

However, the resulting films were found to be fragile and unsuitable for practical applications after crosslinking, as they were observed to break quickly during analysis. These findings indicate that while bacterial activity remains high after film casting, drying remains a critical step affecting bacterial viability.

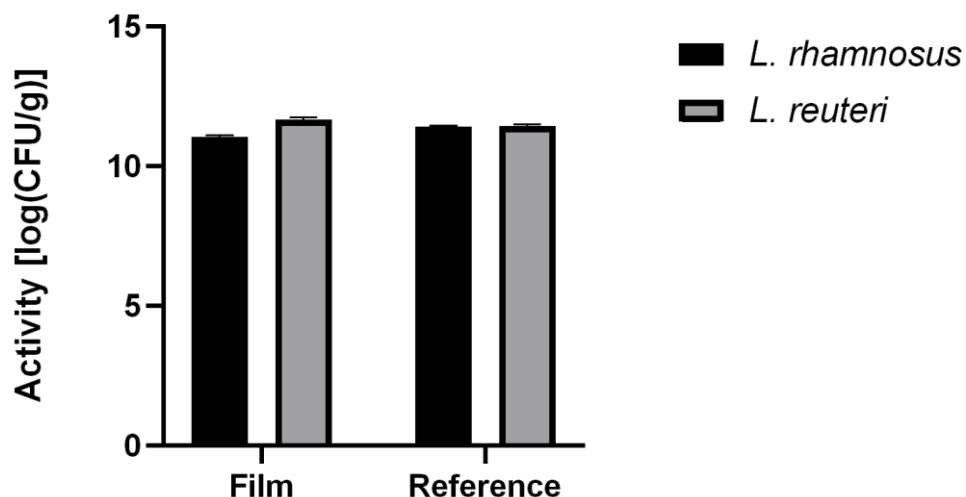


**Figure 6.12.** Assessment of the survival of *L. reuteri* and *L. rhamnosus* embedded within film cased bioink. n=3, with standard deviation (SD).

When comparing the bioprinting process to electromotive film casting, both methods preserved bacterial viability immediately after fabrication, with no significant activity loss observed for *L. rhamnosus* and *L. reuteri*. However, the films produced via the film casting device were fragile and unsuitable for practical applications, breaking down during analysis. These findings further validate the advantage of 3D bioprinting, which produces structurally robust patches with consistent bacterial viability.

Overall, it is shown that 3D bioprinting as an effective and gentle method for incorporating probiotics into hydrogels. The process preserves bacterial activity and structural integrity, making it a promising approach for developing delivery systems for probiotics.

## 6.4. Summary

Hydrogel patches containing the probiotics *L. rhamnosus* and *L. reuteri*, integrated within a gelatin-sodium alginate matrix, were fabricated via 3D bioprinting. The bioprinting process was found to preserve bacterial viability, with minimal reductions in activity observed for both strains post-fabrication. Freeze-drying was identified as the most effective method for drying the patches, with minimal losses in bacterial activity. In contrast, drying at 37 °C with forced air circulation resulted in a complete loss of viability.

The release of bacteria was found to be stable over a 60-minute period, indicating that surface detachment may be the primary release mechanism, rather than dissolution of the hydrogel. The introduction of a grid design to increase the surface area of the patches did not result in enhanced release. This suggests that surface characteristics, rather than area, may govern the release dynamics. Alternatively, the increase in surface area may have been insufficient.

In comparison to bioprinting, electromotive film casting also preserved bacterial viability; however, the resulting films were fragile and unsuitable for practical use. This demonstrates the superiority of bioprinting in the production of structurally stable patches with high bacterial viability.

These findings highlight the potential of three-dimensional bioprinting for the development of probiotic delivery systems. The method is gentle on bacterial viability, provides robust structures, and supports controlled release, making it a promising approach worthy of further investigation. Further work should concentrate on optimizing the design and material properties of the patches in order to enhance functionality and bacterial release.

## 7. Summary & Outlook

This research explores the development of innovative mucoadhesive polymer films containing microencapsulated probiotic bacteria, specifically *L. reuteri* and *L. rhamnosus*, to address the widespread problem of periodontitis. Periodontitis is a chronic inflammatory disease driven by microbial imbalances in the oral cavity. The research's primary goal was to improve the viability, stability, and delivery of these probiotics by embedding them in films designed to adhere to oral surfaces, prolonging their retention time and ensuring targeted release at infection sites.

The study involved several phases: formulation of the polymer films, encapsulation of the bacteria, integration of the encapsulated bacteria into the films, and biological testing to assess efficacy. The results demonstrated that microencapsulation successfully protected the probiotics, and the films adhered well to mucosal surfaces, releasing probiotics over time in the oral environment. In vivo testing indicated that these probiotic films could inhibit harmful bacterial colonization, suggesting a promising non-invasive treatment option for periodontitis.

### 7.1. Film Formulation

The mucoadhesive polymer films were formulated to achieve optimal adhesion, flexibility, and mechanical strength suitable for oral application. Using hydroxypropyl methylcellulose (HPMC) and polyvinyl alcohol (PVA) as primary polymers, the films were designed to form strong bonds with the mucosal surface, prolonging their retention in the oral cavity. Glycerol was included as a plasticizer to enhance flexibility, ensuring that the films could withstand folding and stress without breaking. Different film types were produced, including a thin, flexible HPMC-PVA film and a porous, foamed PVA film with increased loading capacity for probiotics. This versatility in film structure allowed for tailored applications depending on specific treatment needs, such as higher bacterial loading or greater comfort. Testing showed that the films exhibited strong mucoadhesion, suggesting that they could effectively remain in place within the oral cavity to release probiotics over an extended period, making them suitable for localized therapeutic applications in periodontal treatment.

## **7.2. Microencapsulated Bacteria**

To maintain probiotic viability and facilitate controlled release, the bacteria were microencapsulated using a spray-drying process. This technique involved creating a protective matrix around the bacteria to safeguard them from environmental stresses, such as temperature and pH fluctuations. A three-way nozzle configuration was used, optimizing the spray-drying parameters to minimize thermal stress. Eudragit® polymers were employed as encapsulating materials due to their stability and mucoadhesive properties, which enhance retention and protect the probiotics during storage. By adjusting factors like temperature, feed rate, and drying speed, the encapsulation process was fine-tuned to achieve high survival rates, with minimal loss of bacterial viability. The encapsulated bacteria exhibited resilience in preliminary tests, retaining functionality after processing. This microencapsulation approach thus provided a stable and effective means for embedding probiotics within the films, contributing to consistent therapeutic outcomes in oral health applications.

## **7.3. Embedding Bacteria inside Polymer Films**

Following microencapsulation, the encapsulated bacteria were incorporated into the mucoadhesive polymer films. This embedding process involved dispersing the microencapsulated bacteria within a polymer matrix of HPMC and PVA, followed by casting the film using an electromotive film casting device. The goal was to embed the bacteria in the polymer film while maintaining the integrity of the microcapsules. Two main film types were created: a dense, thin HPMC-PVA film and a thicker, porous foamed PVA film. Each film type offered distinct advantages: the thin films were ideal for mucoadhesion and comfort, while the porous films provided increased loading capacity for higher bacterial concentrations. The films were dried under controlled conditions to preserve bacterial viability, with freeze-drying methods also tested to reduce stress on the microorganisms. This integration of probiotics into mucoadhesive films ensured that they could deliver active bacteria directly to affected areas in the oral cavity, enhancing therapeutic potential for periodontitis treatment.

## **7.4. Biological Testing**

Biological efficacy testing involved assessing the viability, adhesion, and probiotic activity of the films within an oral environment. In vitro methods measured bacterial survival and film mucoadhesion, with AFM and tensile testing used to quantify adhesive strength and film flexibility. In vivo testing involved attaching the films to rehydrated bovine enamel mounted on dental splints worn by human volunteers. The films were tested for their ability to release bacteria and promote adhesion to tooth surfaces, real conditions in the oral cavity. Results indicated that the embedded bacteria remained viable and actively adhered to the enamel, reducing colonization by pathogenic bacteria. No adverse reactions were noted in the volunteers, and the films demonstrated strong mucoadhesive properties that allowed for extended bacterial release. This promising outcome suggests that these probiotic films could be a viable, non-invasive therapy for managing periodontitis, supporting oral health by restoring microbial balance and potentially reducing inflammation and infection progression.

## **7.5. Outlook**

This thesis highlights the potential of mucoadhesive polymer films embedded with microencapsulated probiotics as a novel, non-invasive therapeutic approach for periodontitis and other oral health issues. The findings indicate that this method offers a promising alternative to conventional therapies, such as antibiotics or surgical interventions, by targeting and rebalancing the oral microbiome locally without disturbing the overall microbiome. Nevertheless, for this approach to progress from laboratory findings to practical, clinical applications, further research and development are required. The following areas represent key areas for future exploration:

**Optimization of Formulation and Encapsulation:** Although the current study achieved high bacterial survival rates and effective mucoadhesion, further optimization of the encapsulating matrix and film composition could enhance both the longevity of bacterial viability and the film's adhesive properties. The investigation of additional polymers, plasticizers, or other materials may facilitate the enhancement of film flexibility and stability under varying oral conditions, including fluctuations in

## Summary & Outlook

temperature, moisture, and pH levels. In addition to other considerations, polymers capable of releasing bacteria more slowly and over an extended period of time, such as Eudragit RS, could be utilized for microencapsulation. Furthermore, the microencapsulation process can be adapted to allow for dissolution and release of the bacteria at lower pH values, which is a characteristic of inflammatory conditions.

**Scalability and Manufacturing Processes:** The formulation and embedding processes must be adapted for large-scale production. This will entail developing efficient and cost-effective methods for microencapsulation and film casting. It will be necessary to make adjustments to the spray-drying and film-casting processes. However, this objective can be readily achieved, as the processes of spray drying and film casting are both currently employed on a large scale within the industry. Moreover, it is imperative to ascertain the stability over an extended period in accordance with pharmacopoeia and ICH specifications to determine the shelf life.

**Broader Range of Probiotics:** Using more probiotic strains could help develop treatments for specific oral pathogens linked to conditions like gingivitis and halitosis. Adding more strains like *Lactobacillus acidophilus* or *Bifidobacterium bifidum* could improve therapy for specific diseases. For example, *Lactobacillus sp.* inhibit growth of *Streptococcus mutans*, which causes cariogenic diseases.<sup>[177]</sup>

**Clinical trials and long-term efficacy:** To validate these films, clinical trials are needed to evaluate their safety, efficacy, and side effects in a larger patient population. These trials must examine periodontitis symptoms, the microbiome and recurrence rates. The composition of the microbiome in the oral cavity can be identified through the analysis of the genome prior to, during, and following therapeutic intervention. This approach facilitates precise determination of the impact of *L. rhamnosus* and *L. reuteri* on both the pathogenic bacteria and the overall composition of the microbiome. Furthermore, the study will ascertain whether the bacteria establish a permanent colonizing presence.

**Controlled-release mechanisms:** Enhancing the controlled-release profile of the films could improve therapeutic outcomes by ensuring a sustained release of probiotics. It



## Summary & Outlook

would be beneficial to investigate advanced release mechanisms that could respond to pH or enzyme levels. This would allow the film to release probiotics exclusively in the presence of pathogenic bacteria or inflammation. This modification would result in alterations to the composition of the enzymes present in the saliva and the pH value.

**Integration with Other Therapeutic Agents:** Combining probiotics with anti-inflammatory agents, natural extracts, or antimicrobial peptides could provide a more comprehensive treatment for oral diseases. Such agents could act synergistically with the probiotics, reducing inflammation and controlling harmful bacteria. This combination could be particularly efficacious for patients with severe or advanced periodontal disease. For instance, non-steroidal anti-inflammatory rheumatic drugs or glucocorticoids can be administered to mitigate the body's inflammatory response to periodontal disease.<sup>[19]</sup>

**Application to Other Mucosal Environments:** The mucoadhesive film technology developed in this study may extend beyond oral health to other mucosal surfaces. Future research could explore the versatility of these films in delivering probiotics and other therapeutic agents to other body sites.

**Patient Compliance and Usability Studies:** Evaluating the ease of use, comfort, and acceptance of the films from the patient perspective is crucial for successful commercialization. Usability studies on factors like taste, texture, and application duration can inform modifications to enhance compliance, particularly for long-term treatments. This procedure could be conducted as part of a broader efficacy and safety clinical trial.

By advancing in these directions, probiotic mucoadhesive films could become a viable, widely accessible therapy that benefits a range of oral health conditions. Ultimately, this technology has the potential to contribute significantly to personalized and preventive dental care by offering a sustainable, low-impact, and highly targeted treatment option.

## 8. References

- [1] *Probiotics in Food: Health and Nutritional Properties and Guidelines for Evaluation: Report of a Joint FAO/WHO Expert Consultation on Evaluation of Health and Nutritional Properties of Probiotics in Food, Including Powder Milk with Live Lactic Acid Bacteria: Cordoba, Argentina, 1-4 October 2001: Report of a Joint FAO/WHO Working Group on Drafting Guidelines for the Evaluation of Probiotics in Food*, Food And Agriculture Organization Of The United Nations, **2006**.
- [2] C. Hill, F. Guarner, G. Reid, G. R. Gibson, D. J. Merenstein, B. Pot, L. Morelli, R. B. Canani, H. J. Flint, S. Salminen, et al., *Nat Rev Gastroenterol Hepatol* **2014**, 11, 506.
- [3] M. Kechagia, D. Basoulis, S. Konstantopoulou, D. Dimitriadi, K. Gyftopoulou, N. Skarmoutsou, E. M. Fakiri, *ISRN Nutr* **2013**, 2013, 1.
- [4] D. Verma, P. K. Garg, A. K. Dubey, *Arch Microbiol* **2018**, 200, 525.
- [5] M. Di Stefano, A. Polizzi, S. Santonocito, A. Romano, T. Lombardi, G. Isola, *Int J Mol Sci* **2022**, 23, DOI 10.3390/ijms23095142.
- [6] L. Sedghi, V. DiMassa, A. Harrington, S. V. Lynch, Y. L. Kapila, *Periodontol 2000* **2021**, 87, 107.
- [7] K. Lima-Engelmann, M. Schneider, *Current Nutraceuticals* **2022**, 3, DOI 10.2174/2665978604666221122112434.
- [8] M. Kilian, I. L. C. Chapple, M. Hannig, P. D. Marsh, V. Meuric, A. M. L. Pedersen, M. S. Tonetti, W. G. Wade, E. Zaura, *Br Dent J* **2016**, 221, 657.
- [9] M. Minty, T. Canceil, M. Serino, R. Burcelin, F. Tercé, V. Blasco-Baque, *Rev Endocr Metab Disord* **2019**, 20, 449.
- [10] M. A. Listgarten, Peter M Loomer, *Ann Periodontol* **2003**, 8, 182.
- [11] Y. Li, Z. Xing, S. Wang, Y. Wang, Z. Wang, L. Dong, *Acta Biomater* **2023**, 158, 759.
- [12] L. J. Frédéric, B. Michel, T. Selen, *Materials* **2018**, 11, DOI 10.3390/ma11101802.

## References

---

- [13] C. A. Field, M. D. Gidley, P. M. Preshaw, N. Jakubovics, **n.d.**, DOI 10.1111/j.1600-0765.2011.01455.x.Ó.
- [14] S. Murakami, B. L. Mealey, A. Mariotti, I. L. C. Chapple, *J Periodontol* **2018**, *89*, S17.
- [15] M. A. Curtis, P. I. Diaz, T. E. Van Dyke, *Periodontol 2000* **2020**, *83*, 14.
- [16] G. Hajishengallis, R. P. Darveau, M. A. Curtis, *Nat Rev Microbiol* **2012**, *10*, 717.
- [17] R. P. Darveau, G. Hajishengallis, M. A. Curtis, *J Dent Res* **2012**, *91*, 816.
- [18] L. M. Sedghi, M. Bacino, Y. L. Kapila, *Front Cell Infect Microbiol* **2021**, *11*, DOI 10.3389/fcimb.2021.766944.
- [19] T. H. Kwon, I. B. Lamster, L. Levin, *Int Dent J* **2021**, *71*, 462.
- [20] F. Inchingolo, F. S. Martelli, C. G. Isacco, E. Borsani, S. Cantore, F. Corcioli, A. Boddi, K. C. D. Nguyễn, D. De Vito, S. K. Aityan, et al., *Biomedicines* **2020**, *8*, DOI 10.3390/BIOMEDICINES8050115.
- [21] M. R. Jørgensen, C. Kragelund, P. Ø. Jensen, M. K. Keller, S. Twetman, *J Oral Microbiol* **2017**, *9*, DOI 10.1080/20002297.2016.1274582.
- [22] M. S. Kang, J. S. Oh, H. C. Lee, H. S. Lim, S. W. Lee, K. H. Yang, N. K. Choi, S. M. Kim, *Journal of Microbiology* **2011**, *49*, 193.
- [23] N. Romani Vestman, P. Hasslöf, M. K. Keller, E. Granström, S. Roos, S. Twetman, C. Stecksén-Blicks, *Caries Res* **2013**, *47*, 338.
- [24] W. Teughels, A. Durukan, O. Ozcelik, M. Pauwels, M. Quirynen, M. C. Haytac, *J Clin Periodontol* **2013**, *40*, 1025.
- [25] U. Schlagenhauf, J. Rehder, G. Gelbrich, Y. Jockel-Schneider, *J Periodontol* **2020**, *91*, 1328.
- [26] I. Laleman, M. Pauwels, M. Quirynen, W. Teughels, *J Clin Periodontol* **2020**, *47*, 43.
- [27] U. Schlagenhauf, L. Jakob, M. Eigenthaler, S. Segerer, Y. Jockel-Schneider, M. Rehn, *J Clin Periodontol* **2016**, *43*, 948.

## References

---

- [28] A. Alanzi, S. Honkala, E. Honkala, A. Varghese, M. Tolvanen, E. Söderling, *Benef Microbes* **2018**, *9*, 593.
- [29] S. D'Agostino, G. Valentini, F. Iarussi, M. Dolci, *Dent J (Basel)* **2024**, *12*, DOI 10.3390/dj12040102.
- [30] M. K. Keller, E. Brandsborg, K. Holmstrøm, S. Twetman, *Benef Microbes* **2018**, *9*, 487.
- [31] A. Toiviainen, H. Jalasvuori, E. Lahti, U. Gursoy, S. Salminen, M. Fontana, S. Flannagan, G. Eckert, A. Kokaras, B. Paster, et al., *Clin Oral Investig* **2015**, *19*, 77.
- [32] N. Choudhury, M. Meghwal, K. Das, *Food Front* **2021**, DOI 10.1002/fft2.94.
- [33] P. Pupa, P. Apiwatsiri, W. Sirichokchatchawan, N. Pirarat, N. Muangsin, A. A. Shah, N. Prapasarakul, *Sci Rep* **2021**, *11*, DOI 10.1038/s41598-021-93263-z.
- [34] P. Kanmani, R. Satish Kumar, N. Yuvaraj, K. A. Paari, V. Pattukumar, V. Arul, *Biotechnology and Bioprocess Engineering* **2011**, *16*, 1106.
- [35] L. K. Sarao, M. Arora, *Crit Rev Food Sci Nutr* **2017**, *57*, 344.
- [36] D. Dianawati, V. Mishra, N. P. Shah, *Crit Rev Food Sci Nutr* **2016**, *56*, 1685.
- [37] T. B. Lopez-Mendez, E. Santos-Vizcaino, J. L. Pedraz, R. M. Hernandez, G. Orive, *Drug Discov Today* **2021**, *26*, 852.
- [38] K. Kondo, T. Niwa, K. Danjo, *European Journal of Pharmaceutical Sciences* **2014**, *51*, 11.
- [39] M. Chavarri, I. Maranon, M. Carmen, in *Probiotics*, InTech, **2012**.
- [40] E. Ananta, M. Volkert, D. Knorr, *Int Dairy J* **2005**, *15*, 399.
- [41] S. Arslan-Tontul, M. Erbas, *LWT* **2017**, *81*, 160.
- [42] M. . Jantzen, A. Göpel, C. Beermann, *J Appl Microbiol* **2013**, *115*, DOI 10.1111.
- [43] K. S. Yoha, S. Nida, S. Dutta, J. A. Moses, C. Anandharamakrishnan, *Probiotics Antimicrob Proteins* **2022**, *14*, 15.

## References

---

- [44] D. Semyonov, O. Ramon, E. Shimoni, *LWT* **2011**, 44, 1844.
- [45] N. Shetty, Y. Zhang, H. Park, D. Zemlyanov, D. Shah, A. He, P. Ahn, T. T. Mutukuri, H. K. Chan, Q. (Tony) Zhou, *Pharm Res* **2020**, 37, DOI 10.1007/s11095-020-02937-2.
- [46] M. Gover Antoniraj, M. Maria Leena, J. A. Moses, C. Anandharamakrishnan, *Int J Biol Macromol* **2020**, 147, 1268.
- [47] R. M. Pabari, T. Sunderland, Z. Ramtoola, *Expert Opin Drug Deliv* **2012**, 9, 1463.
- [48] A. Al-Khattawi, A. Bayly, A. Phillips, D. Wilson, *Expert Opin Drug Deliv* **2018**, 15, 47.
- [49] A. Kauppinen, J. Broekhuis, N. Grasmeijer, W. Tonnis, J. Ketolainen, H. W. Frijlink, W. L. J. Hinrichs, *European Journal of Pharmaceutics and Biopharmaceutics* **2018**, 123, 50.
- [50] R. M. Pabari, T. Sunderland, Z. Ramtoola, *Expert Opin Drug Deliv* **2012**, 9, 1463.
- [51] F. Wan, M. J. Maltesen, S. K. Andersen, S. Bjerregaard, C. Foged, J. Rantanen, M. Yang, *Pharm Res* **2014**, 31, 1967.
- [52] L. A. Felton, G. Binzet, C. Wiley, D. McChesney, J. McConville, M. Çelik, P. Muttil, *Int J Pharm* **2024**, 658, DOI 10.1016/j.ijpharm.2024.124191.
- [53] M. Maria Leena, M. Gover Antoniraj, J. A. Moses, C. Anandharamakrishnan, *J Drug Deliv Sci Technol* **2020**, 57, DOI 10.1016/j.jddst.2020.101678.
- [54] A. Yousfan, A. O. Al Khatib, A. M. H. Salman, M. H. Abu Elella, G. Barrett, N. Michael, M. G. Zariwala, H. Al-Obaidi, *Mol Pharm* **2024**, DOI 10.1021/acs.molpharmaceut.4c00594.
- [55] N. America, L. America, M. S. Evonik Degussa Argentina A, *Comparison of Protective Coatings Based on Methacrylate Copolymers*, EUDRAGIT® Application Guidelines, **2010**.
- [56] S. Thakral, N. K. Thakral, D. K. Majumdar, *Expert Opin Drug Deliv* **2013**, 10, 131.
- [57] G. Ruíz, E. S. Ghaly, *Revista de la Facultad de Química Farmaceutica* **2006**, 13, 31.
- [58] S. Das, P. K. Suresh, R. Desmukh, *Nanomedicine* **2010**, 6, 318.

## References

---

- [59] C. Eckermann, C. Lasch, A. Luzhetskyy, M. Schneider, *European Journal of Pharmaceutics and Biopharmaceutics* **n.d.**
- [60] A. Bomba, R. Nemcová, S. Gancarcíková, R. Herich, P. Guba, D. Mudronová, *British Journal of Nutrition* **2002**, *88*, S95.
- [61] A. Sohail, M. S. Turner, A. Coombes, B. Bhandari, *Food Bioproc Tech* **2013**, *6*, 2763.
- [62] J. Agudelo, A. Cano, C. González-Martínez, A. Chiralt, *J Funct Foods* **2017**, *37*, 416.
- [63] S. Alaei, H. Omidian, *European Journal of Pharmaceutical Sciences* **2021**, *159*, DOI 10.1016/j.ejps.2021.105727.
- [64] V. V. Khutoryanskiy, *Macromol Biosci* **2011**, *11*, 748.
- [65] A. R. Mackie, F. M. Goycoolea, B. Menchicchi, C. M. Caramella, F. Saporito, S. Lee, K. Stephansen, I. S. Chronakis, M. Hiorth, M. Adamczak, et al., *Macromol Biosci* **2017**, *17*, DOI 10.1002/mabi.201600534.
- [66] E. Hagesaether, M. Hiorth, S. A. Sande, *European Journal of Pharmaceutics and Biopharmaceutics* **2009**, *71*, 325.
- [67] S. Jacob, A. B. Nair, S. H. S. Boddu, B. Gorain, N. Sreeharsha, J. Shah, *Pharmaceutics* **2021**, *13*, DOI 10.3390/pharmaceutics13081206.
- [68] K. Naz, G. Shahnaz, N. Ahmed, N. A. Qureshi, H. S. Sarwar, M. Imran, G. M. Khan, *AAPS PharmSciTech* **2017**, *18*, 1043.
- [69] J. O. Morales, J. T. McConville, *European Journal of Pharmaceutics and Biopharmaceutics* **2011**, *77*, 187.
- [70] O. L. Pop, C. R. Pop, M. Dufrechou, D. C. Vodnar, S. A. Socaci, F. V. Dulf, F. Minervini, R. Suharoschi, *Polymers (Basel)* **2020**, *12*, DOI 10.3390/polym12010012.
- [71] D. M. Rajaram, S. D. Laxman, *Systematic Reviews in Pharmacy* **2016**, *8*, 31.
- [72] Q. D. Pham, S. Nöjd, M. Edman, K. Lindell, D. Topgaard, M. Wahlgren, *Int J Pharm* **2021**, *610*, DOI 10.1016/j.ijpharm.2021.121245.

## References

---

- [73] B. Chatterjee, N. Amalina, P. Sengupta, U. K. Mandal, *J Appl Pharm Sci* **2017**, 7, 195.
- [74] M. P. Deacon, S. McGurk, C. J. Roberts, P. M. Williams, S. J. B. Tendler, M. C. Davies, S. S. Davis, S. E. Harding, *Biochemical Journal* **2000**, 348, 557.
- [75] V. Garsuch, J. Breitreutz, *European Journal of Pharmaceutics and Biopharmaceutics* **2009**, 73, 195.
- [76] F. Laffleur, *Drug Dev Ind Pharm* **2014**, 40, 591.
- [77] M. Hanif, M. Zaman, V. Chaurasiya, *Des Monomers Polym* **2015**, 18, 105.
- [78] J. O. Morales, J. T. McConville, *European Journal of Pharmaceutics and Biopharmaceutics* **2011**, 77, 187.
- [79] P. Kanmani, S. T. Lim, *Food Chem* **2013**, 141, 1041.
- [80] M. Preis, C. Woertz, P. Kleinebudde, J. Breitreutz, *Expert Opin Drug Deliv* **2013**, 10, 1303.
- [81] T. Nyström, *Annu Rev Microbiol* **2004**, 58, 161.
- [82] K. Papadimitriou, Á. Alegría, P. A. Bron, M. de Angelis, M. Gobetti, M. Kleerebezem, J. A. Lemos, D. M. Linares, P. Ross, C. Stanton, et al., *Microbiology and Molecular Biology Reviews* **2016**, 80, 837.
- [83] M. Saarela, M. Rantala, K. Hallamaa, L. Nohynek, I. Virkajärvi, J. Mättö, *J Appl Microbiol* **2004**, 96, 1205.
- [84] J. Wallenius, T. Uuksulainen, K. Salonen, J. Rautio, T. Eerikäinen, *Bioprocess Biosyst Eng* **2011**, 34, 1169.
- [85] A. Hernández, C. U. Larsson, R. Sawicki, E. W. J. van Niel, S. Roos, S. Håkansson, *AMB Express* **2019**, 9, DOI 10.1186/s13568-019-0789-2.
- [86] J. Palmfeldt, B. Hahn-Hagerdal, *Influence of Culture PH on Survival of Lactobacillus Reuteri Subjected to Freeze-Drying*, **2000**.
- [87] A. Siaterlis, G. Deepika, D. Charalampopoulos, *Lett Appl Microbiol* **2009**, 48, 295.

## References

---

- [88] M. Polak-Berecka, A. Wasko, M. Kordowka-Wiater, *Pol J Microbiol* **2010**, 59, 113.
- [89] C. Zhang, Y. Han, Y. Gui, Y. Wa, D. Chen, Y. Huang, B. Yin, R. Gu, *J Ind Microbiol Biotechnol* **2022**, 49, DOI 10.1093/jimb/kuac020.
- [90] A. Lo Curto, I. Pitino, G. Mandalari, J. R. Dainty, R. M. Faulks, M. S. John Wickham, *Food Microbiol* **2011**, 28, 1359.
- [91] S. Koch, G. Oberson, E. Eugster-Meier, L. Meile, C. Lacroix, *Int J Food Microbiol* **2007**, 117, 36.
- [92] A. Terpou, A. Papadaki, I. K. Lappa, V. Kachrimanidou, L. A. Bosnea, N. Kopsahelis, *Nutrients* **2019**, 11, DOI 10.3390/nu11071591.
- [93] J. Prasad, P. McJarrow, P. Gopal, *Appl Environ Microbiol* **2003**, 69, 917.
- [94] E. R. Fischer, B. T. Hansen, V. Nair, F. H. Hoyt, D. W. Dorward, *Curr Protoc Microbiol* **2012**, DOI 10.1002/9780471729259.mc02b02s25.
- [95] S. A. and K. S. B. and A. A. M. Akhtar Kalsoom and Khan, in *Handbook of Materials Characterization* (Ed: S. K. Sharma), Springer International Publishing, Cham, **2018**, pp. 113–145.
- [96] A. Ul-Hamid, *SpringerInternationalPublishing* **2018**.
- [97] M. Koch, M. K. Włodarczyk-Biegun, **2020**, DOI 10.1101/2020.03.18.997668.
- [98] J. Grobelny, DelRio FW, Pradeep N, Kim DI, Hackley VA, Cook RF, *National Cancer Institute's Nanotechnology Characterization Laboratory Assay Cascade Protocols. Bethesda* **2009**.
- [99] T. Nandi, Sri Rama Koti Ainavarapu, *Emerg Top Life Sci* **2021**, 5, 103.
- [100] T. M. Ho, F. Abik, K. S. Mikkonen, *Crit Rev Food Sci Nutr* **2022**, 62, 4908.
- [101] T. Ando, *Curr Opin Chem Biol* **2019**, 51, 105.
- [102] M. Davidovich-Pinhas, H. Bianco-Peled, *Expert Opin Drug Deliv* **2010**, 7, 259.
- [103] J. Mohammad, M. Thariq, N. Saba, *Mechanical and Physical Testing of Biocomposites, Fibre-Reinforced Composites and Hybrid Composites*, **2019**.



## References

---

- [104] ISO 527-3:2018, **2018**.
- [105] J. Yan, X. Chen, S. Yu, H. Zhou, *J Drug Deliv Sci Technol* **2017**, *40*, 157.
- [106] S. Hekmat, H. Soltani, G. Reid, *Innovative Food Science and Emerging Technologies* **2009**, *10*, 293.
- [107] S. A. Hayek, R. Gyawali, S. O. Aljaloud, A. Krastanov, S. A. Ibrahim, *Journal of Dairy Research* **2019**, *86*, 490.
- [108] B. V. R. Tata, B. Raj, *Confocal Laser Scanning Microscopy: Applications in Material Science and Technology*, **1998**.
- [109] P. O. Bayguinov, D. M. Oakley, C. C. Shih, D. J. Geanon, M. S. Joens, J. A. J. Fitzpatrick, *Curr Protoc Cytom* **2018**, *85*, DOI 10.1002/cpcy.39.
- [110] C. L. Smith, *Curr Protoc Microbiol* **2006**, *00*, DOI 10.1002/9780471729259.mc02c01s01.
- [111] F. E. Dewhirst, T. Chen, J. Izard, B. J. Paster, A. C. R. Tanner, W. H. Yu, A. Lakshmanan, W. G. Wade, *J Bacteriol* **2010**, *192*, 5002.
- [112] Buchi, *Spray-Drying*, **2021**.
- [113] Y. C. Huang, M. K. Yeh, S. N. Cheng, C. H. Chiang, *J Microencapsul* **2003**, *20*, 459.
- [114] K. Cal, K. Sollohub, *J Pharm Sci* **2010**, *99*, 575.
- [115] K. Sollohub, K. Cal, *J Pharm Sci* **2010**, *99*, 587.
- [116] K. Kondo, T. Niwa, K. Danjo, *European Journal of Pharmaceutical Sciences* **2014**, *51*, 11.
- [117] M. Gagneten, S. Passot, S. Cenard, S. Ghorbal, C. Schebor, F. Fonseca, *Appl Microbiol Biotechnol* **2024**, *108*, DOI 10.1007/s00253-024-13186-3.
- [118] R. J. B. Heinemann, R. A. Carvalho, C. S. Favaro-Trindade, *Innovative Food Science and Emerging Technologies* **2013**, *19*, 227.
- [119] M. He, L. Zhu, N. Yang, H. Li, Q. Yang, *Int J Pharm* **2021**, *604*, DOI 10.1016/j.ijpharm.2021.120759.

## References

---

- [120] B. M. A. Silva, A. F. Borges, C. Silva, J. F. J. Coelho, S. Simões, *Int J Pharm* **2015**, 494, 537.
- [121] S. Alaei, H. Omidian, *European Journal of Pharmaceutical Sciences* **2021**, 159, DOI 10.1016/j.ejps.2021.105727.
- [122] S. Shukla, **2011**, 2, 3061.
- [123] K. A. Gaidhani, M. Harwalkar, D. Bhambere, P. S. Nirgude, Kunal et al. *World Journal of Pharmaceutical Research World Journal of Pharmaceutical Research SJIF Impact Factor 5* **2015**, 4, 517.
- [124] I. Roy, M. N. Gupta, *Biotechnol Appl Biochem* **2004**, 39, 165.
- [125] H. Kawasaki, T. Shimanouchi, Y. Kimura, *J Chem* **2019**, 2019, DOI 10.1155/2019/9502856.
- [126] F. Franks, *Freeze-Drying of Bioproducts: Putting Principles into Practice*, **1998**.
- [127] S. Aliyazdi, S. Frisch, A. Hidalgo, N. Frank, D. Krug, R. Müller, U. F. Schaefer, T. Vogt, B. Loretz, C. M. Lehr, *Biofabrication* **2023**, 15, DOI 10.1088/1758-5090/acd95e.
- [128] K. S. Yoha, T. Anukiruthika, W. Anila, J. A. Moses, C. Anandharamakrishnan, *LWT* **2021**, 146, DOI 10.1016/j.lwt.2021.111461.
- [129] Y. Liu, X. Yin, X. Xia, Z. Liu, L. Chen, M. Dong, *Food Science and Human Wellness* **2023**, 12, 477.
- [130] Y. Liu, X. Yin, X. Xia, Z. Liu, L. Chen, M. Dong, *Food Science and Human Wellness* **2023**, 12, 477.
- [131] J. O. Morales, J. T. McConville, *European Journal of Pharmaceutics and Biopharmaceutics* **2011**, 77, 187.
- [132] I. Khadra, M. A. Obeid, C. Dunn, S. Watts, G. Halbert, S. Ford, A. Mullen, *Int J Pharm* **2019**, 561, 43.
- [133] S. Mansuri, P. Kesharwani, K. Jain, R. K. Tekade, N. K. Jain, *React Funct Polym* **2016**, 100, 151.
- [134] R. Shaikh, T. Raj Singh, M. Garland, A. Woolfson, R. Donnelly, *J Pharm Bioallied Sci* **2011**, 3, 89.

## References

---

- [135] J. D. Smart, *Adv Drug Deliv Rev* **2005**, 57, 1556.
- [136] S. Golshani, A. Vatanara, M. Amin, *Recent Advances in Oral Mucoadhesive Drug Delivery*, **2022**.
- [137] Q. Zhang, X. Li, B. R. Jasti, *Int J Pharm* **2021**, 609, DOI 10.1016/j.ijpharm.2021.121218.
- [138] T. H. Kim, J. S. Ahn, H. K. Choi, Y. J. Choi, C. S. Cho, *A Novel Mucoadhesive Polymer Film Composed of Carbopol, Poloxamer and Hydroxypropylmethylcellulose*, **2007**.
- [139] E. Karavas, E. Georgarakis, D. Bikiaris, *European Journal of Pharmaceutics and Biopharmaceutics* **2006**, 64, 115.
- [140] N. Jaipakdee, T. Pongjanyakul, E. Limpongsa, *International Journal of Applied Pharmaceutics* **2018**, 10, 115.
- [141] Y. Ikeuchi-Takahashi, C. Ishihara, H. Onishi, *Drug Dev Ind Pharm* **2017**, 43, 1489.
- [142] N. A. Peppas, N. K. Mongia, *Ultrapure Poly(Vinyl Alcohol) Hydrogels with Mucoadhesive Drug Delivery Characteristics*, **1997**.
- [143] C. F. Vecchi, G. B. Cesar, P. R. de Souza, W. Caetano, M. L. Bruschi, *Pharm Dev Technol* **2021**, 26, 138.
- [144] P. J. Bora, A. G. Anil, P. C. Ramamurthy, Y. H. Lee, *Macromol Rapid Commun* **2021**, 42, DOI 10.1002/marc.202000763.
- [145] G. Broeckx, D. Vandenheuvel, I. J. J. Claes, S. Lebeer, F. Kiekens, *Int J Pharm* **2016**, 505, 303.
- [146] X. Gao, J. Kong, H. Zhu, B. Mao, S. Cui, J. Zhao, *J Appl Microbiol* **2022**, 132, 802.
- [147] Y. Wang, K. Kho, W. S. Cheow, K. Hadinoto, *Int J Pharm* **2012**, 424, 98.
- [148] J. Schmitz, E. Manevich, M. Tschöpe, R. Alon, K. E. Gottschalk, *Soft Matter* **2009**.
- [149] J. Bohn, A. Yüksel-Dadak, S. Dröge, H. König, *J Biotechnol* **2017**, 244, 4.

## References

---

- [150] N. Wiemer, A. Wetzel, M. Schleiting, P. Krooß, M. Vollmer, T. Niendorf, S. Böhm, B. Middendorf, *Materials* **2020**, *13*, DOI 10.3390/ma13143128.
- [151] A. Abdkader, P. Penzel, D. Friese, M. Overberg, L. Hahn, M. Butler, V. Mechtcherine, C. Cherif, *Materials* **2023**, *16*, DOI 10.3390/ma16062459.
- [152] B. D. Sahm, A. B. V. Teixeira, A. C. dos Reis, *Japanese Dental Science Review* **2023**, *59*, 160.
- [153] S. Y. Khin, H. M. S. H. Soe, C. Chansriniyom, N. Pornputtapong, R. Asasutjarit, T. Loftsson, P. Jansook, *Molecules* **2022**, *27*, DOI 10.3390/molecules27154755.
- [155] C. Iaconelli, G. Lemetais, N. Kechaou, F. Chain, L. G. Bermúdez-Humarán, P. Langella, P. Gervais, L. Beney, *J Biotechnol* **2015**, *214*, 17.
- [156] C. Iaconelli, G. Lemetais, N. Kechaou, F. Chain, L. G. Bermúdez-Humarán, P. Langella, P. Gervais, L. Beney, *J Biotechnol* **2015**, *214*, 17.
- [157] M. Moayyedi, M. H. Eskandari, A. H. E. Rad, E. Ziaee, M. H. H. Khodaparast, M. T. Golmakani, *J Funct Foods* **2018**, *40*, 391.
- [158] P. Gong, L. Zhang, X. Han, N. Shigwedha, W. Song, H. Yi, M. Du, C. Cao, *Drying Technology* **2014**, *32*, 793.
- [159] X. T. Liu, C. L. Hou, J. Zhang, X. F. Zeng, S. Y. Qiao, *Lett Appl Microbiol* **2014**, *59*, 398.
- [160] J. Prasad, P. McJarrow, P. Gopal, *Appl Environ Microbiol* **2003**, *69*, 917.
- [161] M. Chaouat, C. Le Visage, W. E. Baille, B. Escoubet, F. Chaubet, M. A. Mateescu, D. Letourneur, *Adv Funct Mater* **2008**, *18*, 2855.
- [162] M. A. Momoh, F. C. Kenechukwu, P. O. Nnamani, J. C. Umetiti, *Drug Deliv* **2015**, *22*, 837.
- [163] Y. Zhang, X. Wu, L. Meng, Y. Zhang, R. Ai, N. Qi, H. He, H. Xu, X. Tang, *Int J Pharm* **2012**, *436*, 341.
- [164] J. Sahoo, P. N. Murthy, S. Biswal, Manik, *AAPS PharmSciTech* **2009**, *10*, 27.
- [165] M. Brennan, B. Wanismail, M. C. Johnson, B. Ray, *Cellular Damage in Dried Lactobacillus Acidophilus*, **1986**.

## References

---

- [166] P. G. Cataldo, P. Klemm, M. Thüring, L. Saavedra, E. M. Hebert, R. K. Hartmann, M. Lechner, *BMC Genom Data* **2021**, 22, DOI 10.1186/s12863-021-00983-2.
- [167] I. Ravn, I. Dige, R. L. Meyer, B. Nyvad, *Caries Res* **2012**, 46, 107.
- [168] W. Teughels, M. Van Essche, I. Sliepen, M. Quirynen, *Periodontol 2000* **2008**, 48, 111.
- [169] H. Yli-Knuuttila, J. Snäll, K. Kari, J. H. Meurman, *Oral Microbiol Immunol* **2006**, 21, 129.
- [170] A. J. Flichy-Fernández, T. Alegre-Domingo, D. Peñarrocha-Oltra, M. Peñarrocha-Diago, *Med Oral Patol Oral Cir Bucal* **2010**, 15, DOI 10.4317/medoral.15.e677.
- [171] J. H. Meurman, I. Stamatova, *Oral Dis* **2007**, 13, 443.
- [172] G. B. Proctor, *Periodontol 2000* **2016**, 70, 11.
- [173] M. Hannig, *Eur J Oral Sci* **1999**, 107.
- [174] M. Popović, M. Stojanović, Z. Veličković, A. Kovačević, R. Miljković, N. Mirković, A. Marinković, *Int J Biol Macromol* **2021**, 183, 423.
- [175] D. Shahrampour, M. Khomeiri, S. M. A. Razavi, M. Kashiri, *LWT* **2020**, 118, DOI 10.1016/j.lwt.2019.108758.
- [176] P. K. Akman, F. Bozkurt, K. Dogan, F. Tornuk, F. Tamturk, *Journal of Food Measurement and Characterization* **2021**, 15, 84.
- [177] R. Wasfi, O. A. Abd El-Rahman, M. M. Zafer, H. M. Ashour, *J Cell Mol Med* **2018**, 22, 1972.

## Publication Report

### Paper

“Development of Mucoadhesive Polymer Films as a Delivery System for Microencapsulated *Lactobacillus reuteri* – Strategies to Improve Bacterial Viability” by Charlotte Eckermann, Constanze Lasch, Sangeun Lee, Andriy Luzhetskyy and Marc Schneider

Prepared for submission

“Probiotic-Embedded Polymer Films for Oral Health: Development, Characterization, and Therapeutic Potential” by Charlotte Eckermann, Florian Schäfer, Marc Thiel, Agnes-Valencia Weiss, Christian Motz, Karen Lienkamp, Matthias Hannig, Marc Schneider

Prepared for submission

### Posters

“Development of Mucoadhesive Probiotic Films”

*DPHG Annual Meeting, Marburg 2023*

“Development and Characterization of Mucoadhesive Probiotic Films”

*CRS Local Chapter, Annual Meeting, Würzburg 2023*

“Development of Mucoadhesive Probiotic Films containing *Lactobacillus reuteri*”

*CRS Local Chapter, Annual Meeting, Bad Dürkheim 2024*

## **Oral Talk**

“Enhancing viability of Lactobacilli in mucoadhesive polymer films”

GPEN Annual Meeting, Copenhagen 2024

## Acknowledgements

Mit großer Dankbarkeit möchte ich mich bei all jenen bedanken, die mich während meiner Promotionszeit begleitet und unterstützt haben.

Mein besonderer Dank gilt meinem Erstgutachter und Betreuer, Prof. Dr. Marc Schneider (Biopharmazie und Pharmazeutische Technologie), für seine wertvollen Ideen, die kontinuierlichen Möglichkeiten zur Weiterentwicklung sowie den regelmäßigen, fachlichen Austausch, der meine Arbeit maßgeblich bereichert hat.

Ebenso danke ich meinem Zweitgutachter, Prof. Dr. Andriy Luzhetskyy (Pharmazeutische Biotechnologie), für seine inspirierenden neuen Perspektiven und das Einbringen biotechnologischer Aspekte in meine Arbeit.

Ein großer Dank geht an Dr. Constanze Lasch aus der pharmazeutischen Biotechnologie für ihre Zuversicht, Ideen und großartige Unterstützung bei der Arbeit mit den Bakterien. Mein Dank gilt zudem Prof. Dr. Matthias Hannig (Klinik für Zahnerhaltungskunde, Parodontologie und präventive Zahnheilkunde), der mit seiner Unterstützung bei den in vivo-Versuchen sowie der Bereitstellung der Zahnschienen entscheidend zum Gelingen dieser Arbeit beigetragen hat.

Ein herzliches Dankeschön an Karola Lima Engemann, meine Vorgängerin, für die ausgezeichnete Einarbeitung, die Möglichkeit, auf ihren Ergebnissen aufzubauen, und die tolle Betreuung zu Beginn meiner Promotion. Deine Unterstützung hat mir den Start erheblich erleichtert.

Danken möchte ich ebenfalls Samy Aliyazdi (Helmholtzinstitut für Pharmazeutische Forschung) für die Einführung in den 3D-Druck und seine Unterstützung bei der Formulierung des Bioinks. Ein weiterer Dank geht an Dr. Agnes-Valencia Weiß für ihre Hilfe an dem AFM- und Mukoadhäsionsversuchen.

Mein Dank gilt zudem Dr. Florian Schäfer und Prof. Christian Motz (Materialwissenschaften) für ihre Unterstützung bei den Mukoadhäsionsversuchen sowie Marc Thiel und Prof. Karen Lienkamp (Polymerwerkstoffe) für ihre Expertise in der Reißfestigkeitsprüfung.



## Acknowledgments

---

Weiterhin danke ich der Lactopia GmbH Saarbrücken für die Bereitstellung der Bakterienstämme *Lactobacillus rhamnosus* und *Lactobacillus reuteri*.

Ein besonderer Dank geht an das Saarland University Seed Grant (Saarbrücken, Germany) für die finanzielle Unterstützung dieser Forschungsarbeit.

Ich danke allen Studierenden, die an meiner Arbeit mitgewirkt haben – insbesondere Yannik Fuchs (Wahlpflichtpraktikant) und Jan Bernard (Masterarbeit) für ihre wertvollen Beiträge zur Generierung weiterer Ergebnisse.

Ein großes Dankeschön an meine aktuellen und ehemaligen Kollegen, die die Zeit in der Arbeitsgruppe unvergesslich gemacht haben. Vielen Dank für die vielen gemeinsamen Mittagspausen, Feierabendbiere und Grillabende, die stets für eine tolle Atmosphäre gesorgt haben: Philipp, Kristela, Lena, Karola, Tom, Johannes, Jannis, Christof, Mark, Chathuri, Saad, Akram, Thu, Karola, Tom, Johannes, Camilla und Marijas.

Ein herzliches Dankeschön geht an mein großartiges Büro – die Jetski Gang: Elena, Sabrina, Armin und Justin. Ihr wart mein zweites Zuhause am Arbeitsplatz und habt meine Promotionszeit mit vielen gemeinsamen Erlebnissen, auch außerhalb der Arbeit, bereichert. Ich hoffe, dass wir auch nach dieser Zeit weiterhin Lost Places erkunden, gemeinsam essen, wandern und unsere Freundschaft lebendig halten.

Justin, ich bin unheimlich froh, dich zuerst als Kollegen kennengelernt zu haben und noch mehr darüber, dass du schnell mehr als das wurdest. Danke für deine Unterstützung, deine kreativen Lösungen für jedes Problem und dafür, dass du immer mitgedacht hast. Ich bin sehr glücklich, mit dir das Saarland erkundet zu haben und dass wir gemeinsam den nächsten Schritt aus Saarbrücken heraus wagen.

Ein großer Dank geht an das „Boulderteam“ für die vielen gemeinsamen Stunden in der Halle, auf dem Fahrrad oder einfach als großartige Ablenkung von der Arbeit. Ihr habt meine Zeit in Saarbrücken zu einer besonderen gemacht.

Abschließend danke ich meiner Familie von Herzen für das beständige Mitfiebern – auch über das Studium hinaus in der Promotion. Danke für euer offenes Ohr, eure Unterstützung und dass ihr immer für mich da wart.

# Curriculum Vitae

<b>Personal Dates</b>  Charlotte Eckermann	Mainzer Straße 56 66121 Saarbrücken 0163-4705113 charlotte.eckermann@web.de
<b>Education &amp; Work</b>  August 2001- July 2005  August 2005- June 2013  June 2013   October 2014 – October 2019  August 2016  September 2016 – June 2017  October 2019  November 2019 – April 2020  May – December 2020   January 2021  January 2021   February 2021 – August 2021   September 2021 – August 2024   September 2021 – August 2024	Primary School Am Sandberge, Hanover  St. Ursula Schule, Hanover  Abitur   Study of Pharmacy, Albert-Ludwigs-University, Freiburg  First state examination pharmacy  Erasmus internship, Copenhagen University  Second state examination pharmacy  Internship, Löwen Apotheke, Freiburg  Diploma thesis, Pharmaceutical Technology Prof. Dr. Süss, Albert-Ludwigs-University, Freiburg  Third state examination pharmacy  Licensed as a pharmacist   Pharmacist, Hubertus Pharmacy Caunes, Freiburg  Research assistant, Biopharmaceutics and Pharmaceutical Technology, Prof. Dr. Schneider, Saarland University  PhD student, Biopharmaceutics and Pharmaceutical Technology, Prof. Dr. Schneider, Saarland University

<b>Internships and HiWi-positions</b>	
March 2015	Four-week clinical elective in the pharmacy at the Grosser Hillen, Hanover, Germany
September - October 2015	Four-week clinical elective in the hospital pharmacy of the Diakoniekrankehaus Friederikenstift, Hanover, Germany
February – August 2017	Six-month independent laboratory project "Enhanced delivery of peptide drugs through conjugation to a cell-penetrating peptide", Copenhagen University, Copenhagen
July – September 2017	Ten-week internship in the bacteriology department of Boehringer Ingelheim Veterinary Research Center GmbH & Co.KG, Hannover, Germany
October 2017 – March 2018	Student assistant in the internship "Qualitative Analysis" Pharmacy, Albert-Ludwigs-University, Freiburg, Germany
March 2018 – April 2018	Student assistant in the practical course "General and Inorganic Chemistry for Biologists and Geologists", Albert-Ludwigs-University, Freiburg
October 2018 – March 2019	Student assistant in the practical course "Qualitative Analysis" Pharmacy, Albert-Ludwigs-University, Freiburg
May 2019 – September 2019	Student assistant Erasmus Coordination Pharmacy, Albert-Ludwigs-University, Freiburg